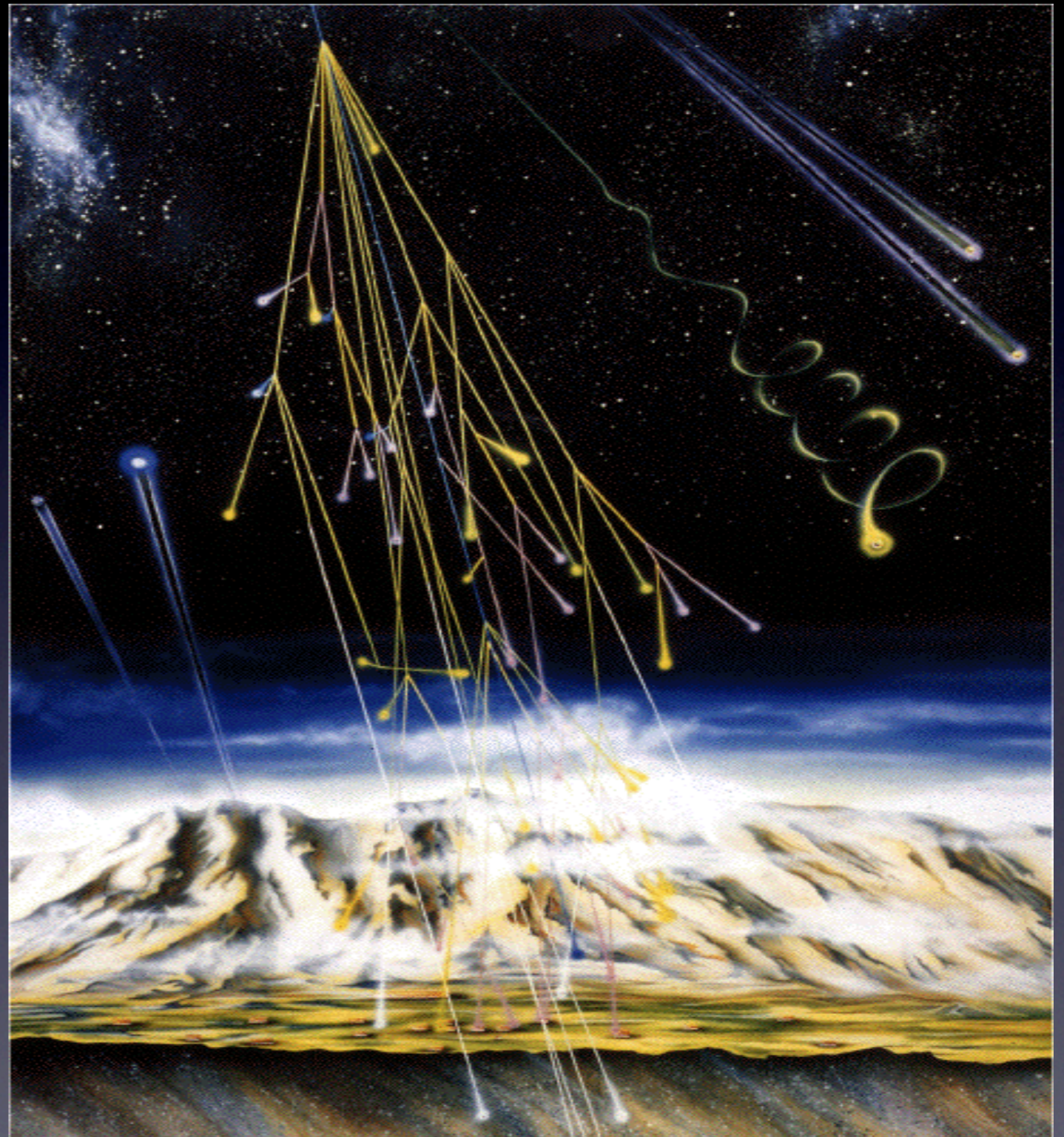


Overview in TeV Cherenkov Experiments

overview

- Introduction of the IACT technique:
 - Pioneering experiments
 - Sensitivity through the IACT generation experiments
- Running IACT experiment
 - Scientific achievements
- Perspectives in the field
 - CTA



The Very Beginning of the Atmospheric Air Cherenkov Telescope Technique

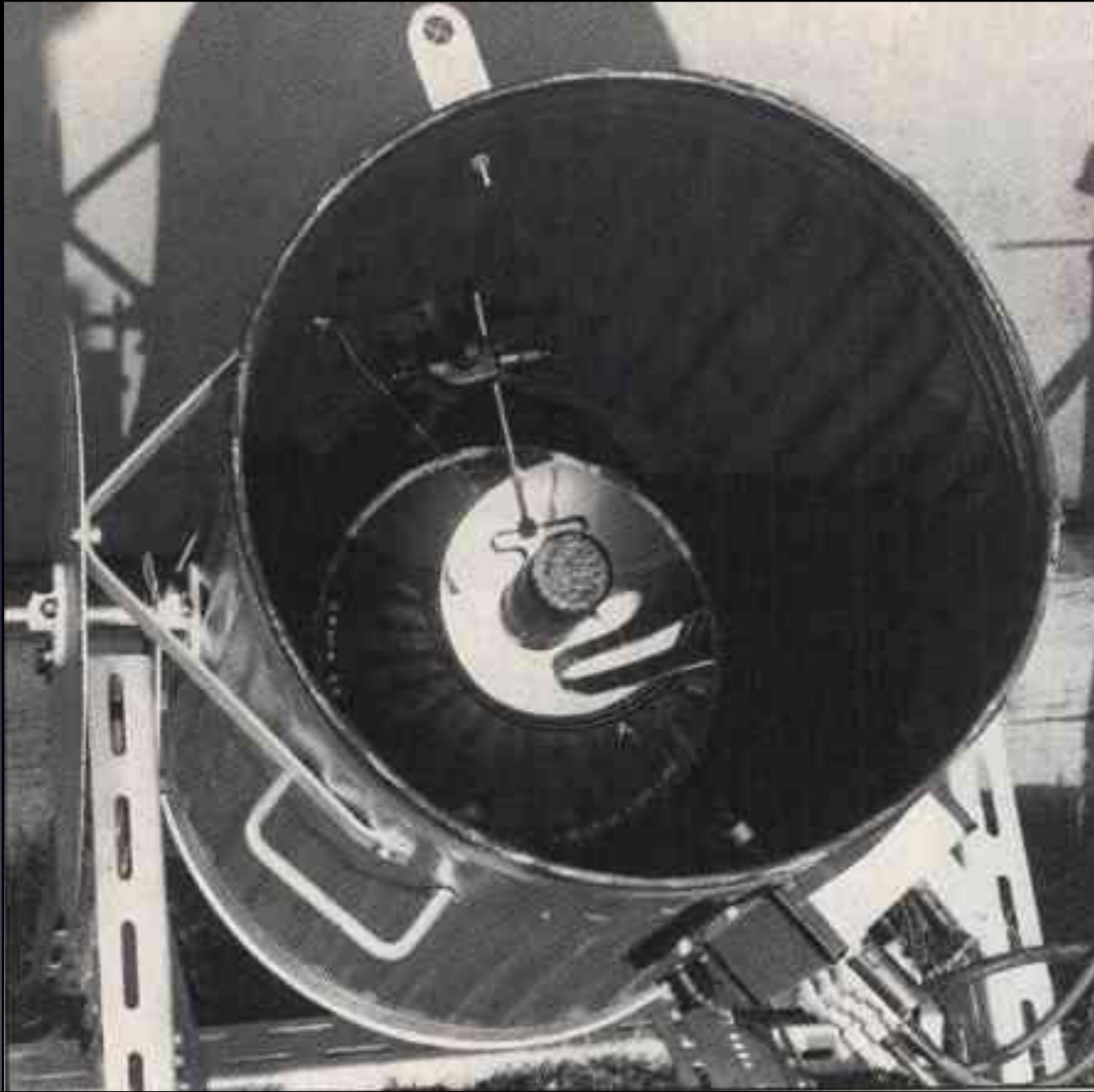


1948

- Blackett (Nobel prize laureate) was the first to mention that there shall be **Cherenkov light component from relativistic particles in air showers** (mostly e^- , e^+ , μ^- , μ^+) marginally contributing ($\sim 10^{-4}$) to the **intensity of the light of night sky** (LONS)

- Until that the Cherenkov light has been detected only in solids and liquids

The Very Beginning of the Atmospheric Air Cherenkov Telescope Technique



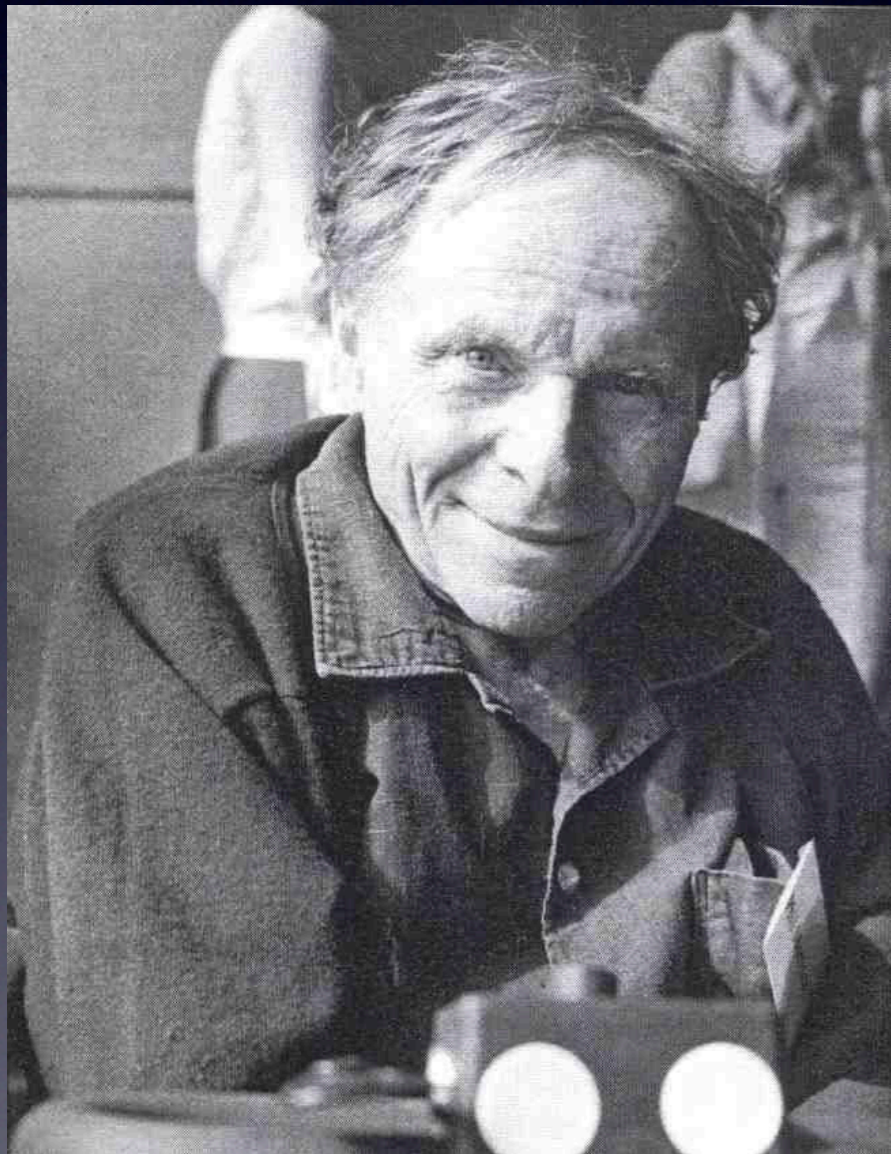
Courtesy of Razmik Mirzoyan

1953

By using a garbage can, a 60 cm diameter mirror in it and a PMT in its focus Galbraith and Jelly had discovered the Cherenkov light pulses from the extensive air showers.

The Very Beginning of the Atmospheric Air Cherenkov Telescope Technique

Seminal paper by
Phillip Morrison,
1958



IL NUOVO CIMENTO

VOL. VII, N. 6

16 Marzo 1958

On Gamma-Ray Astronomy.

P. MORRISON

Department of Physics, Cornell University - Ithaca, N. Y.

(ricevuto il 22 Dicembre 1957)

Summary. — Photons in the visible range form the basis of astronomy. They move in straight lines, which preserves source information, but they arise only very indirectly from nuclear or high-energy processes. Cosmic-ray particles, on the other hand, arise directly from high-energy processes in astronomical objects of various classes, but carry no information about source direction. Radio emissions are still more complex in origin. But γ -rays arise rather directly in nuclear or high-energy processes, and yet travel in straight lines. Processes which might give rise to continuous and discrete γ -ray spectra in astronomical objects are described, and possible source directions and intensities are estimated. Present limits were set by observations with little energy or angular discrimination; γ -ray studies made at balloon altitudes, with feasible discrimination, promise valuable information not otherwise attainable.

Courtesy of Razmik Mirzoyan

1. — The nature of the problem.

Astronomy is based on information carried by incoming radiation of optical frequencies. The photons in this channel retain the momentum with which they were originally emitted; with precision in direction which is

The Very Beginning of the Atmospheric Air Cherenkov Telescope Technique

Also proposed at higher energies independently by in the same time by

Giuseppe Cocconi, 1959

AN AIR SHOWER TELESCOPE
AND THE DETECTION OF 10^{12} eV PHOTON SOURCES
Giuseppe Cocconi *
CERN - Geneva.

1) This paper discusses the possibility of detecting high energy photons produced by discrete astronomical objects. Sources of charged particles are not considered as the emanating produced by the magnetized plasmas filling the interstellar spaces probably obliterates the original directions of movement.

2) Here are some numerical estimates.

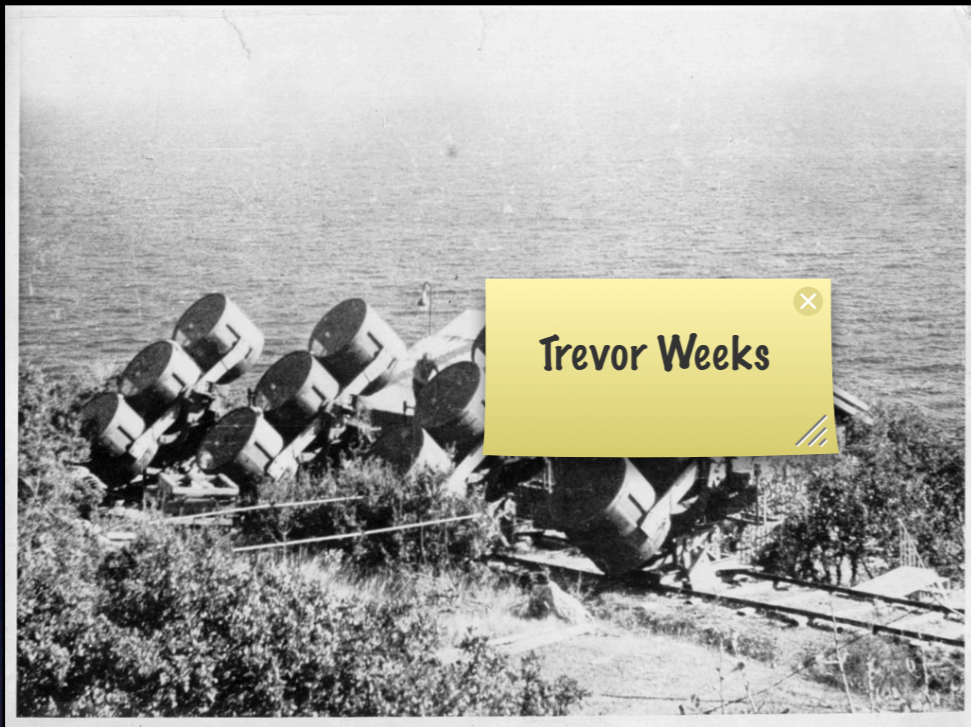
The Crab Nebula: Visual magnitude of polarized light $m = 9$.
Magnetic field in the gas shell $H \approx 10^{-4}$ gauss.
Therefore: $U_\nu = 10^{12}$ eV and $R(10^{12}$ eV) $\approx 10^{-3.2} \text{ m}^{-2} \text{ s}^{-1}$.

The signal is thus about 10^3 times larger than the background (2). Probably in the Crab Nebula the electrons are not in equilibrium with the trapped cosmic rays, and our estimate is over-optimistic. However, this source can probably be detected even if its efficiency in producing high energy photons is substantially smaller than postulated above.

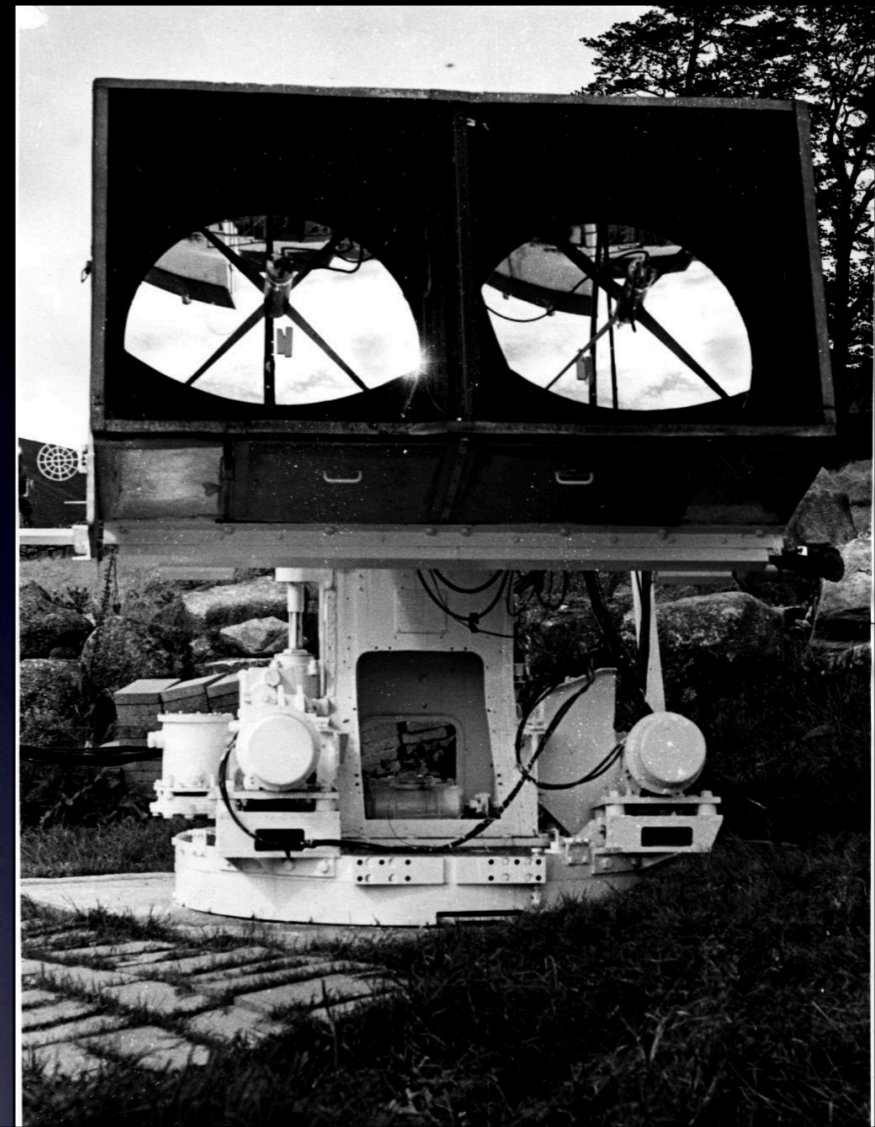
M87, the Jet Nebula: $m = 13.5$ $H \approx 10^{-4}$ gauss.
 $R(10^{12}$ eV) $\approx 10^{-5} \text{ m}^{-2} \text{ s}^{-1}$, still well above the background (2). For this object our evaluation is probably not fundamentally wrong.

Courtesy of Razmik Mirzoyan

The Very Beginning of the Atmospheric Air Cherenkov Telescope Technique



Crimea Experiment
1959-1965, Chudakov, et al.,
(SNR, radio galaxies)



Telescope Glencullen, Ireland
~1962-66 University College,
Dublin group led by Neil Porter (in
collaboration with J.V. Jelley)

Courtesy of Razmik Mirzoyan

The Very Beginning of the Atmospheric Air Cherenkov Telescope Technique



Crimea Experiment
1959-1965, C
(SNR, radio galaxi



Work on the Mt. Hopkins Observatory proceeds at an astonishing pace. The laser and Baker-Nunn systems are now installed and operating and the large optical reflector is scheduled to arrive by the end of next month. In preparation for the LOR installation, Trevor Weekes (above, left) and George Rieke have conducted seeing tests with two movable searchlight reflectors. Look carefully – some outcroppings at the base of Mt. Hopkins are visible upside-down in the reflector.



n, Ireland
College,
Neil Porter(in
V.Jelley)

Courtesy of Razmik Mirzoyan

in the reflector.
[unclear] – some outcroppings at the base of Mt. Hopkins are visible upside-down
conducted seeing tests with two movable searchlight reflectors. Look care-
fully for the LOR installation. Trevor Weekes (above, left) and George Rieke

The 1st Statement in the Literature on the Potential of Imaging Stereo Detector: Zatsepin 1965

THE ANGULAR DISTRIBUTION OF INTENSITY OF CERENKOV RADIATION FROM EXTENSIVE COSMIC-RAY AIR SHOWERS

V. I. ZATSEPIN

P. N. Lebedev Physics Institute, Academy of Sciences, U.S.S.R.

Submitted to JETP editor March 2, 1964

J. Exptl. Theoret. Phys. (U.S.S.R.) 47, 689-696 (August, 1964)

The angular distribution of intensity is calculated for the Cerenkov radiation produced in the terrestrial atmosphere by extensive air showers of cosmic rays. Calculations are made for showers arriving from the zenith and for conditions of observation at sea level and at an altitude of 3860 m above sea level. Photographic observation of the shape of the flash of light against the celestial sphere, as obtained in [2,3] is evidently in satisfactory agreement with the calculations.

1. INTRODUCTION

IN the registration of extensive air showers (EAS) by means of Cerenkov counters, [1,2] a knowledge of the angular distribution of the Cerenkov radiation is important primarily from the methodological point of view (choice of the angle subtended by the Cerenkov counters to obtain optimal signal-to-noise ratio, estimates of the accuracy of the angular coordinates of high-energy primary particles, and so on). Besides this, the angular distribution of the light from showers is already itself the object of physical investigation, [3] and therefore it is important to ascertain what kind of information about a shower can be obtained from such data. The present calculation has been made for this purpose, and is based on the following ideas.

Cerenkov radiation is mainly caused by the electronic component, which makes up the bulk of the charged particles in a shower. Owing to multiple Coulomb scattering by the nuclei of atoms in the air, electrons of energy E at a depth p have a Gaussian distribution of distances r from the axis of the shower, and a Gaussian distribution of angles relative to a mean angle ψ , which depends on r . The dispersions of the transverse and angular distributions depend on E . The energy spectrum of the electrons is an equilibrium one and does not depend on the degree of development of the shower in depth. For the case of primary photons the variation of the electrons with height is taken to be that given by the electromagnetic cascade theory, [4] and for the case of primary protons, that given by the calculations of Nikol'skii and Pomanskii, [5] The light emitted by the electrons is at the angle ψ_{Cer} with the direction of their

motion. Neither the scattering of the light by density inhomogeneities in the air nor absorption of the light is taken into account.

2. STATEMENT OF PROBLEM AND METHOD OF CALCULATION

The purpose of the calculation is to determine the number I of light quanta in the frequency range from λ_1 to λ_2 that fall on unit area of the earth's surface at distance R from the axis of the shower, and in the direction from any given point of the celestial sphere.

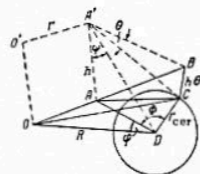


FIG. 1

Let us turn to Fig. 1. Here O is the trace of the axis of the shower on the earth's surface, D is the point of observation, and A' is an arbitrary point which is at height h over the level of observation and is characterized by the angular coordinates ψ (the zenith angle) and φ (the azimuthal angle). We agree to measure the azimuthal angle from the direction from the point of observation D to the trace O of the axis of the shower on the earth's surface. The figure $OBCD$ lies in the plane of the drawing, and $OO'A'B$ in the perpendicular plane. We shall determine for the neighborhood of

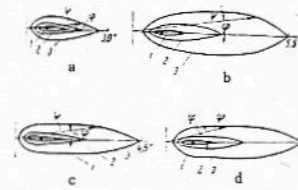


FIG. 6. Contours of equal intensity in light flashes from showers from primary protons and primary photons of various energies, for sea level and $R = 100$ m from the axis. The curves 1, 2, 3 correspond to intensity values $10^{-3} I_{\text{max}}(100)$, $10^{-2} I_{\text{max}}(100)$, and $10^{-1} I_{\text{max}}(100)$. Diagrams a and b correspond to primary photons of energies 10^9 and 5×10^8 BeV, and diagrams c and d to primary protons of energies 1.5×10^9 and 4.5×10^8 BeV.

primary photons. For lower energies of the primary particles ($E_0 \approx 10^{12}$ eV) the situation is somewhat better (Fig. 6). Here the shape of the line $I = 10^{-3} I_{\text{max}}$ in showers from photons differs appreciably from that of the corresponding line in showers from protons. This difference, however, is entirely due to the difference in the shapes of the cascade curves. If we allow for the fact that owing to fluctuations the cascade curves for proton showers can differ decidedly from the average curve, the difference in the shape of the light spots which we have mentioned can also be insufficient for a reliable distinction between showers produced by photons and those produced by protons. Figures 7 and 8, which are analogous to Figs. 2 and 3, give an idea of the angular distribution of the light in showers from primary protons when the observation is at altitude 3860 meters above sea level. A comparison of Figs. 3 and 8 shows that on mountains the spot of light from a shower from a proton

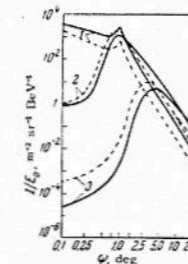


FIG. 7. Section of angular distribution of the intensity of Cerenkov light against zenith angle for azimuthal angle $\varphi = 0$, for altitude 3860 m above sea level. Curves 1, 2, and 3 are for the respective distances 0, 100, and 400 m from the axis of the shower. The solid curves correspond to a primary proton with energy 4.5×10^8 BeV, and the dashed curves to one with energy 1.5×10^9 BeV.

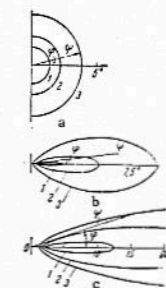


FIG. 8. Contours of equal intensity in the light flash at various distances from the axis of a shower arising from a primary proton with $E_0 = 4.5 \times 10^8$ BeV (3860 m above sea level). Curves 1, 2, and 3 correspond to the intensities $10^{-3} I_{\text{max}}(R)$, $10^{-2} I_{\text{max}}(R)$, and $10^{-1} I_{\text{max}}(R)$, and diagrams a, b, and c are for distances 0, 100, and 400 m from the axis of the shower.

with $E = 4.5 \times 10^{16}$ eV is considerably larger than that from such a shower at sea level. This difference is mainly due to the different distance of the registering device from the maximum of the shower. Thus the shape of the spot of light is sensitive to the height of the maximum of the shower, and at least in principle an analysis of the shape can be used also to determine the position of the maximum of a shower.

The present calculations have been made on the same assumptions as the calculations of the spatial distribution of the light made in [6], and therefore they can be checked directly by calculating the total luminous flux density

$$Q(R, E_0) = \int_0^{2\pi} \int_0^{\pi/2} I(E_0, R, \psi, \varphi) \sin \psi d\psi d\varphi \quad (11)$$

at a given distance from the axis of the shower and comparing it with the results obtained in [6]. Calculations by Eq. (11) have been made for sea level for $R = 100$ m and $R = 400$ m. The results agreed with the results of [6] to an accuracy of several percent.

CONCLUSION

The calculations that have been made enable us to draw the following conclusions:

1. Since the maximum intensity of the light from a shower does not coincide with the direction of arrival of the primary particle, in researches in which the determination of the angular coordinates of the primary particle is made by photographing the light flash from the shower one should seek improved accuracy in this determination by photo-

The 1st Statement in the Literature on the Potential of Imaging Stereo Detector: Zatsepin 1965

THE ANGULAR DISTRIBUTION OF INTENSITY OF CERENKOV RADIATION FROM EXTENSIVE COSMIC-RAY AIR SHOWERS

V. I. ZATSEPIN

P. N. Lebedev Physics Institute, Academy of Sciences, U.S.S.R.

Submitted to JETP editor March 2, 1964

J. Exptl. Theoret. Phys. (U.S.S.R.) 47, 689-696 (August, 1964)

The angular distribution of intensity is calculated for the Cerenkov radiation from extensive air showers of cosmic rays. Calculations are made for showers arriving from the zenith and for conditions of observation at an altitude of 3860 m above sea level. Photographic observation of the shape of the light flash against the celestial sphere, as obtained in [2,3] is evidently in satisfactory agreement with the calculations.

1. INTRODUCTION

In the registration of extensive air showers (EAS) by means of Cerenkov counters, [1,2] a knowledge of the angular distribution of the Cerenkov radiation is important primarily from the methodological point of view (choice of the angle subtended by the Cerenkov counters to obtain optimal signal-to-noise ratio, estimates of the accuracy of the angular coordinates of high-energy primary particles, and so on). Besides this, the angular distribution of the light from showers is already itself the object of physical investigation, [3] and therefore it is important to ascertain what kind of information about a shower can be obtained from such data. The present calculation has been made for this purpose, and is based on the following ideas.

Cerenkov radiation is mainly caused by the electronic component, which makes up the bulk of the charged particles in a shower. Owing to multiple Coulomb scattering by the nuclei of atoms in the air, electrons of energy E at a depth p have a Gaussian distribution of distances r from the axis of the shower, and a Gaussian distribution of angles relative to a mean angle ψ , which depends on r . The dispersions of the transverse and angular distributions depend on E . The energy spectrum of the electrons is an equilibrium one and does not depend on the degree of development of the shower in depth. For the case of primary photons the variation of the electrons with height is taken to be that given by the electromagnetic cascade theory, [4] and for the case of primary protons, that given by the calculations of Nikol'skii and Pomanskii, [5] The light emitted by the electrons is at the angle ψ_{Cer} with the direction of their

motion. Neither the inhomogeneities of the light is taken into

2. STATEMENT OF THE METHOD OF CALCULATION

The purpose of the calculation is to determine the number I of light photons from λ_1 to λ_2 that fall on a surface at distance R and in the direction ψ and in the direction of the celestial sphere.

Let us turn to the axis of the shower. The point of observation is at the zenith and is characterized by the zenith angle ψ (the zenith angle). We agree to take the direction of the trace O of the shower as the direction of the drawing, and the plane of the drawing as the plane of the shower. We shall determine the intensity I of the light flash from the shower at the angle ψ relative to the axis of the shower.

CONCLUSION

The calculations that have been made enable us to draw the following conclusions:

1. Since the maximum intensity of the light from a shower does not coincide with the direction of arrival of the primary particle, in researches in which the determination of the angular coordinates of the primary particle is made by photographing the light flash from the shower one should seek improved accuracy in this determination by photographing the shower simultaneously from several positions.

2. If the distance from the axis of the shower to the detector is determined from independent data, then an analysis of the shape of the light flash from the shower and its total intensity gives information both about the initial energy of the primary particle and about the position in the atmosphere of the maximum of the shower, and can thus be used for the analysis of fluctuations in the development of showers in the atmosphere.

In conclusion I regard it as my pleasant duty to express my gratitude to A. E. Chudakov for suggesting this topic and for helpful discussions.

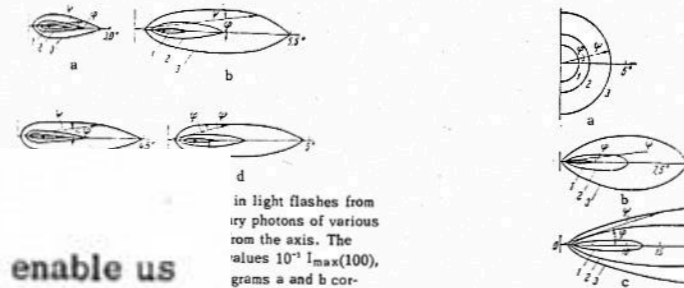


FIG. 8. Contours of equal intensity in the light flash at various distances from the axis of a shower arising from a primary proton with $E_{\text{ep}} = 4.5 \times 10^6$ BeV (3860 m above sea level). Curves 1, 2, and 3 correspond to the intensities $10^{-1} I_{\text{max}}(R)$, $10^{-2} I_{\text{max}}(R)$, and $10^{-3} I_{\text{max}}(R)$, and diagrams a, b, and c are for distances 0, 100, and 400 m from the axis of the shower.

in light flashes from extensive air showers. The angular distribution of the light from the shower is sensitive to the height of the maximum of the shower, and at least in principle an analysis of the shape of the spot of light is sensitive to the height of the maximum of the shower. Thus the shape of the spot of light is sensitive to the height of the maximum of the shower, and at least in principle an analysis of the shape of the spot of light can be used also to determine the position of the maximum of a shower.

FIG. 8. Contours of equal intensity in the light flash at various distances from the axis of a shower arising from a primary proton with $E_{\text{ep}} = 4.5 \times 10^6$ BeV (3860 m above sea level). Curves 1, 2, and 3 correspond to the intensities $10^{-1} I_{\text{max}}(R)$, $10^{-2} I_{\text{max}}(R)$, and $10^{-3} I_{\text{max}}(R)$, and diagrams a, b, and c are for distances 0, 100, and 400 m from the axis of the shower.

The present calculations have been made on the same assumptions as the calculations of the spatial distribution of the light made in [6], and therefore they can be checked directly by calculating the total luminous flux density

$$Q(R, E_0) = \int_0^{2\pi} \int_0^{\pi/2} I(E_0, R, \psi, \varphi) \sin \psi d\psi d\varphi \quad (11)$$

at a given distance from the axis of the shower and comparing it with the results obtained in [6]. Calculations by Eq. (11) have been made for sea level for $R = 100$ m and $R = 400$ m. The results agreed with the results of [6] to an accuracy of several percent.

CONCLUSION

The calculations that have been made enable us to draw the following conclusions:

1. Since the maximum intensity of the light from a shower does not coincide with the direction of arrival of the primary particle, in researches in which the determination of the angular coordinates of the primary particle is made by photographing the light flash from the shower one should seek improved accuracy in this determination by photographing the shower simultaneously from several positions.

Imaging Detector to reveal Cherenkov light from Atmospheric showers



30h for 20 sigma signal from crab

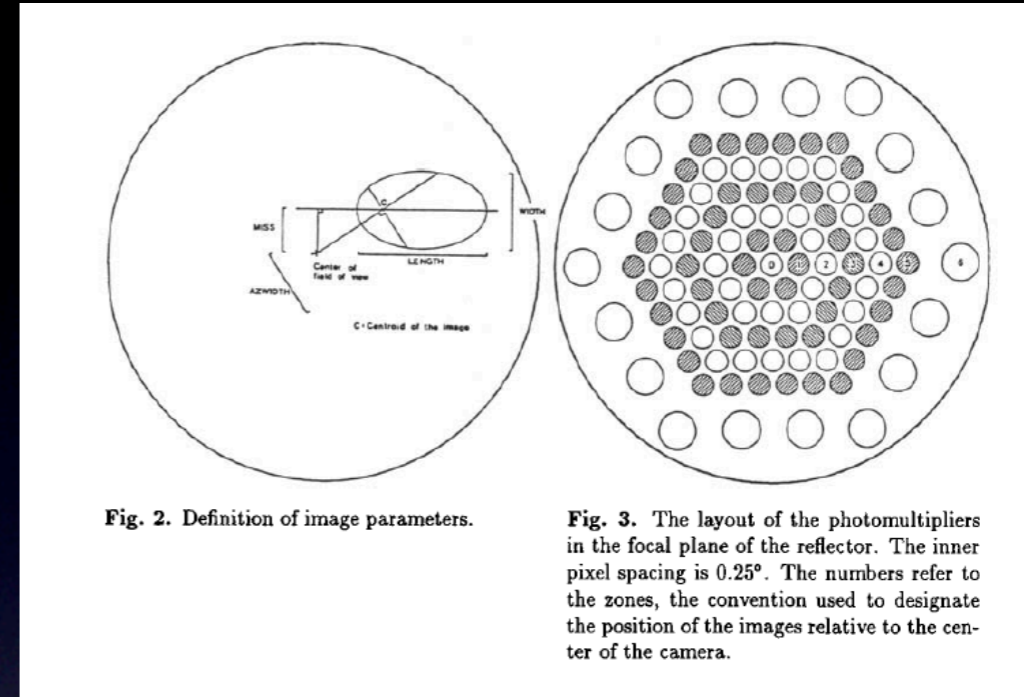


Fig. 2. Definition of image parameters.

Fig. 3. The layout of the photomultipliers in the focal plane of the reflector. The inner pixel spacing is 0.25° . The numbers refer to the zones, the convention used to designate the position of the images relative to the center of the camera.

1988-89

Observations of TeV Photons at the Whipple Observatory

R. C. Lamb,¹ C. W. Akerlof,² M. F. Cawley,³ E. Colombo,⁴ D. J. Fegan,⁵ A. M. Hillas,⁶
P. W. Kwok,⁴ M.J.Lang,⁴ D. A. Lewis,¹ D. J. Macomb,¹ D. I. Meyer,² K. S. O'Flaherty,⁵
P.T.Reynolds,⁴ G. Vacanti,¹ and T.C.Weekes⁴

¹Iowa State University, Ames, IA 50011 USA

²University of Michigan, Ann Arbor, MI 48109 USA

³St. Patrick's College, Maynooth, Co. Kildare, IRELAND

⁴Harvard-Smithsonian Center for Astrophysics, P.O. Box 97, Amado, Arizona 85645 USA

⁵University College, Dublin, IRELAND

⁶University of Leeds, Leeds, UK

Abstract

The Whipple Observatory 10 m gamma-ray telescope has been used to search for TeV gamma-ray emission from a number of objects. This paper reports observations of six galactic and three extragalactic objects using the Cherenkov image technique. With the introduction of a high-resolution camera ($1/4^\circ$ pixel) in 1988, the Crab Nebula was detected at a significance level of 20σ in 30 hours of on-source observation. Upper limits at a fraction of the Crab flux are set for most of the other objects, based on the absence of any significant dc excess or periodic effect when an *a priori* Monte Carlo determined imaging selection criterion (the "azwidth cut") is employed. There are weak indications that one source, Hercules X-1, may be an episodic emitter. The Whipple detection system will be improved shortly with the addition of a second reflector 11 m in diameter (GRANITE) for stereoscopic viewing of showers. The combination of the two-reflector system should have a signal-to-noise advantage of 10^3 over a simple nonimaging Cherenkov receiver.

E-M shower + Cherenkov light emission.

IACT Technique

Gamma-ray

Particle shower

~ 10 km

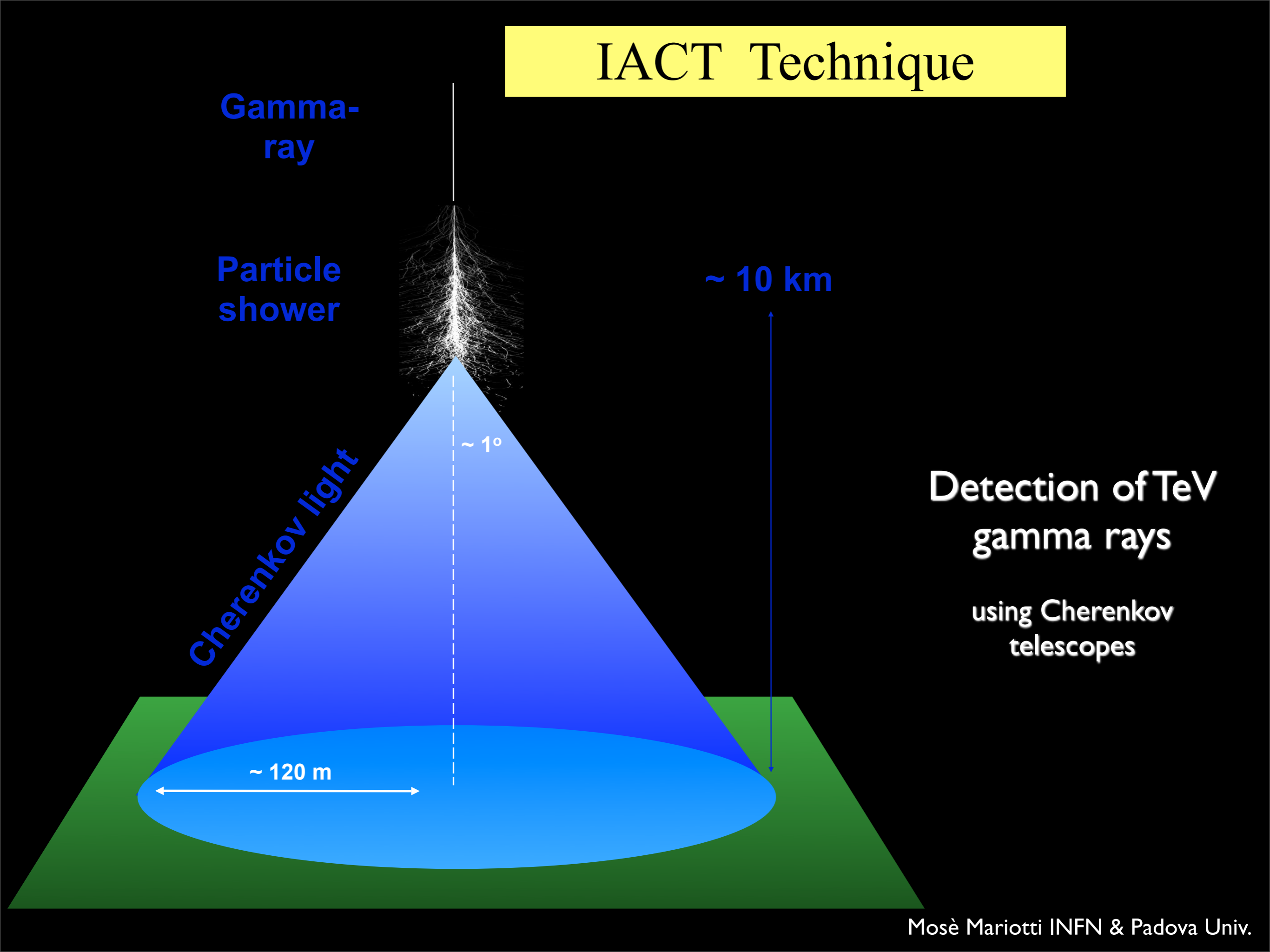
Cherenkov light

~ 1°

Detection of TeV
gamma rays

using Cherenkov
telescopes

~ 120 m



IACT Technique

Gamma-ray

Particle shower

~ 10 km

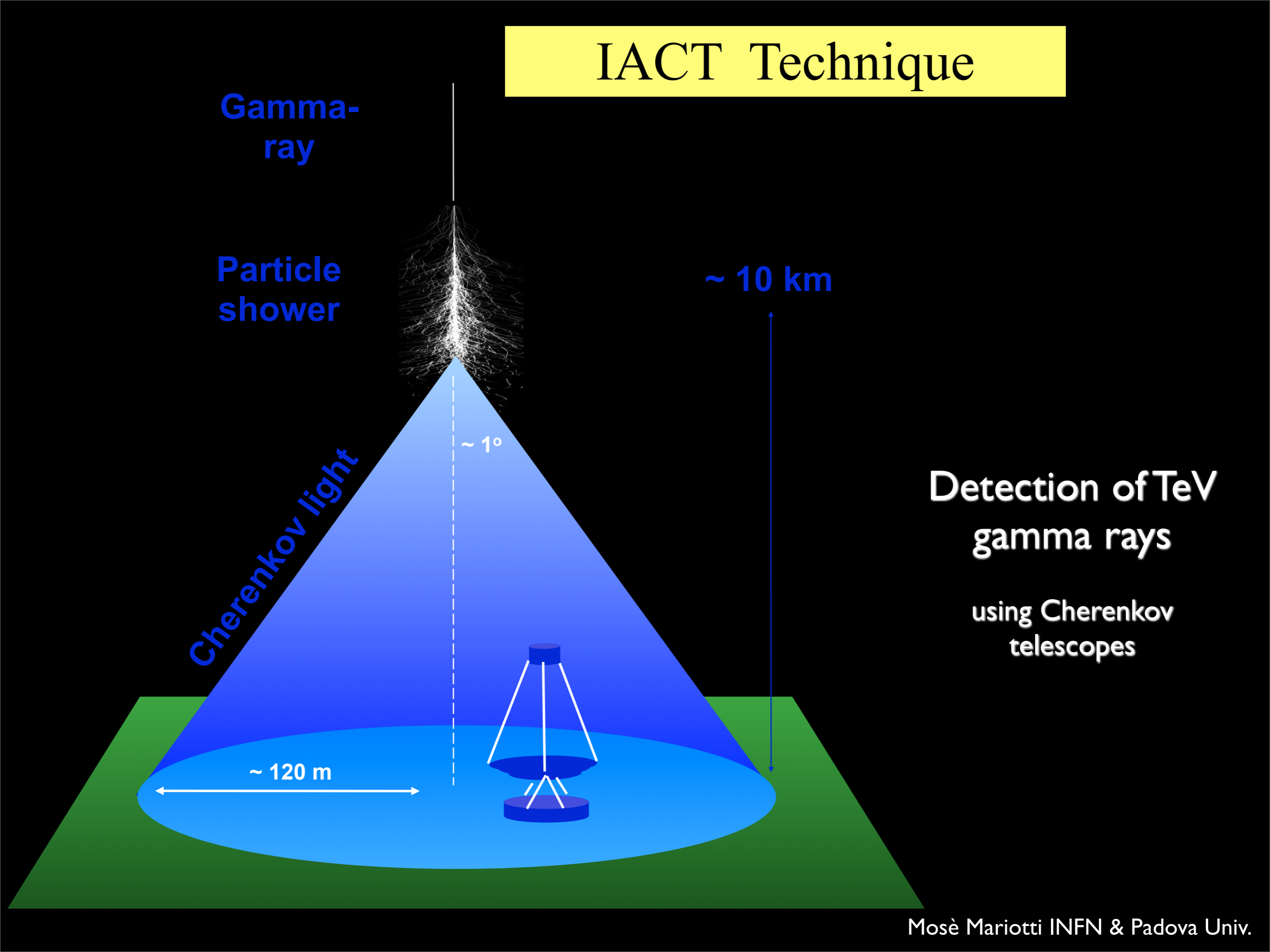
Cherenkov light

~ 1°

Detection of TeV
gamma rays

using Cherenkov
telescopes

~ 120 m



IACT Technique

Gamma-ray

Particle shower

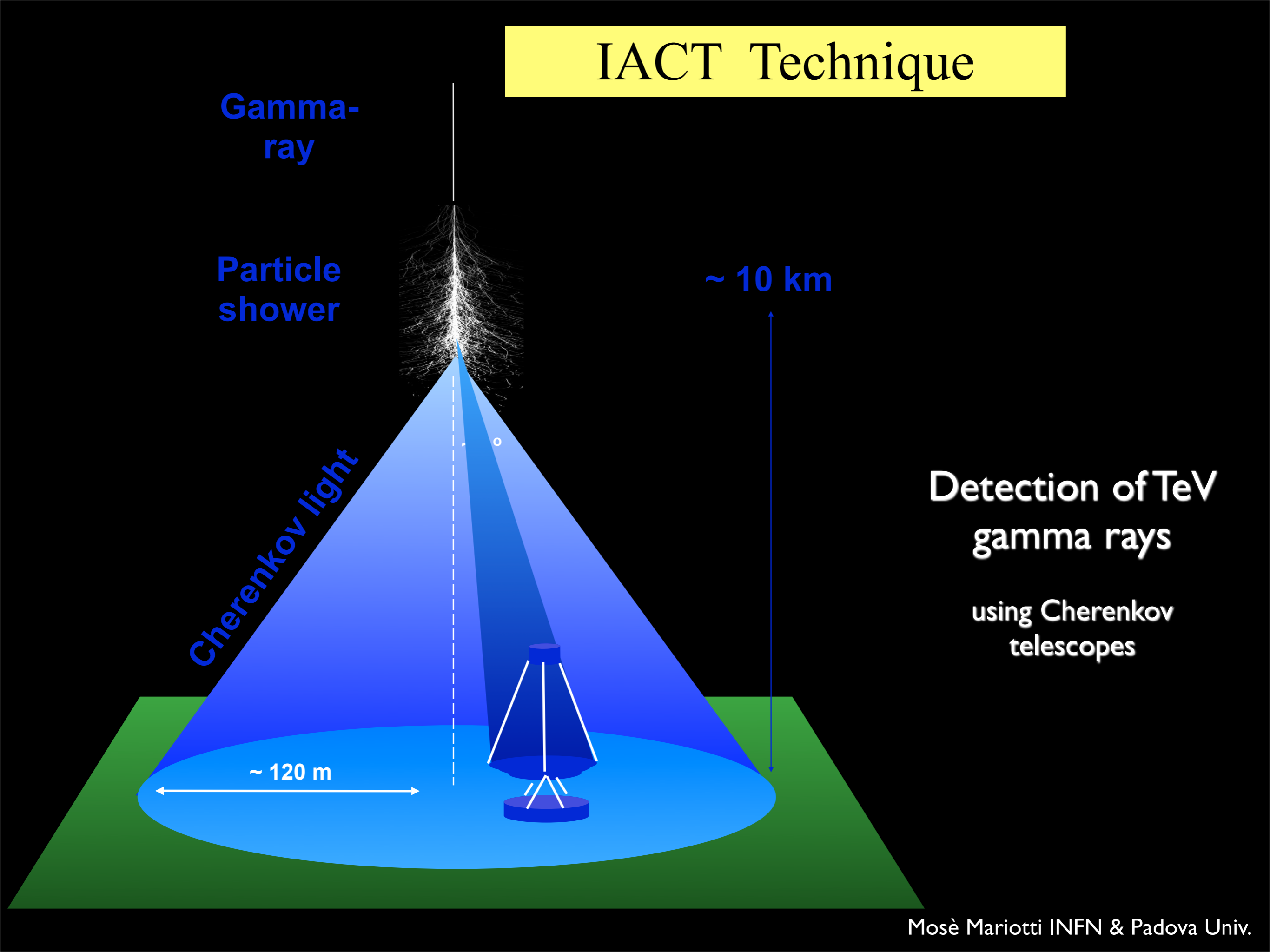
~ 10 km

Cherenkov light

Detection of TeV
gamma rays

using Cherenkov
telescopes

~ 120 m



IACT Technique

Gamma-ray

Particle shower

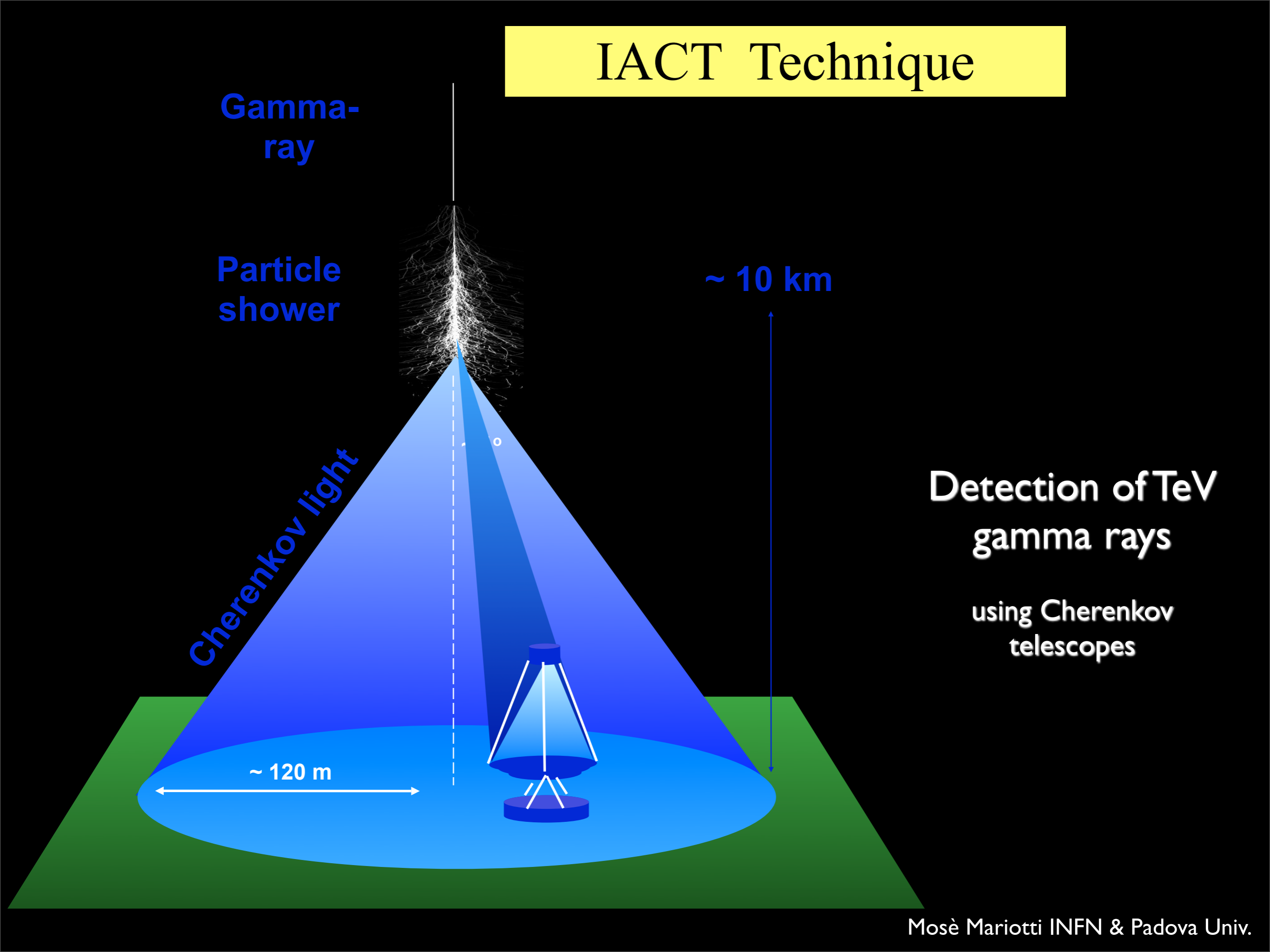
~ 10 km

Cherenkov light

Detection of TeV
gamma rays

using Cherenkov
telescopes

~ 120 m



IACT Technique

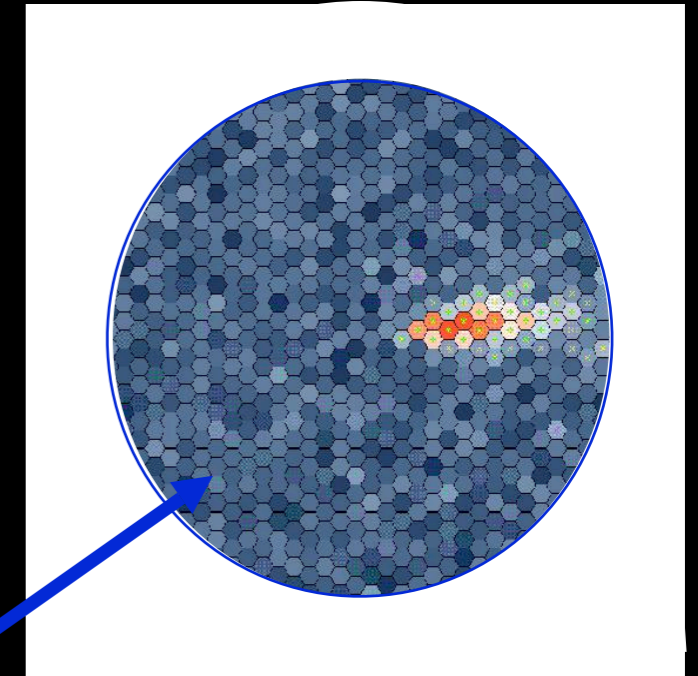
Gamma-ray

Particle shower

Cherenkov light

~ 10 km

~ 120 m



Detection of TeV
gamma rays

using Cherenkov
telescopes

Atmosphere

~ 10 km

Primary γ -ray

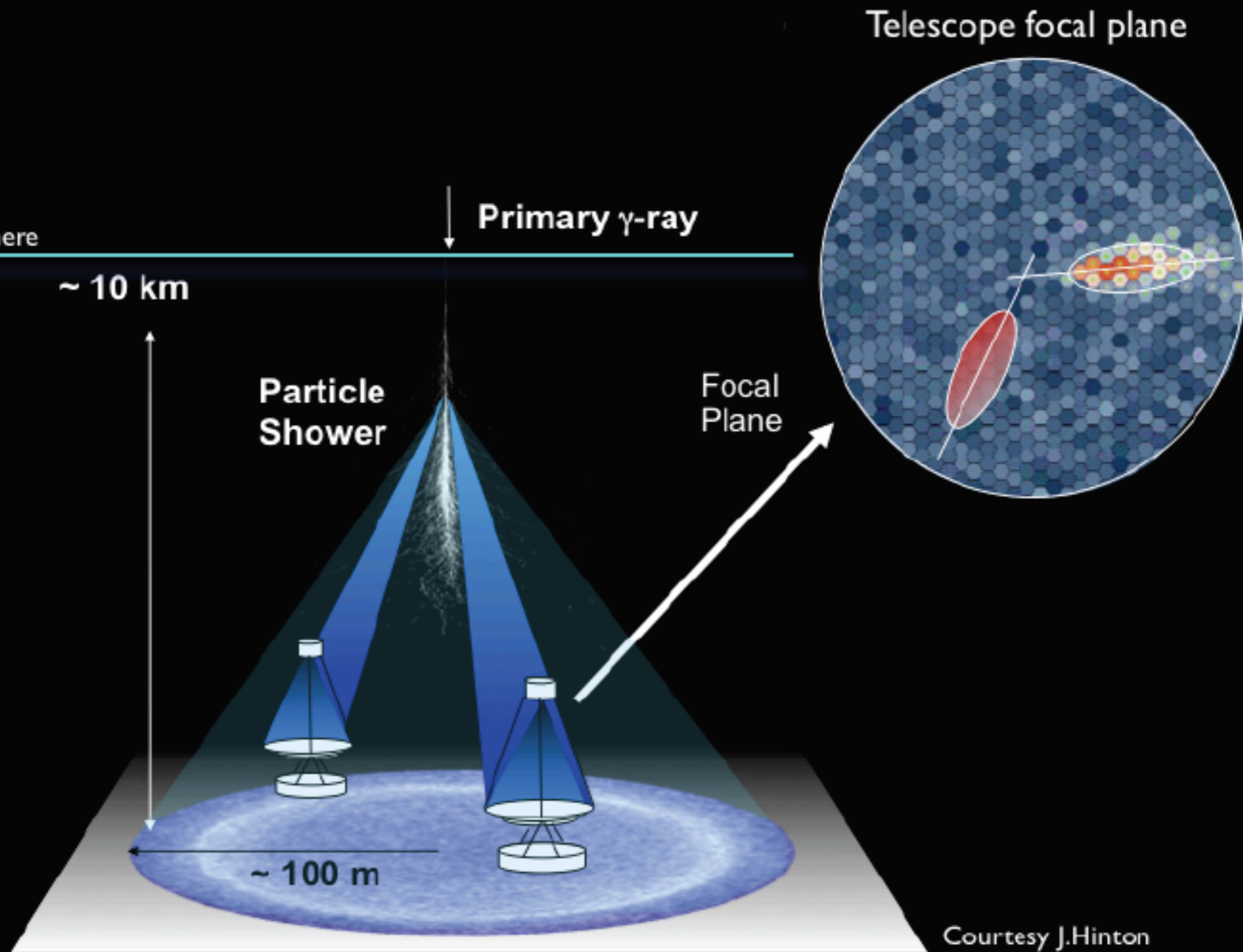
Particle Shower

Focal Plane

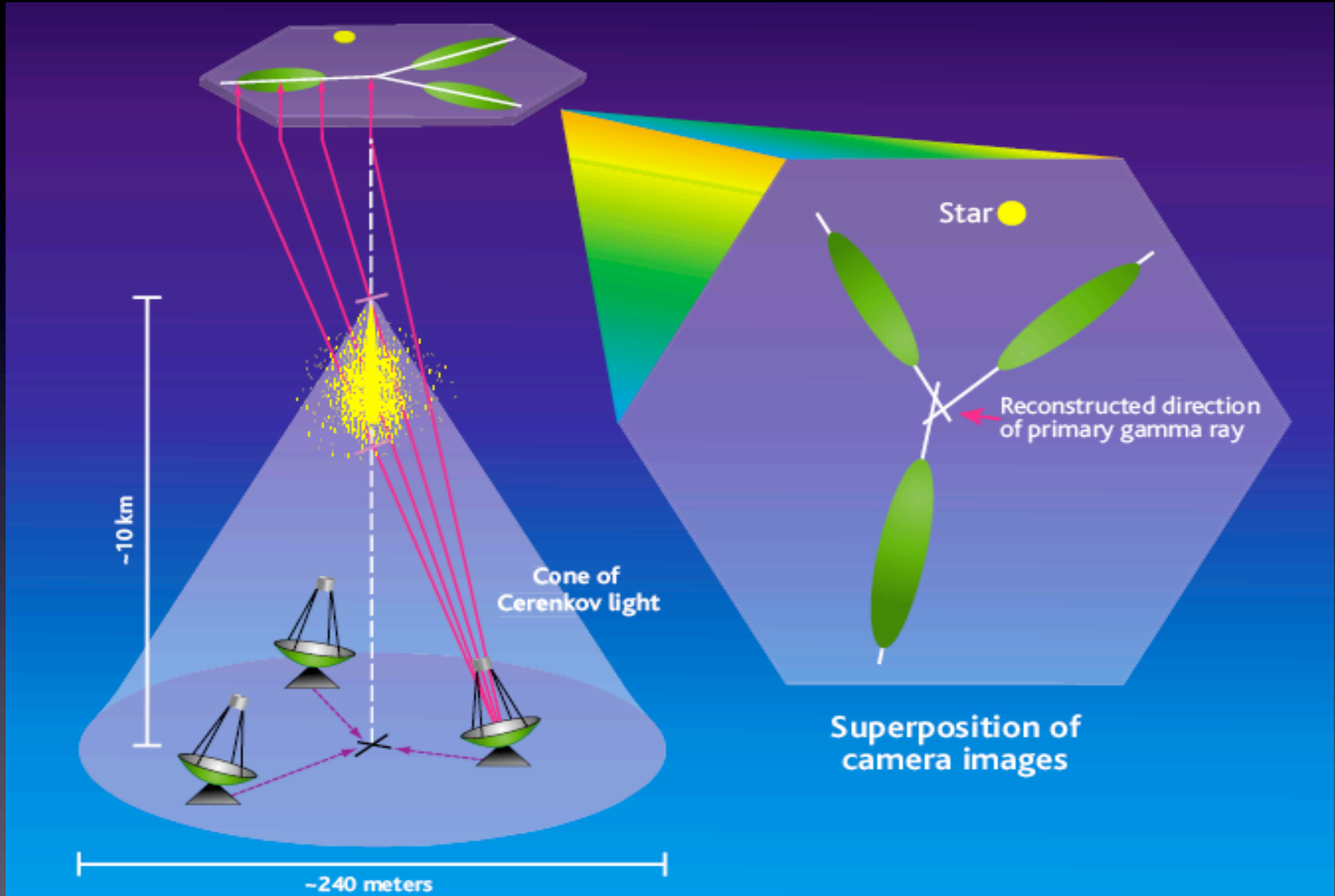
Telescope focal plane

~ 100 m

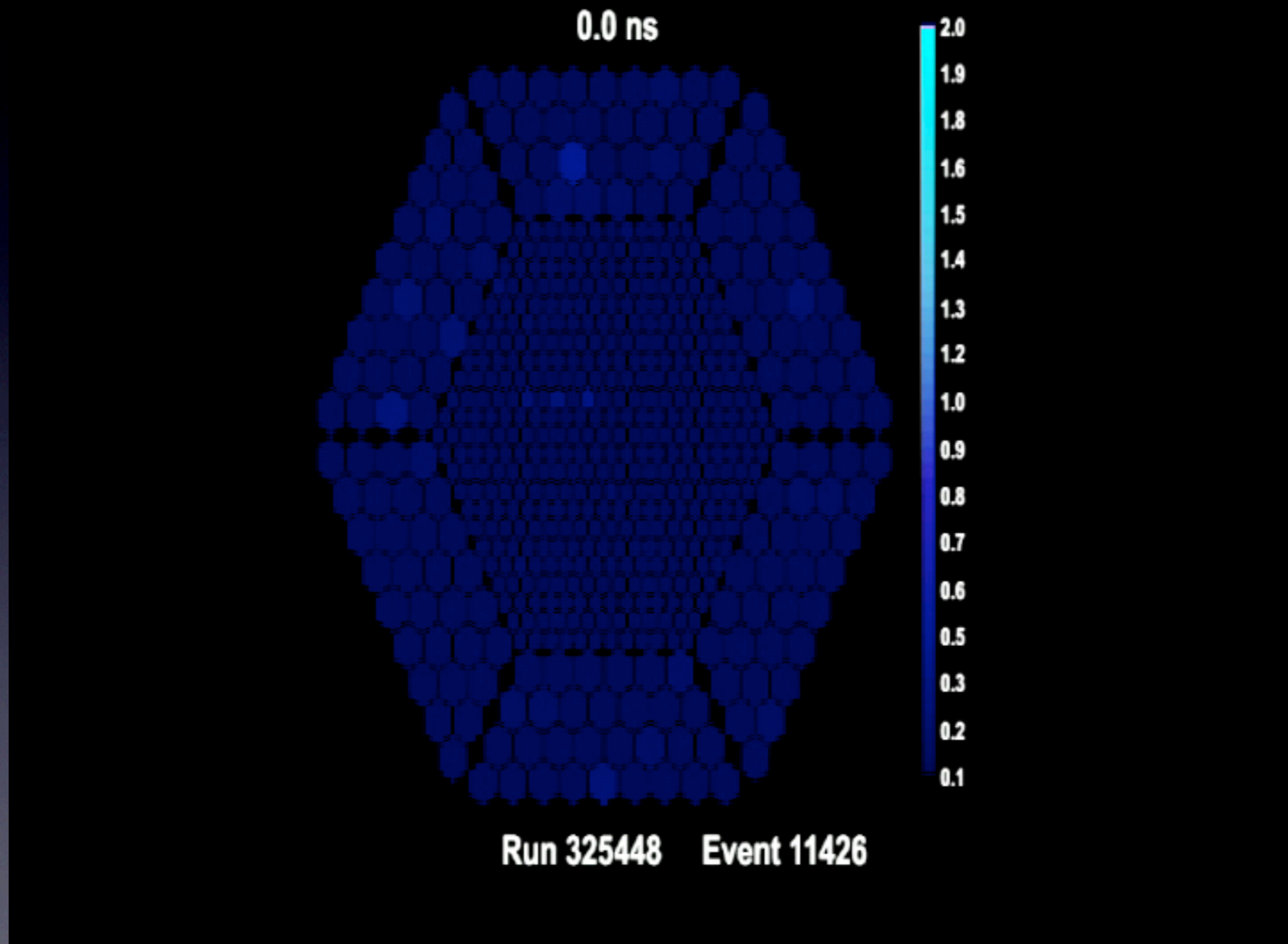
Courtesy J.Hinton



The stereoscopic concept



E-M shower in the atmosphere



Evolution of sensitivity

Crab discovery Wipple

5 sigma crab in 2h

HEGRA, Wipple granite

5 sigma crab in 6 min

MAGIC, HESS, Veritas

5 sigma crab <20 s

Detectors in Gamma-Ray Astrophysics

Low Energy Threshold

EGRET, AGILE, FERMI

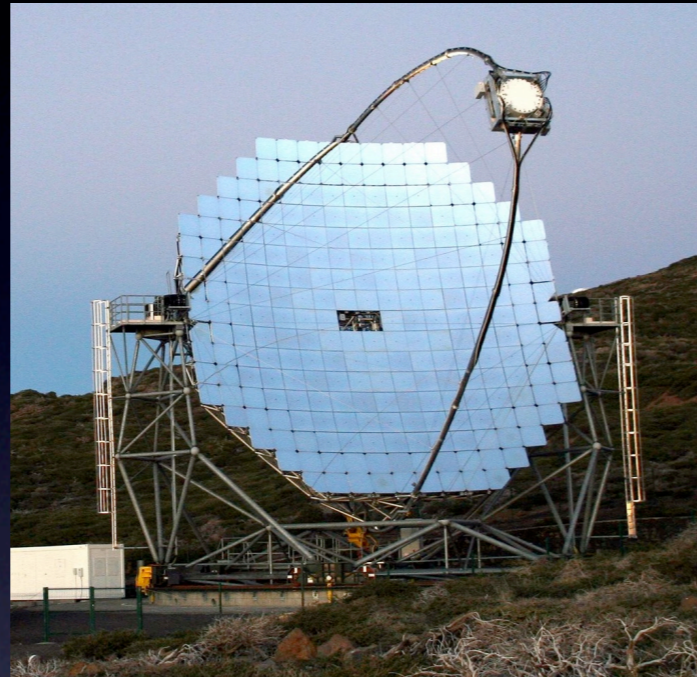


Energy Range 0.1-100 GeV
Area: 1 m²
~ Background Free
Angular Resolution 0.1° - 0.3°
Aperture 2.4 sr
Duty Cycle > 90%

Unbiased Sky Survey (<100 GeV)
Extended Sources
Transients (AGN, GRBs) <100 GeV
Simultaneous ν Observations

High Sensitivity

HESS, MAGIC, CANGAROO, VERITAS



Energy Range 20 GeV-50 TeV
Area > 10⁵ m²
Background Rejection > 99.8%
Angular Resolution 0.05°
Aperture 0.003 sr
Duty Cycle 10%

High Resolution Energy Spectra
Studies of known sources
Surveys of limited regions of sky

Large Aperture/High Duty Cycle

Milagro, Tibet, ARGO, HAWC



Energy Range 0.1-100 TeV
Area > 10⁴ m²
Background Rejection > 95%
Angular Resolution 0.3° - 0.7°
Aperture > 2 sr
Duty Cycle > 90%

Unbiased Sky Survey
Extended Sources
Transients (GRB's)
Simultaneous ν Observations

running IACTs

HESS I: Array 4 tel. of 12m
HESS II: 28m diameter (2013)
1800 m asl
> 2003



MAGIC:
Array 2 telescopes
17m diameters
2200 m asl
>2004

Array 4 telescopes of
12m diam.
Central mast mounting
1800 m asl
>2007

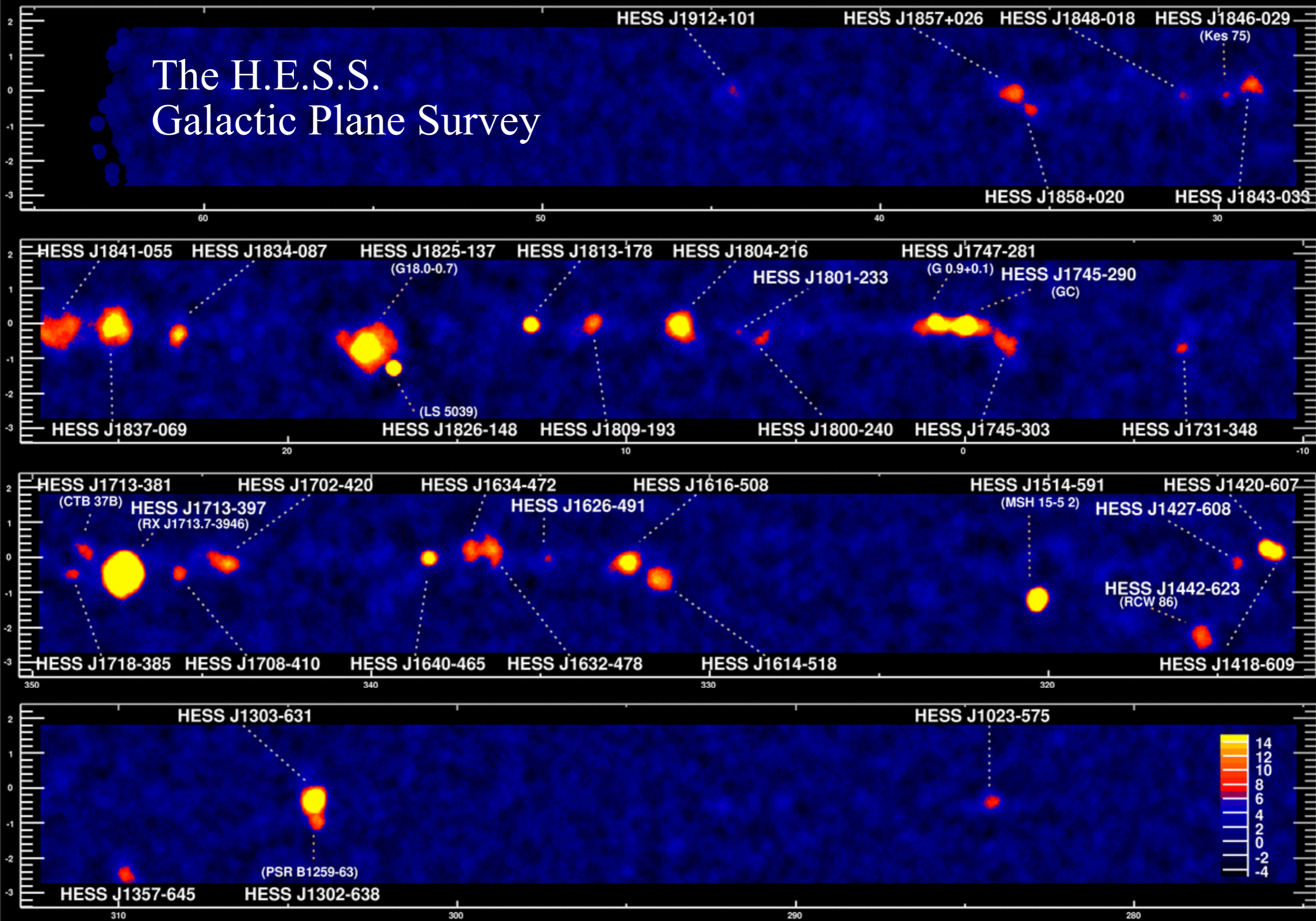


Scientific achievements

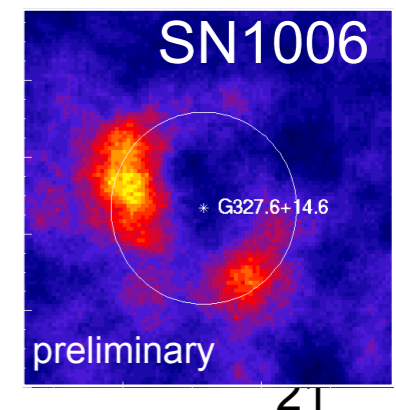
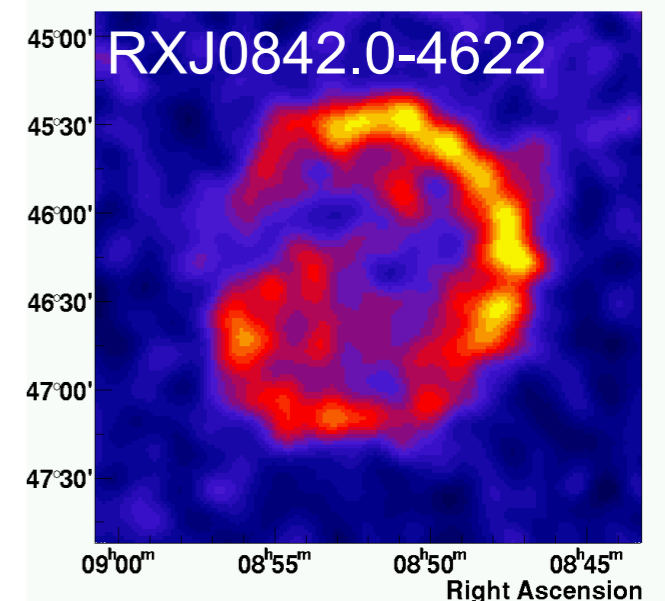
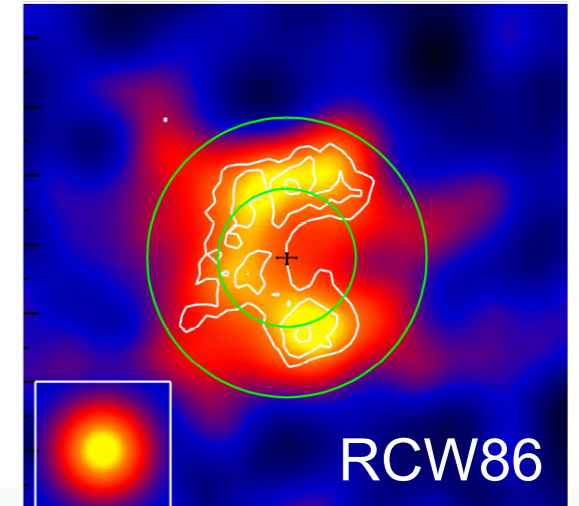
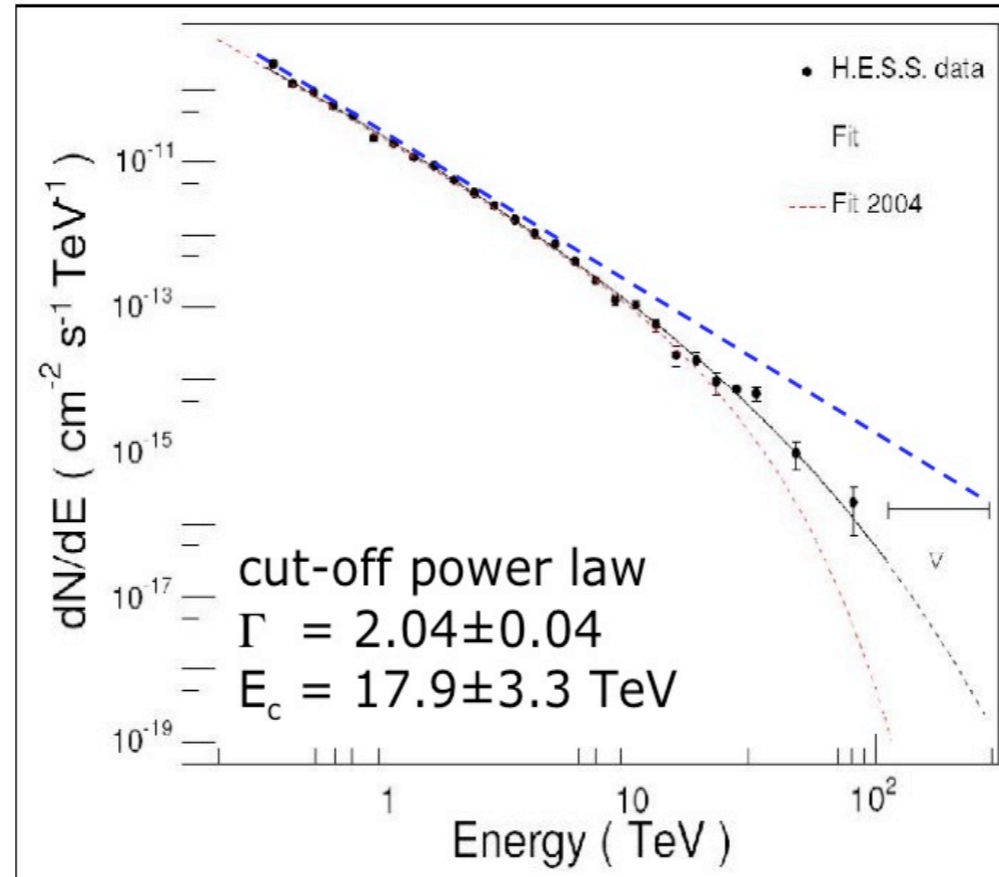
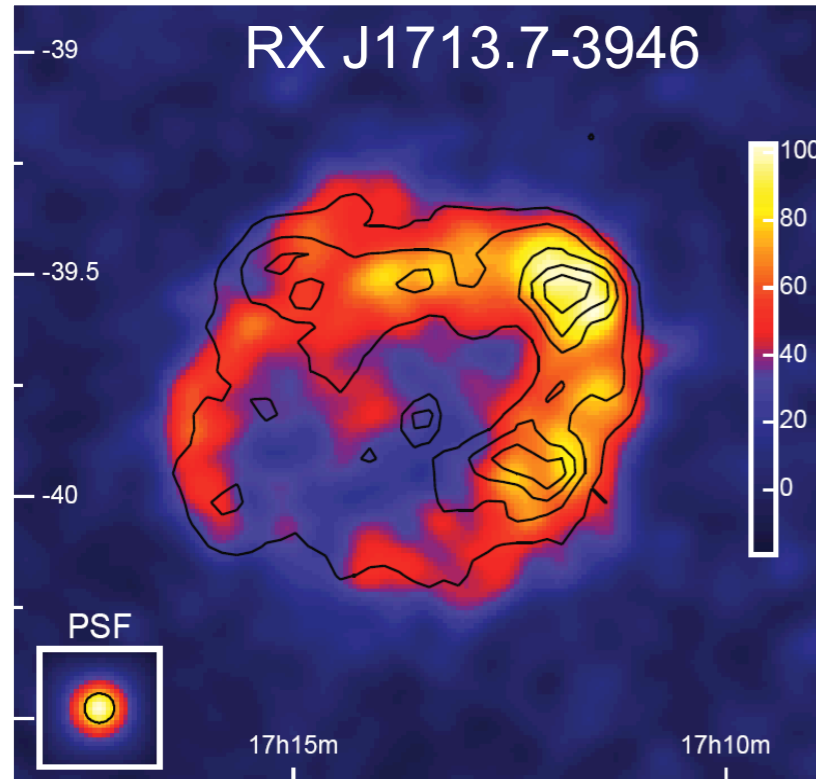
Key elements:

- high sensitivity
- high angular resolution

The H.E.S.S. Galactic Plane Survey



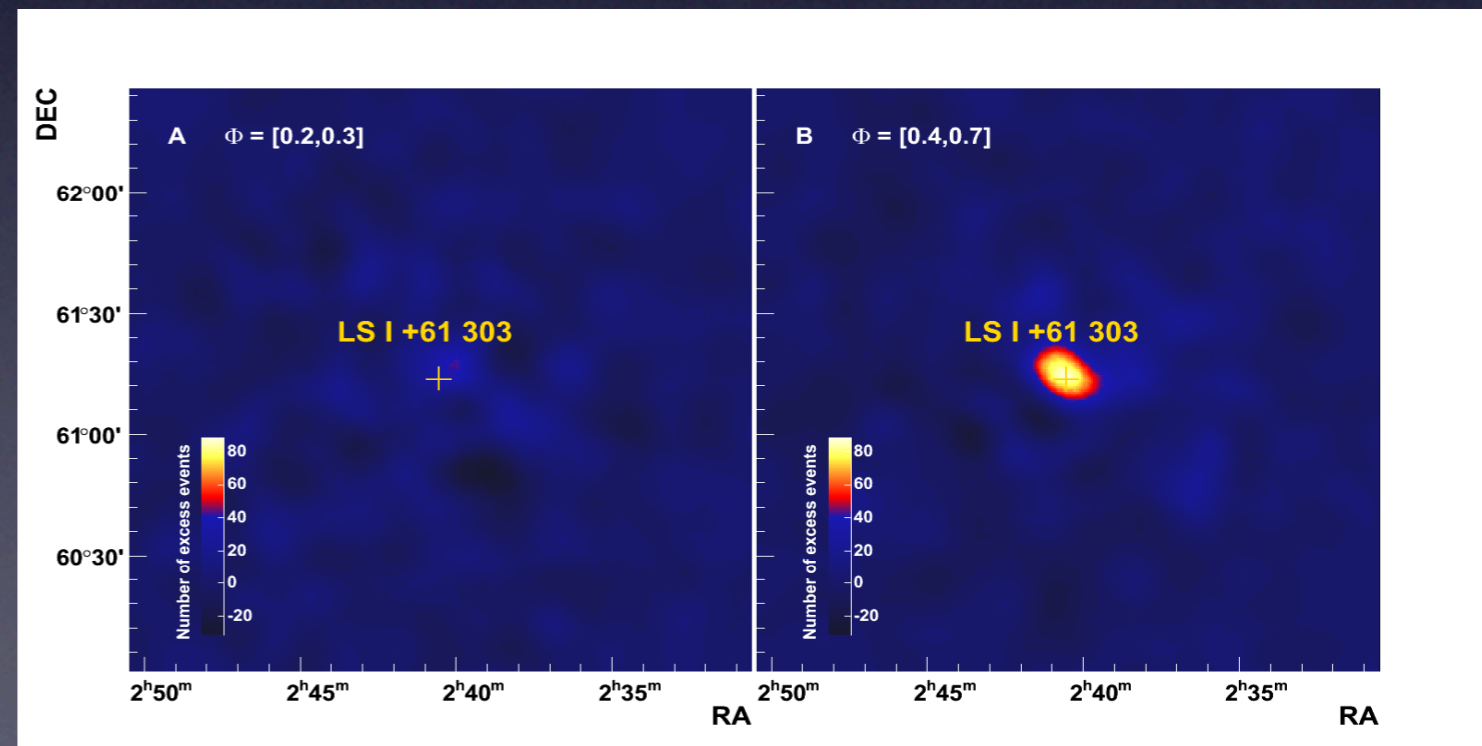
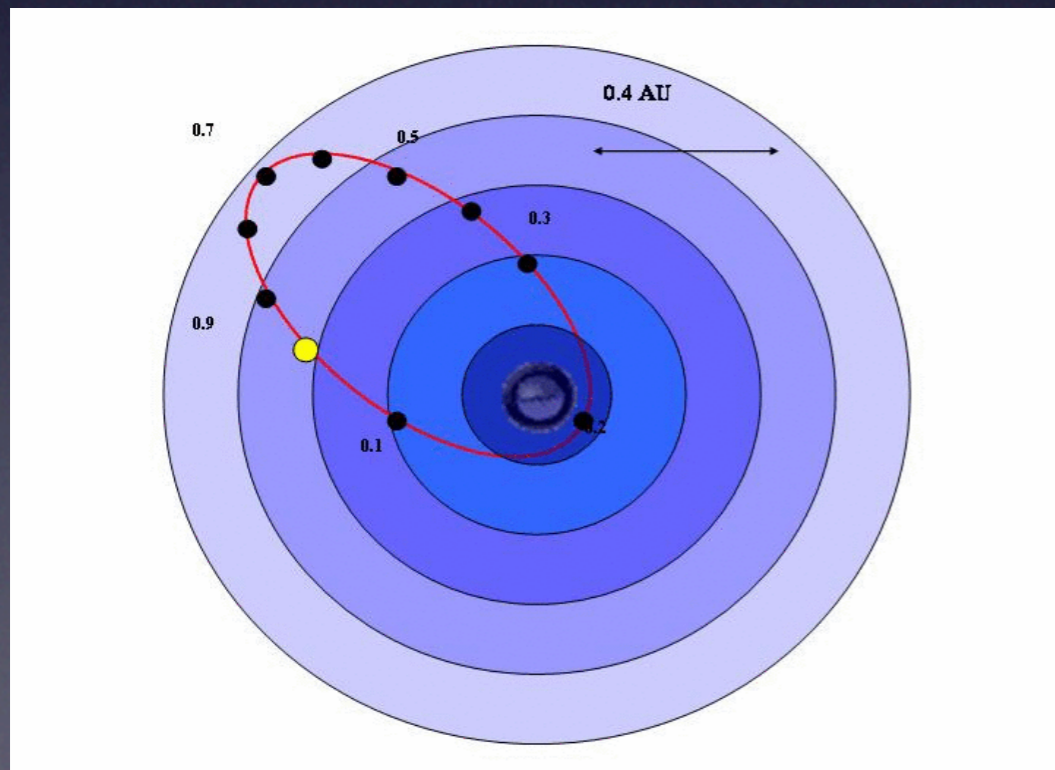
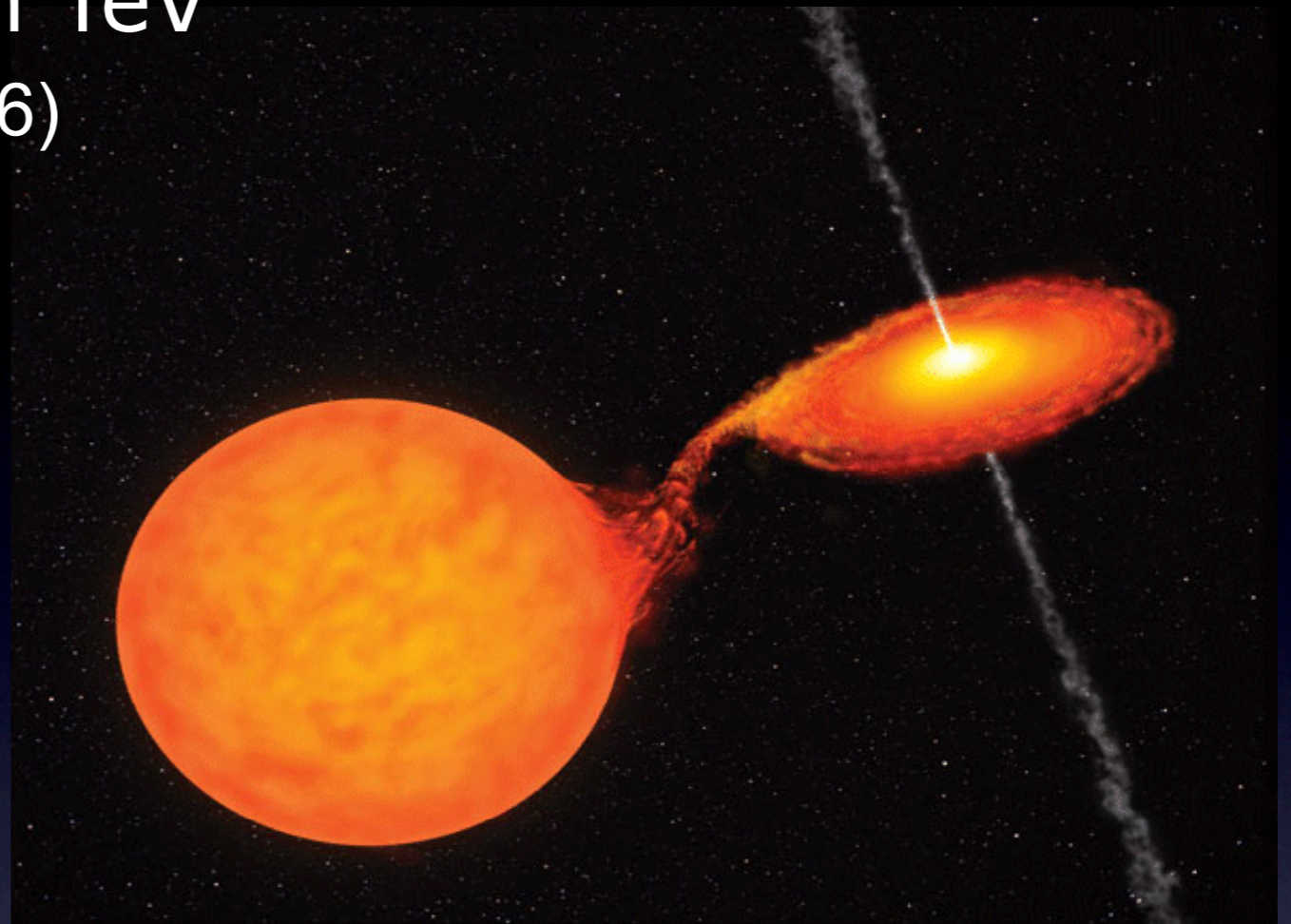
Shell-Type Supernova Remnants



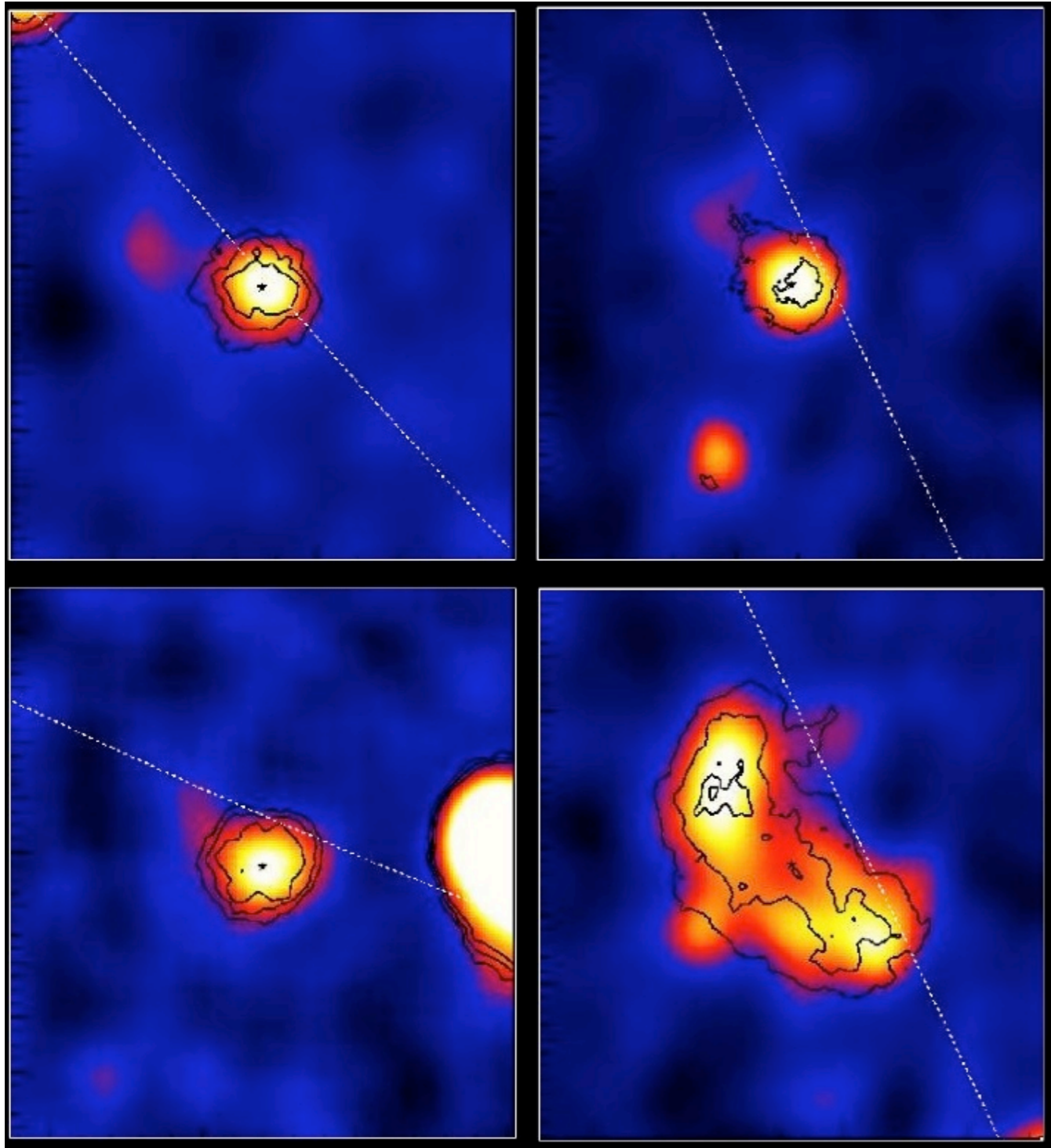
- proof of γ -ray emission SNR shells
- particle acceleration beyond 100 TeV
- H.E.S.S. Nature 2004, A&A 2006

First uQuasar observed in TeV by MAGIC (*Science*, May 2006)

“Variable Very High
Energy Gamma-Ray
Emission from the
mQSR LS I+61 303”,
Science, May 2006.



H.E.S.S. “Dark” Sources



- no counterparts in other energy bands seen
- aligned with the galactic plane
- extended (~ 10 arcmin)
- usually hard spectra ($\Gamma \sim 2.1 \dots 2.5$)
- maximum energy output in VHE γ -rays?
- hadron accelerators?
- old PWN?
- GRB remnants?

H.E.S.S. A&A, 477 (2008)

Rapid variability

astro-ph/0702008
arXiv:0708.2889

MAGIC, Mkn 501
Doubling time ~ 2 min

HESS PKS 2155

$z = 0.116$

July 2006

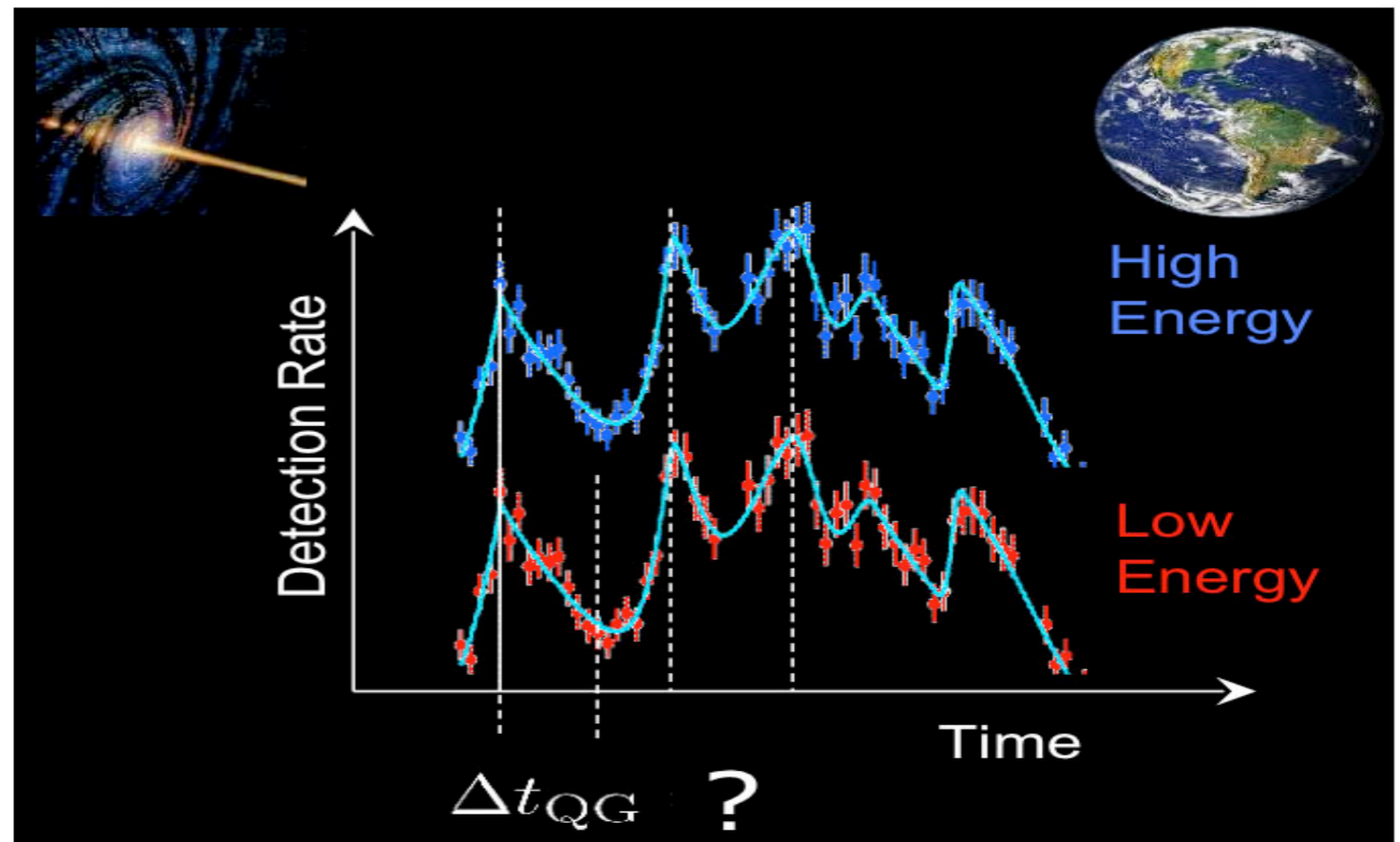
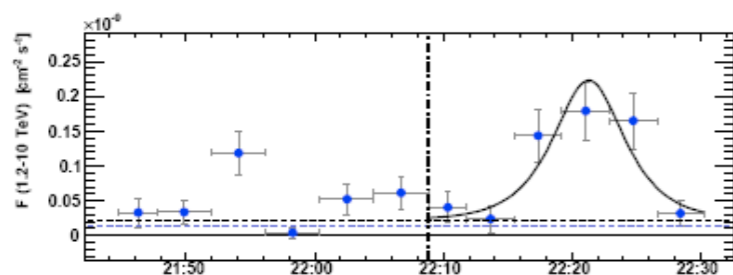
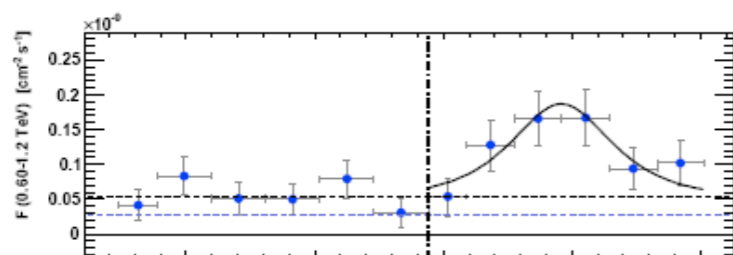
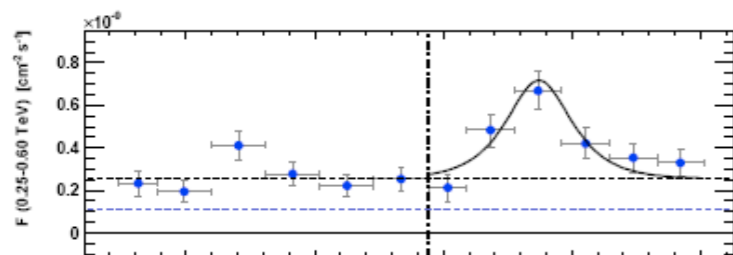
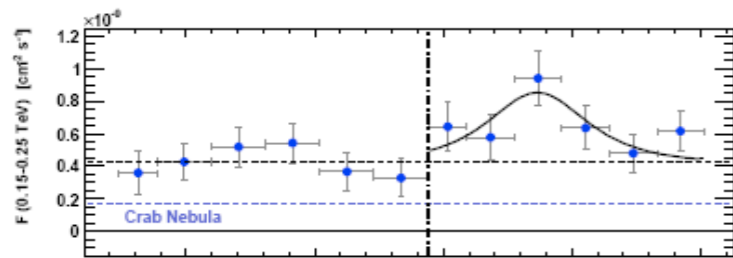
Peak flux ~ 15 x Crab
 ~ 50 x average

Doubling times
1-3 min

H.E.S.S.

arXiv:0706.0797

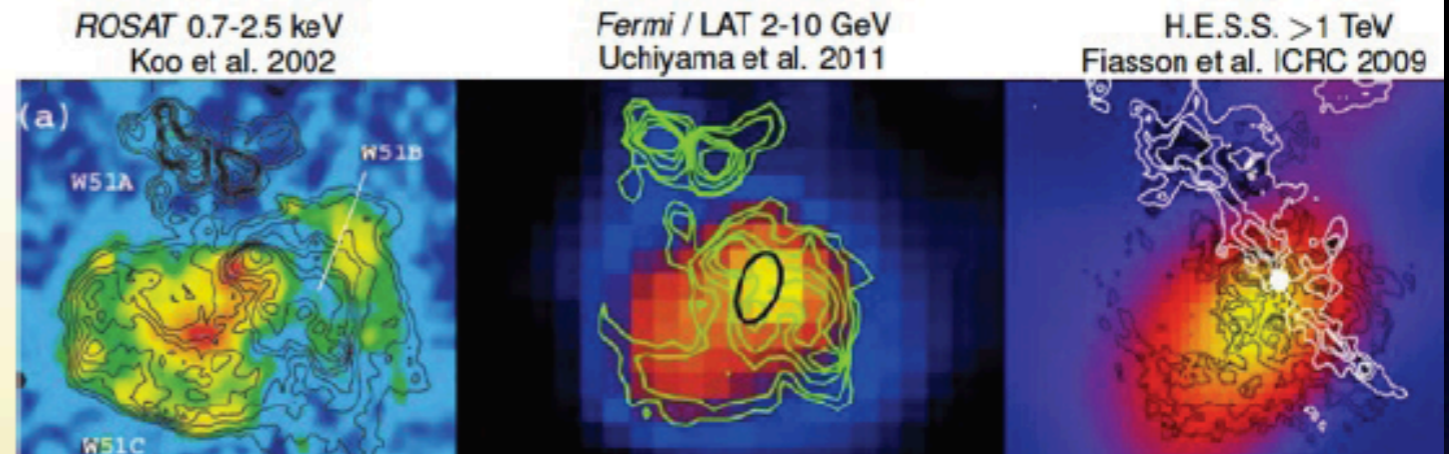
$R_{\text{BH}}/c \sim 1 \dots 2 \cdot 10^4$ s



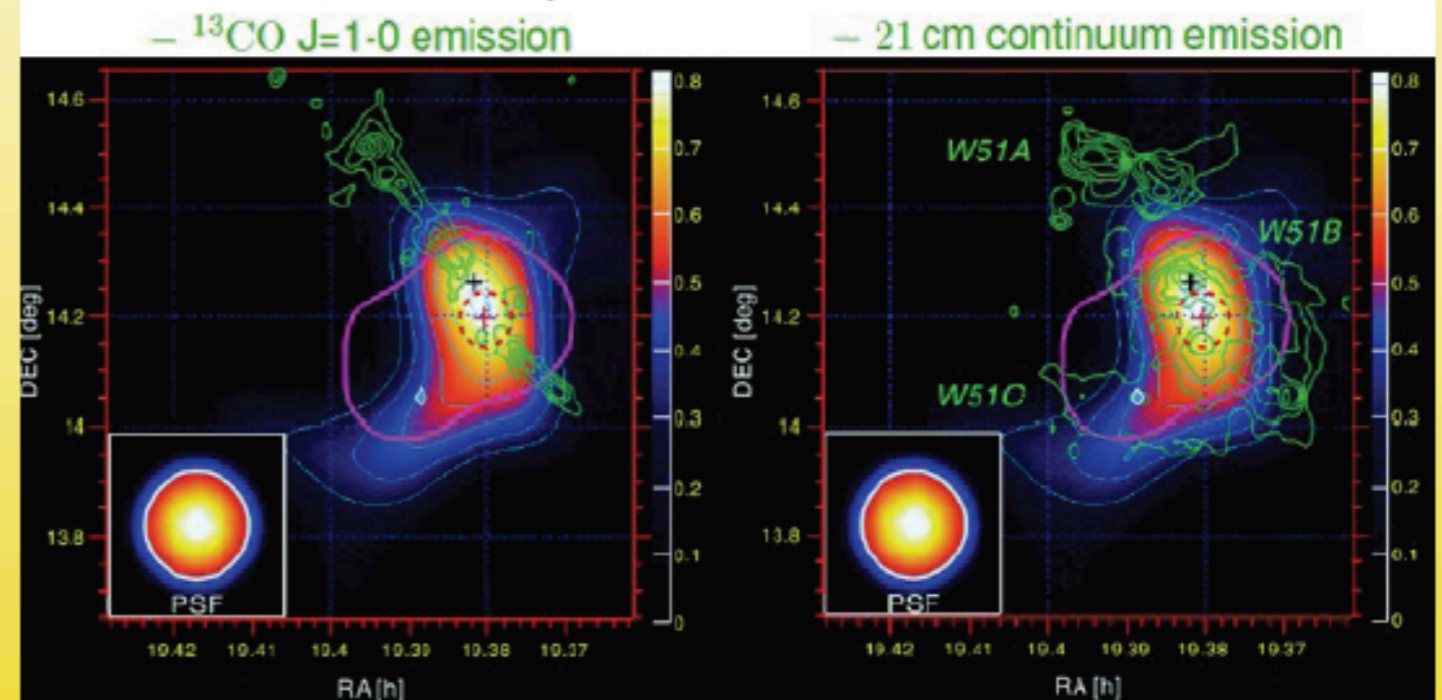
W51

Aleksic et al. (2012) A&A 541, 13

- W51C ($d \sim 5.5$ kpc) is a medium age (~ 30 kyr) supernova remnant [SNR]
- Possible Pulsar Wind Nebula associated to W51C (Koo et al. 2005)
- The SNR interacts with W51B (Koo et al. 1997a&b, Green et al. 1997)
- Discovered by Fermi-LAT (\sim GeV) and H.E.S.S. (> 1 TeV)
- High CR ionization, $\sim 100 \times$ ISM value (Ceccarelli et al. 2011)
- MAGIC stereo data taken in 2010 and 2011 (53h), 11σ signal, clearly extended

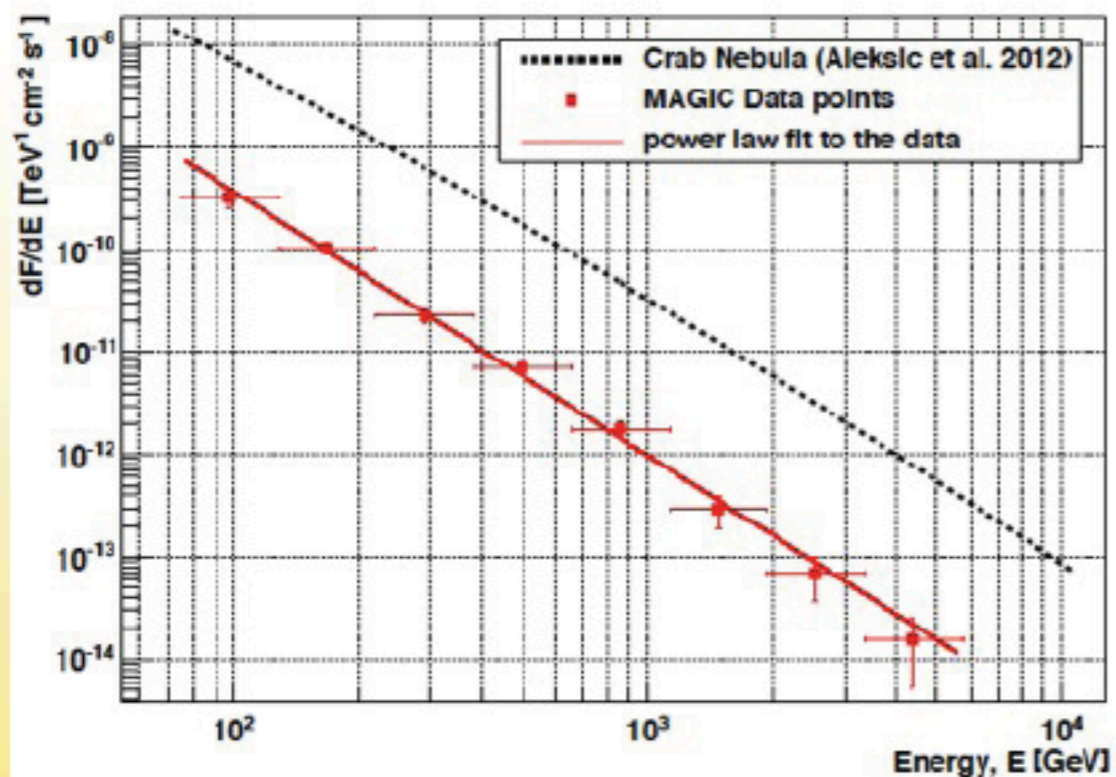


MAGIC maps in $0.3 \text{ TeV} < E < 1.0 \text{ TeV}$



The emission arises in the interaction zone between the cloud and W51C. Neither from the complete shell nor the complete cloud.

W51

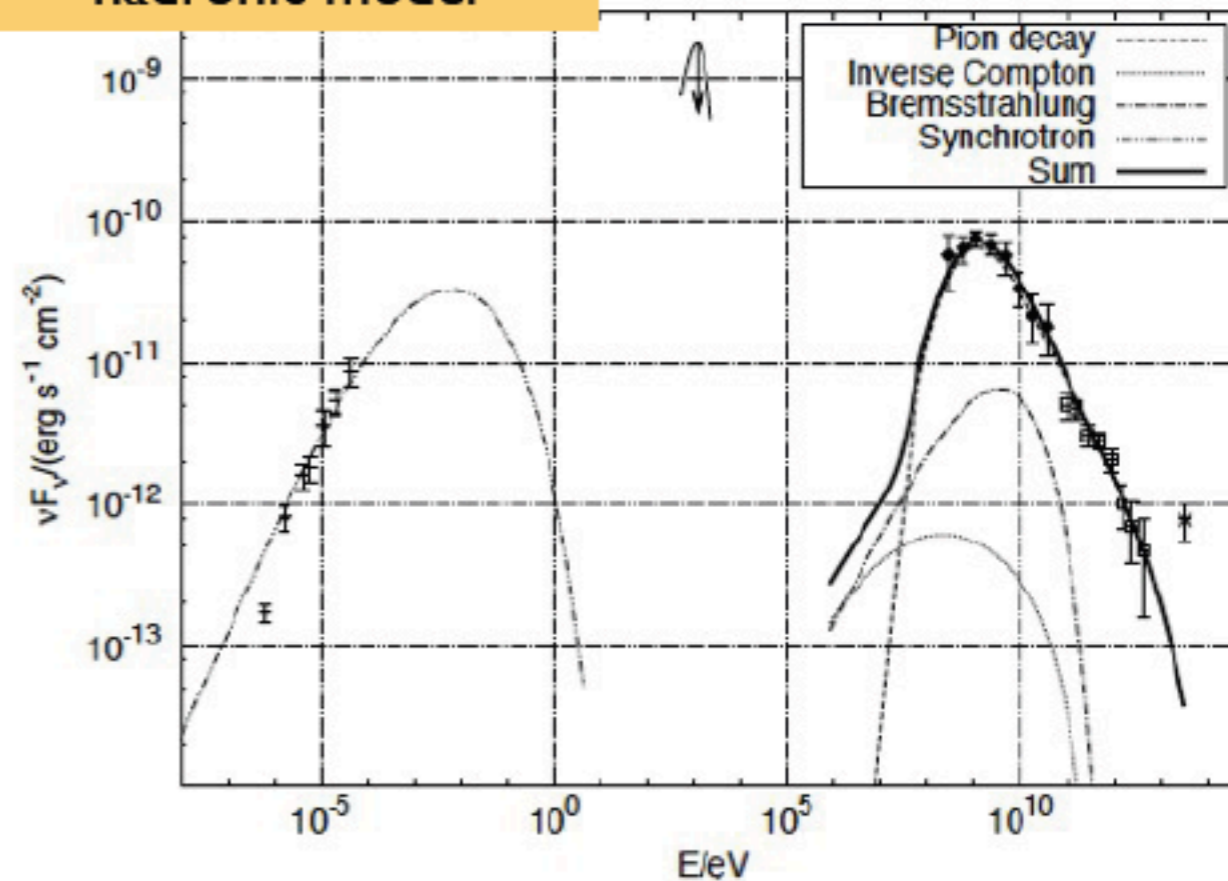


Differential energy spectrum:

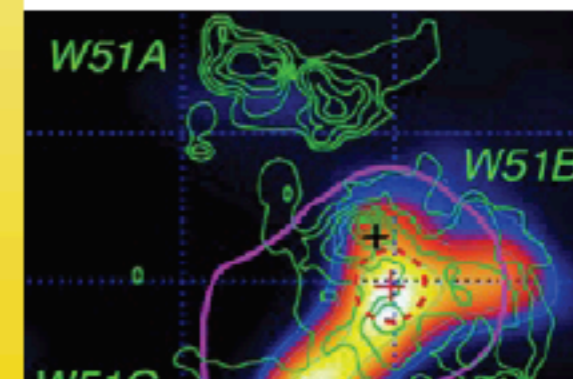
$$\frac{dF}{dE} = (9.7 \pm 1.0_{\text{stat}}) \times 10^{-13} \left(\frac{E}{\text{TeV}}\right)^{(-2.58 \pm 0.07_{\text{stat}})} [\text{TeV}^{-1} \text{cm}^{-2} \text{s}^{-1}]$$

- Emission probably hadronic (at least simple leptonic models fail)
- VHE emission from interaction zone
- Feature towards possible PWN

hadronic model



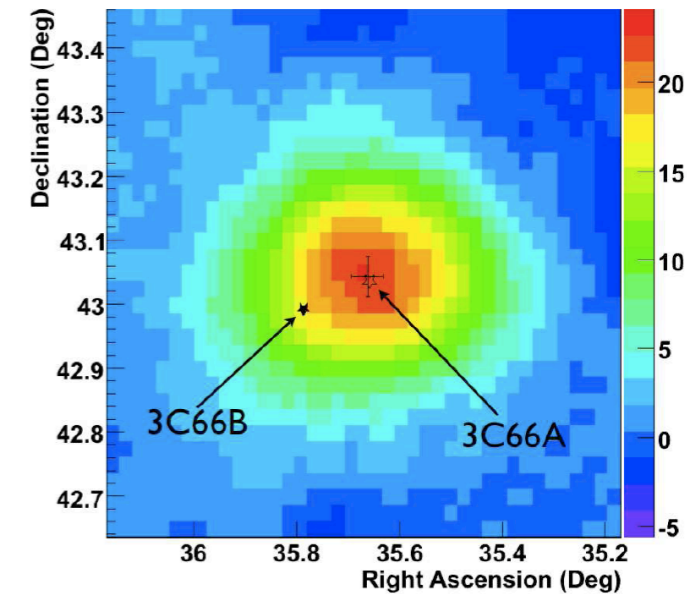
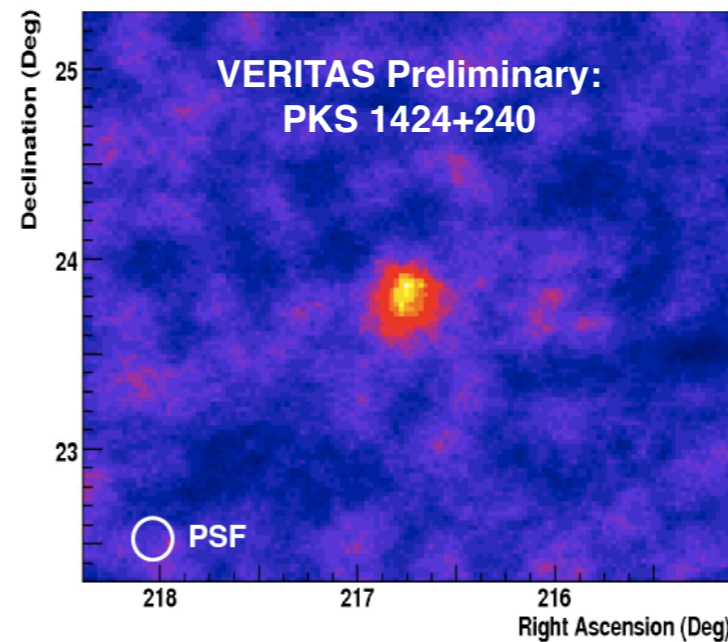
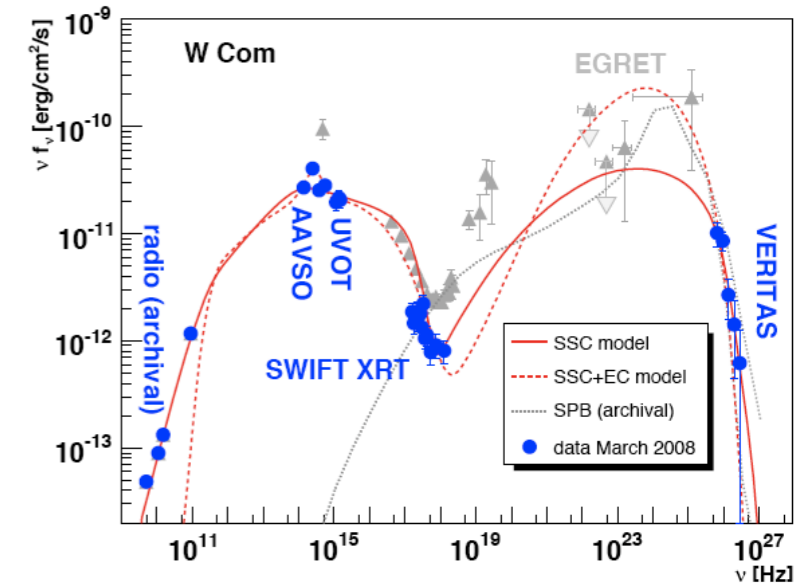
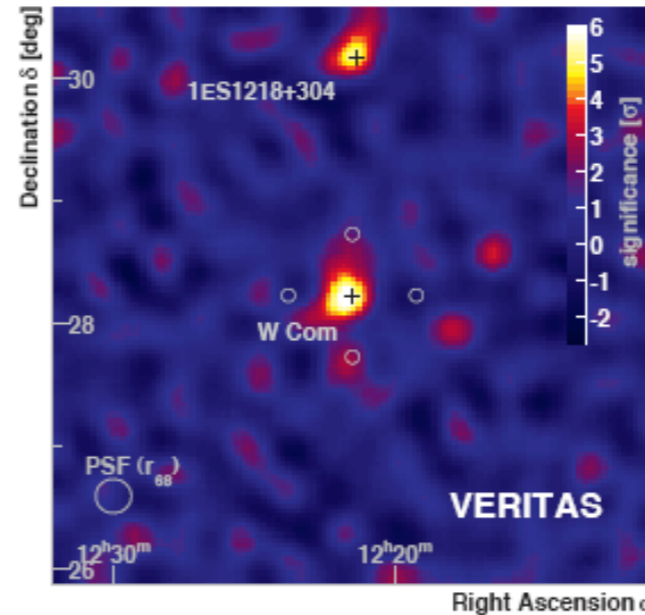
MAGIC map at E > 1.0 TeV



VERITAS Blazar Discovery Program



- Discovered 5 VHE blazars
 - First 3 IBL: Significance maps shown
 - W Comae & 3C 66A seen during flares
 - 2 HBL: Constant flux & not too distant
- Every discovery has MWL data
 - Data are contemporaneous
 - Swift, Chandra, RXTE, optical, radio
 - SSC models work for HBL, not well for IBL
 - IBL need external-Compton contribution
- Another ~50 blazars observed
 - Avg exposure of ~6 h; Avg. limit <2% Crab
 - Limits are most-constraining ever for most

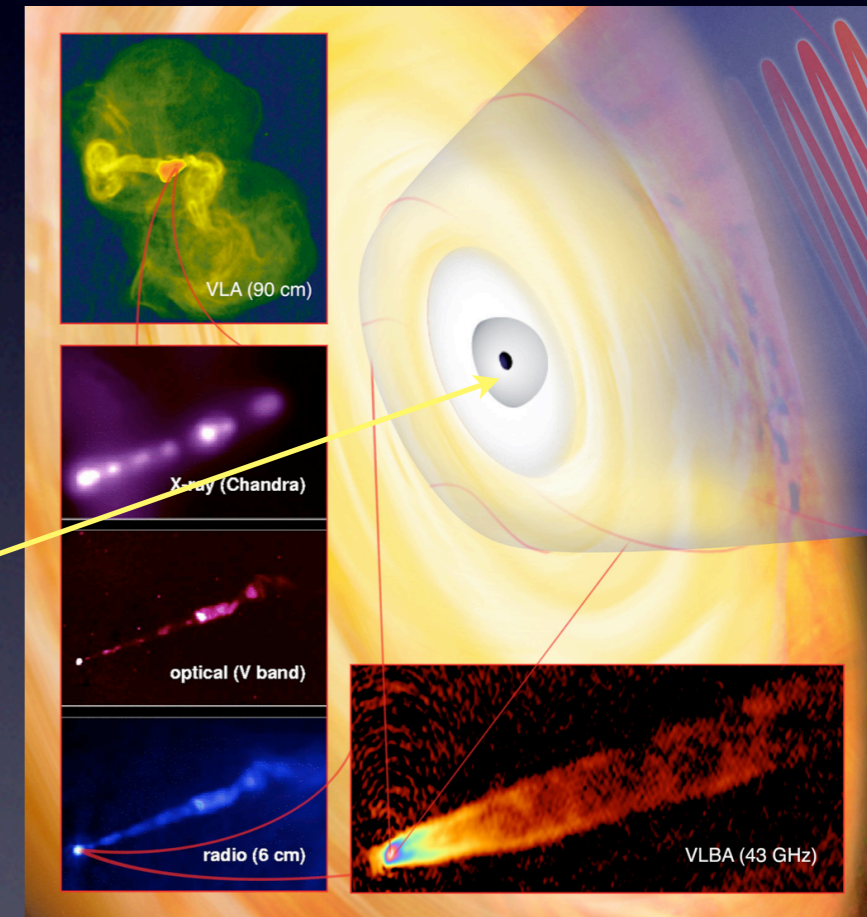
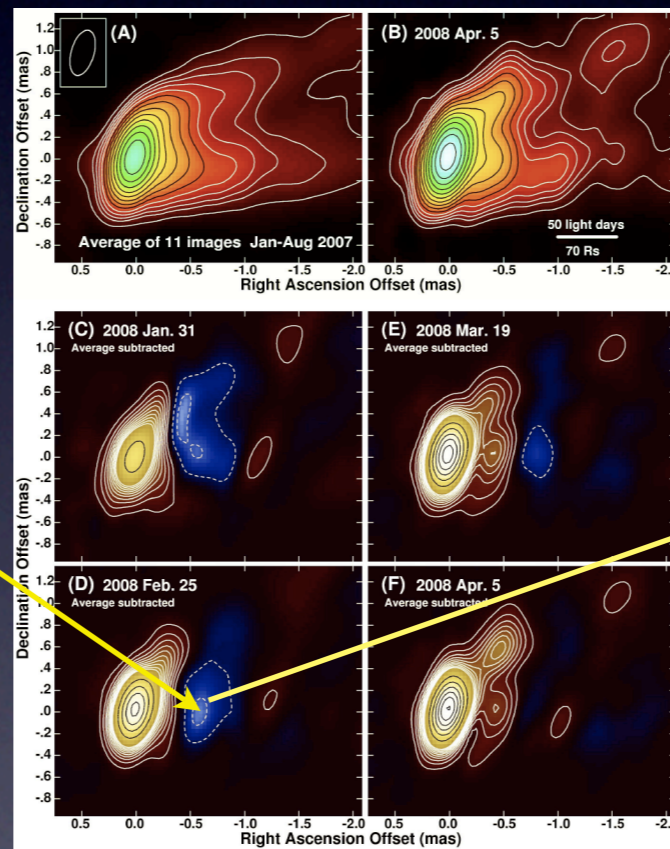
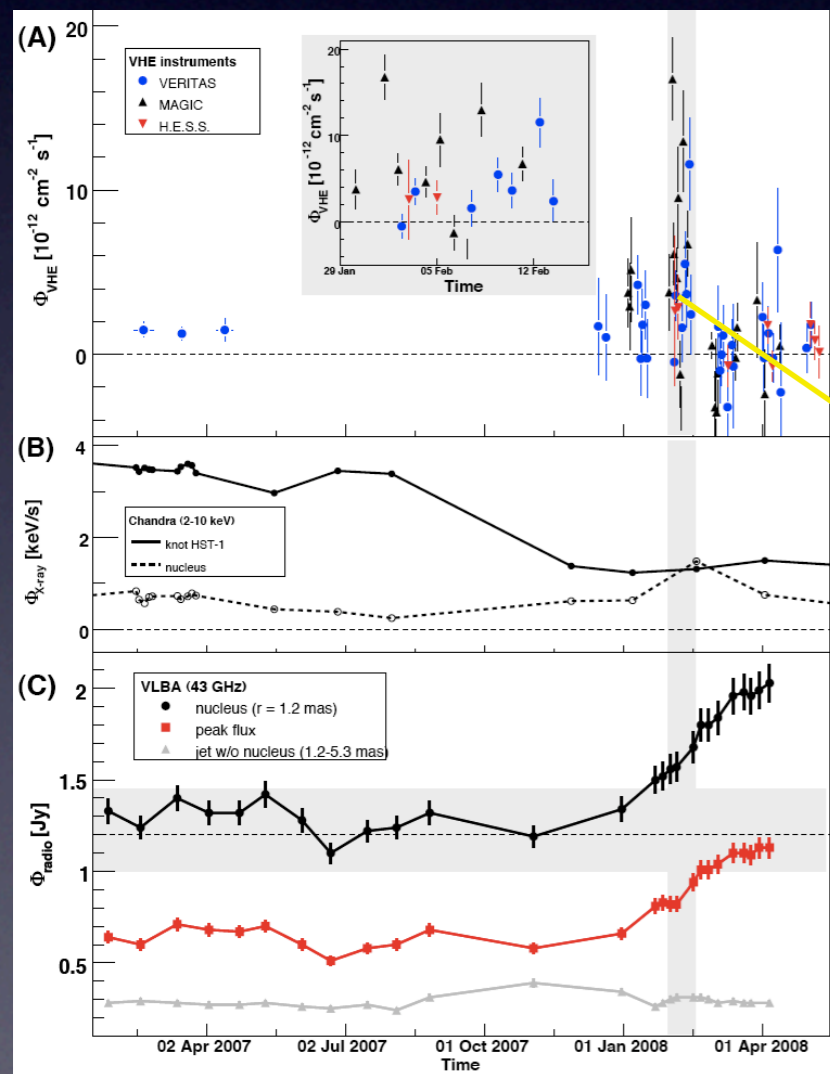
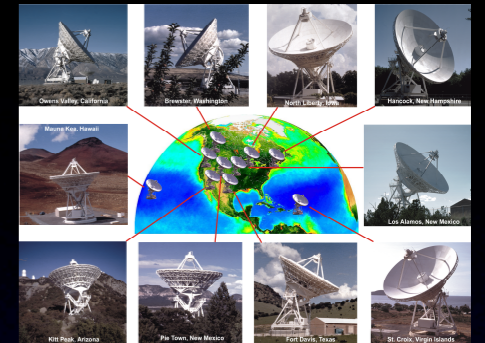


PKS 1424+240 is 1st VHE discovery triggered by Fermi-LAT results

Radio Imaging of the Very-High-Energy Gamma-Ray Emission Region in the Central Engine of a Radio Galaxy

“Combining Observations at Lowest and Highest Energies Reveals the Location of the Particle Acceleration in the Giant Radio Galaxy Messier 87”

(**Science** July 2009)



MAGIC + HESS + VERITAS + VLBA

Scientific achievements

Key elements:

- high sensitivity
- Low energy threshold

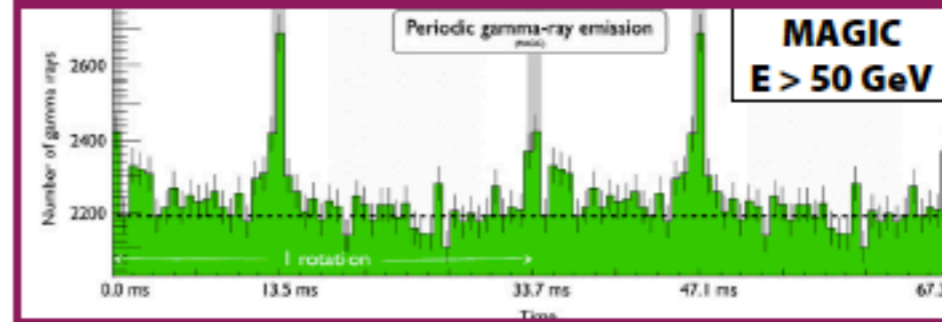
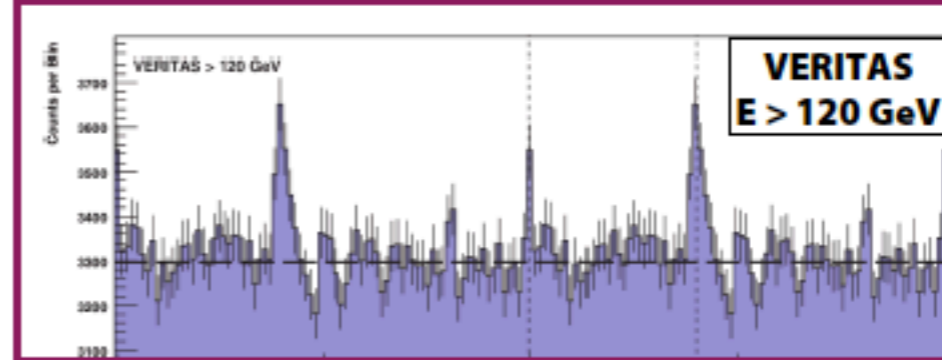
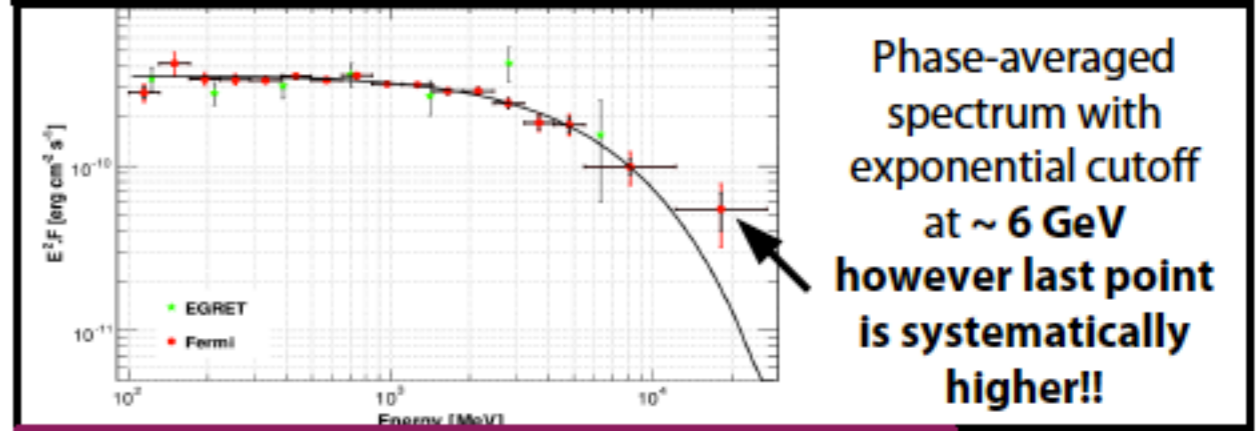
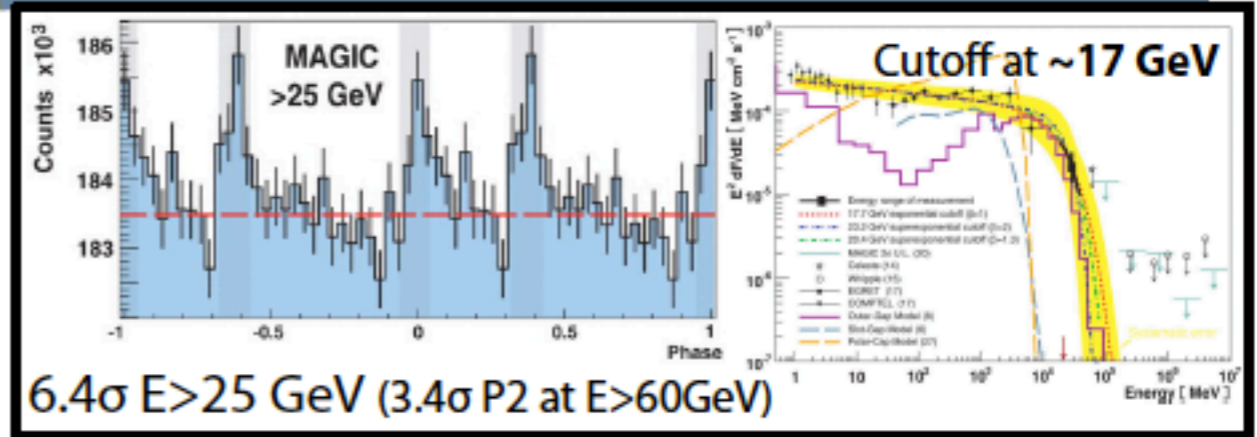
Crab Pulsar: recent VHE history

2008 – 2010:

- MAGIC (mono) discovery at $E > 25$ GeV: rules out Polar Cap model (Aliu et. al 2008, Science 322:1221) →
- Fermi-LAT: P1+P2 cutoff at $E \sim 6$ GeV, around P2 cutoff is up to $E > 10$ GeV (Abdo et. al 2010, Science 322:1221) →

2011 – 2012:

- VERITAS: pulsed emission at $E > 100$ GeV, excludes exponential cutoff (Fermi Symposium, Rome 2011, Aliu et. al 2011, Science 334:69) →
- MAGIC mono: phase-dep. spectrum $25 < E < 100$ GeV, excludes exp. cutoff (ICRC, Beijing 2011, Aleksić et. al 2011, ApJ 742:43) →
- MAGIC stereo: phase-dependent spectrum up to 400 GeV (Aleksić et. al 2012, A&A 540:A69) →



Breakthrough VHE measurements

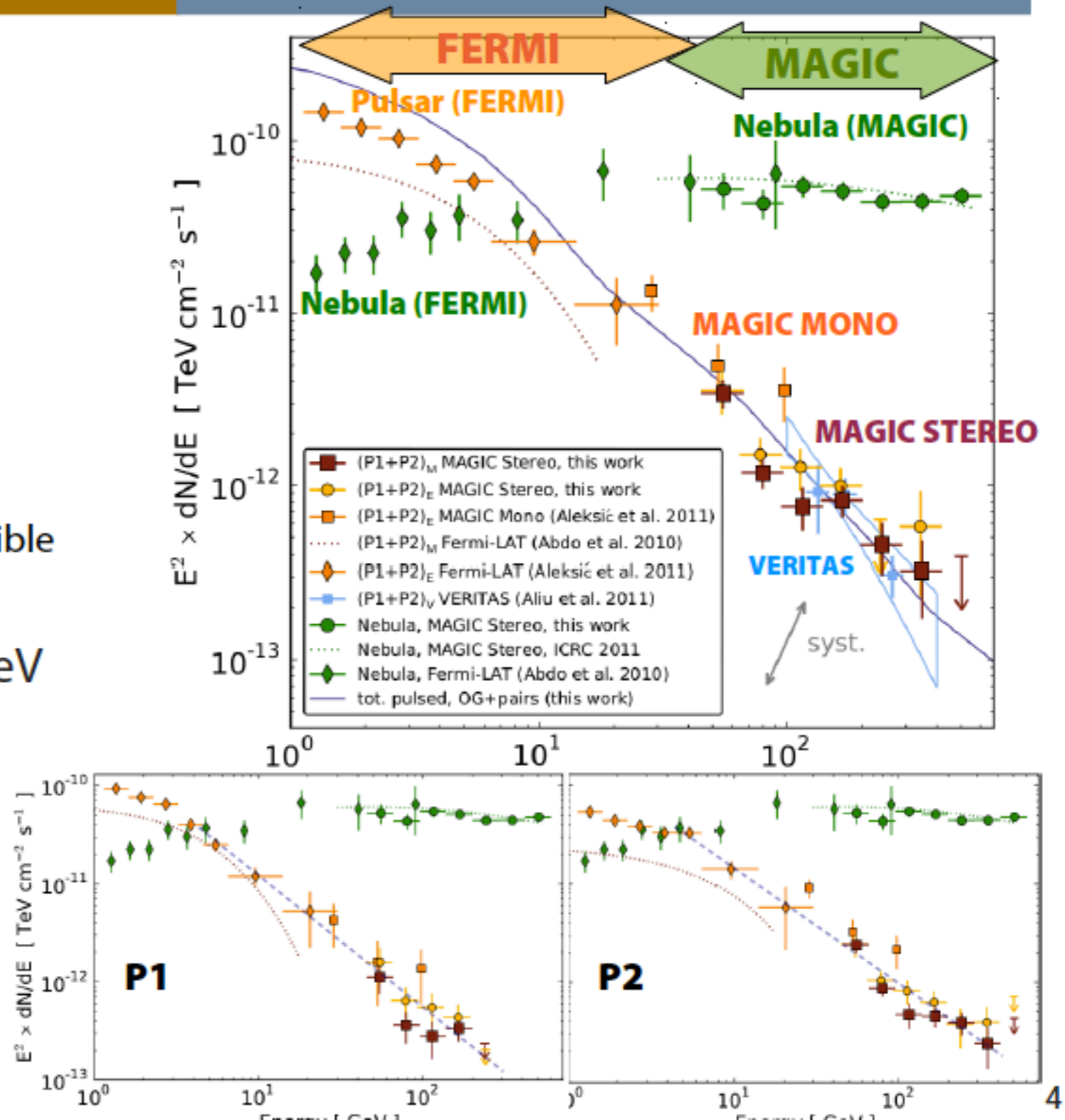
Exclude exp. cutoff hypothesis

Challenge all existing theoretical models

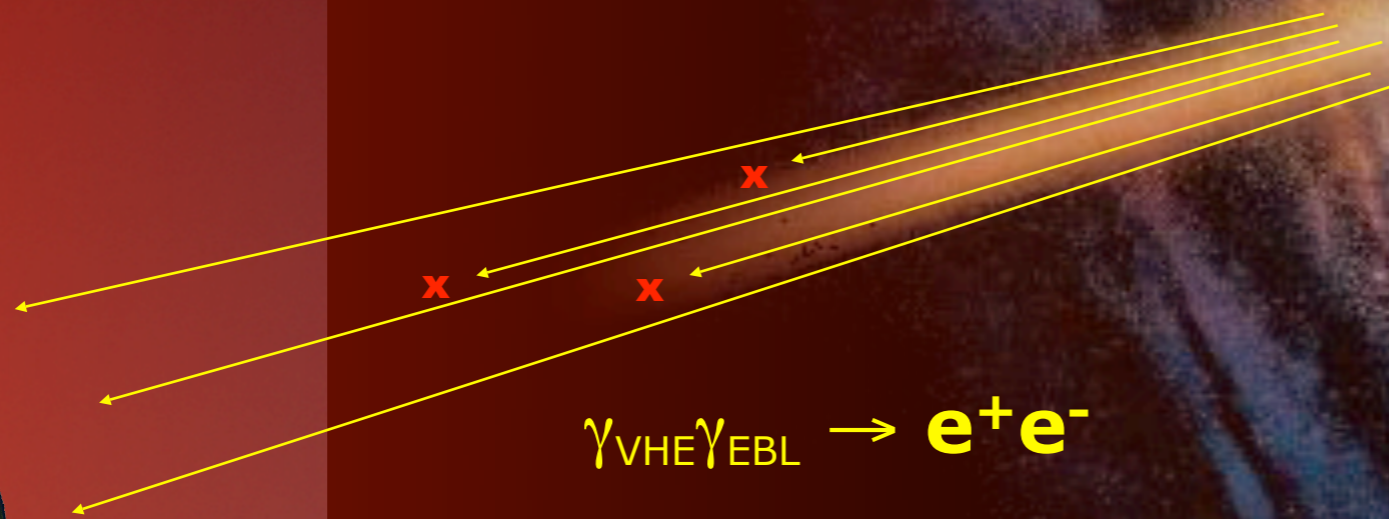
Crab Pulsar: stereo observations

- Stereo spectrum:
Power law, joins Fermi-LAT, MAGIC mono and VERITAS
- Double-check with Nebula spectrum: ok down to 50 GeV
- Phase-averaged index :

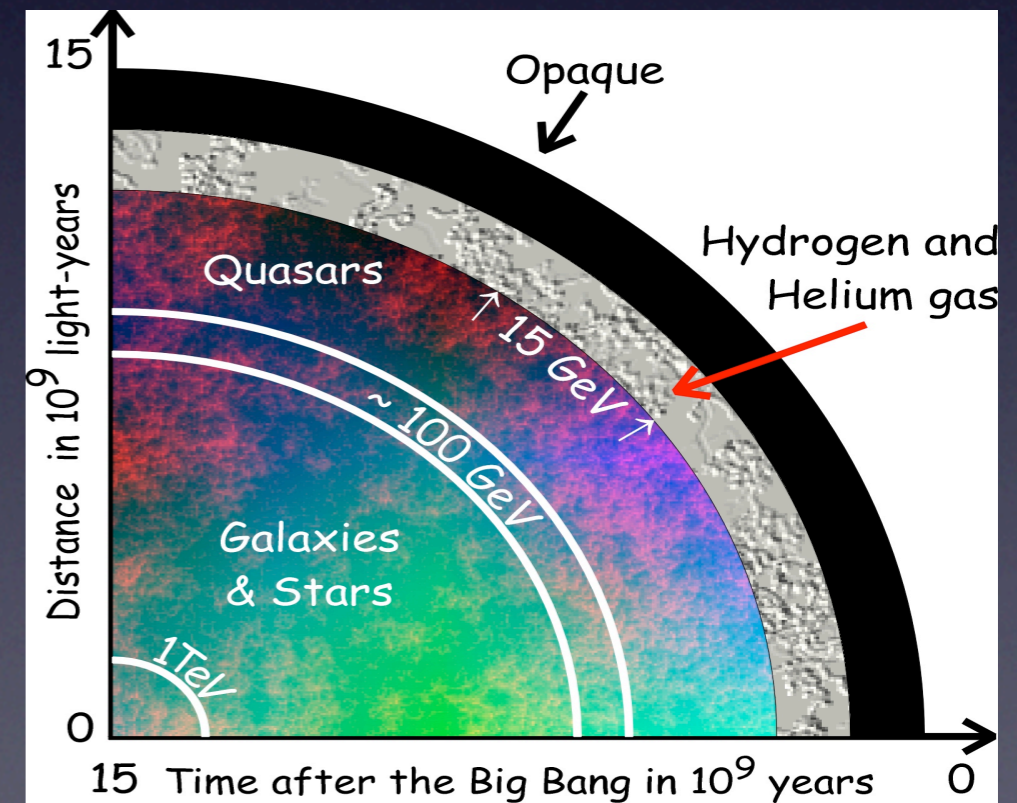
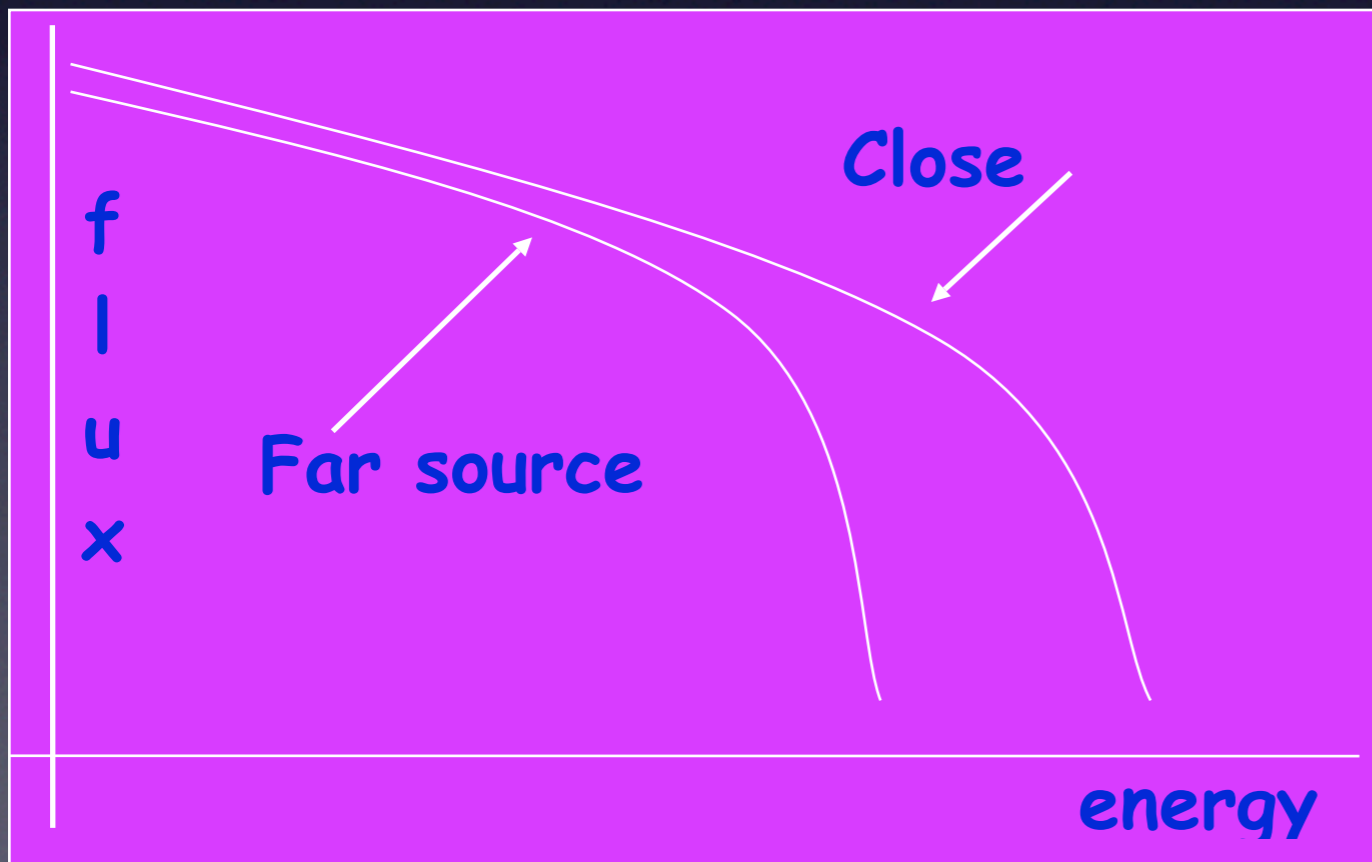
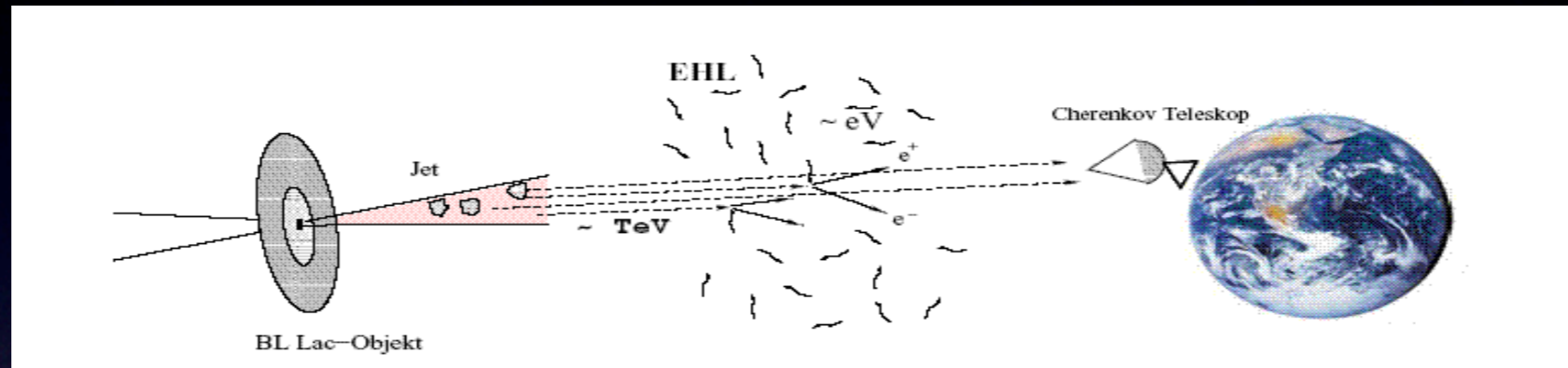
P1+P2	: $\Gamma = -3.6 \pm 0.3$	}	Compatible
P1	: $\Gamma = -4.0 \pm 0.8$		
P2	: $\Gamma = -3.4 \pm 0.3$		
- P1/P2 ratio $\sim 0.4 \pm 0.2$ at 100 GeV
- No significant yearly variability
- Systematic uncertainties:
17% energy scale
19% flux normalization
0.2 photon index



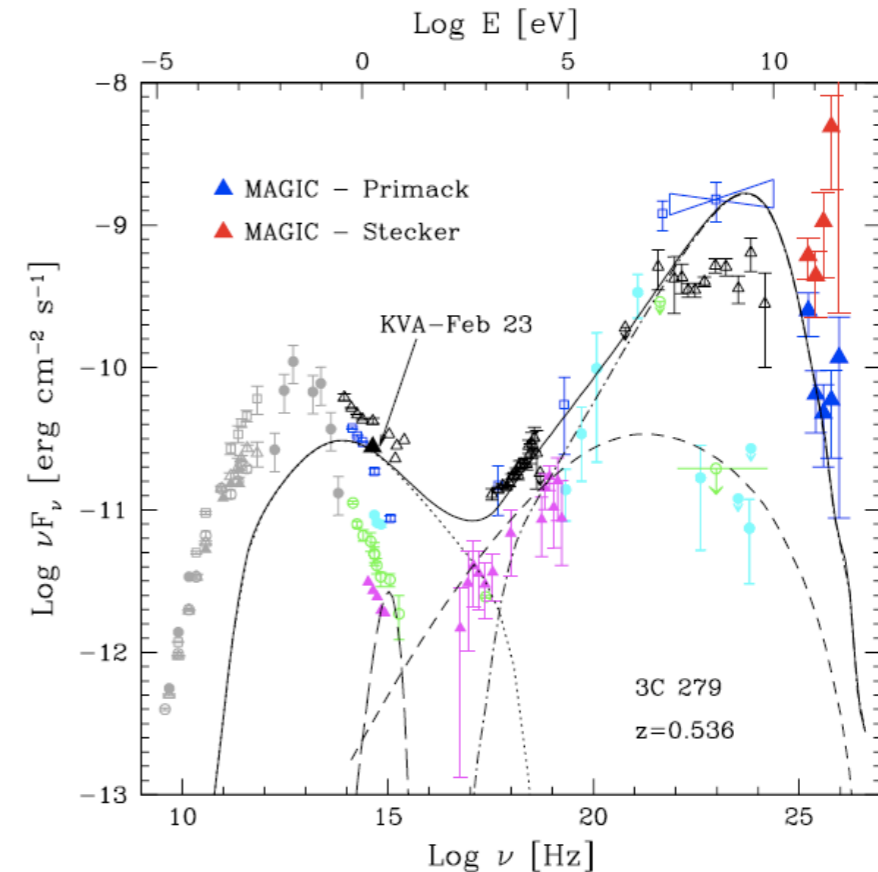
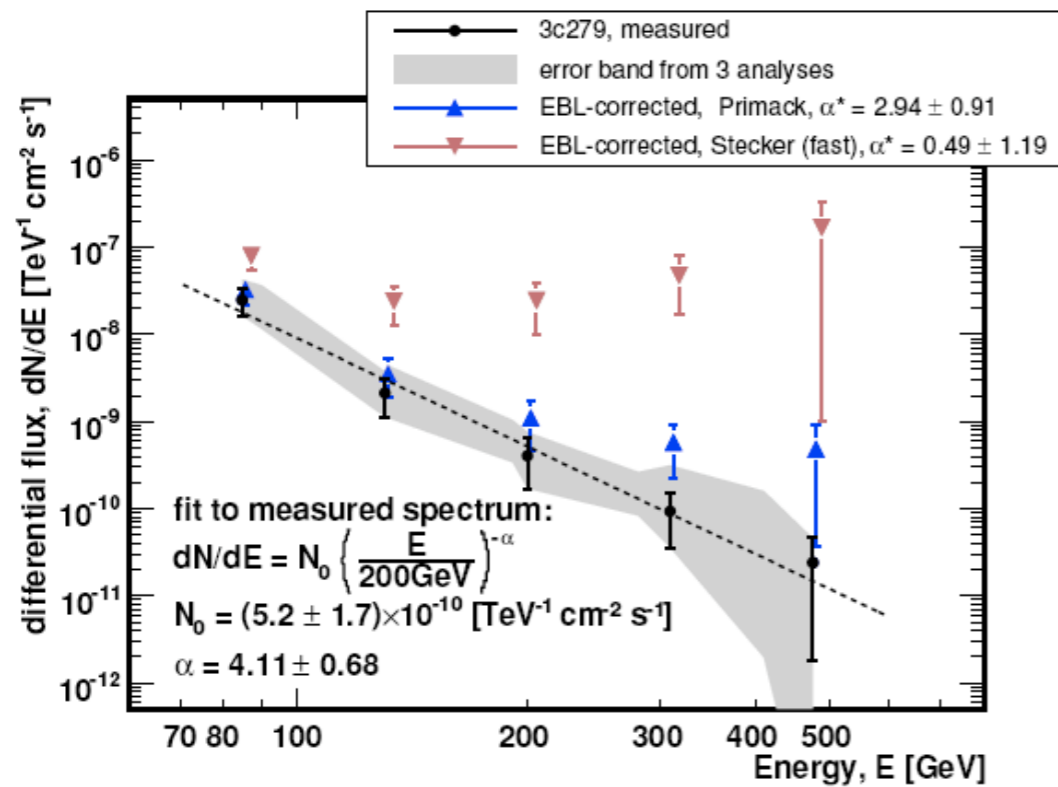
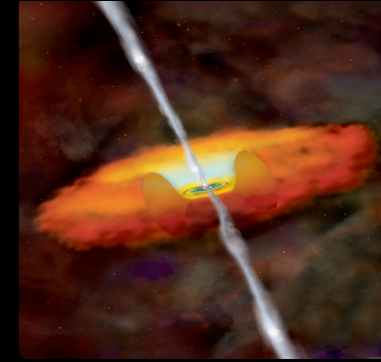
Extragalactic sources and EBL



Pair Creation; $\gamma_{HE} + \gamma_{EBL} \rightarrow e^+ + e^-$

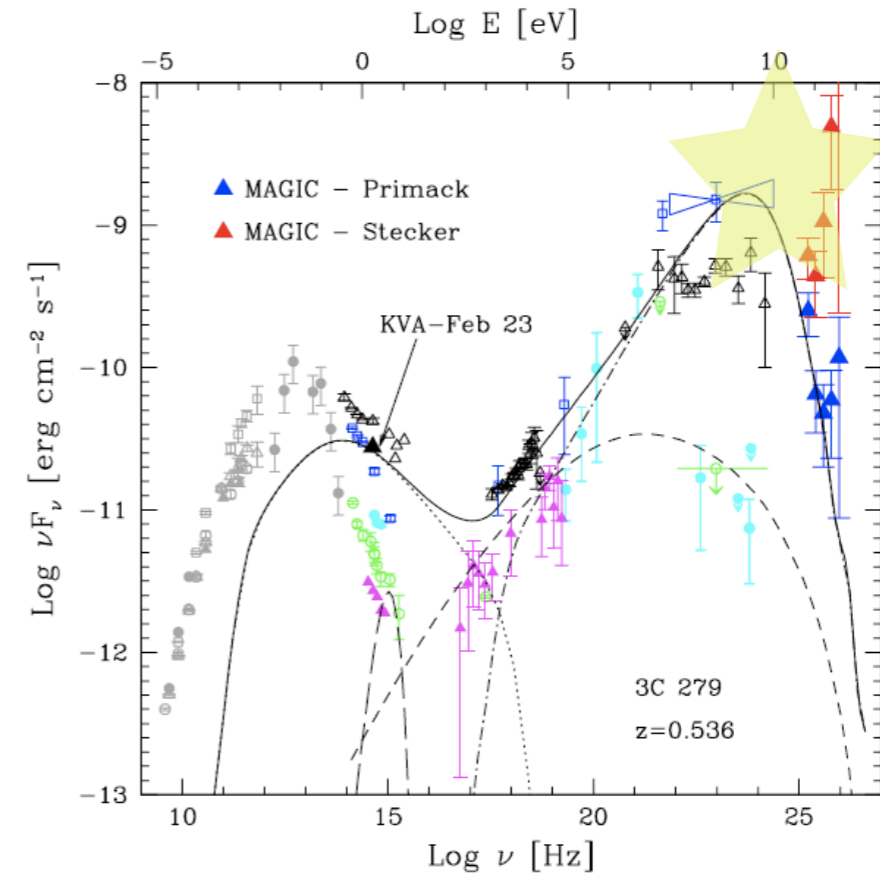
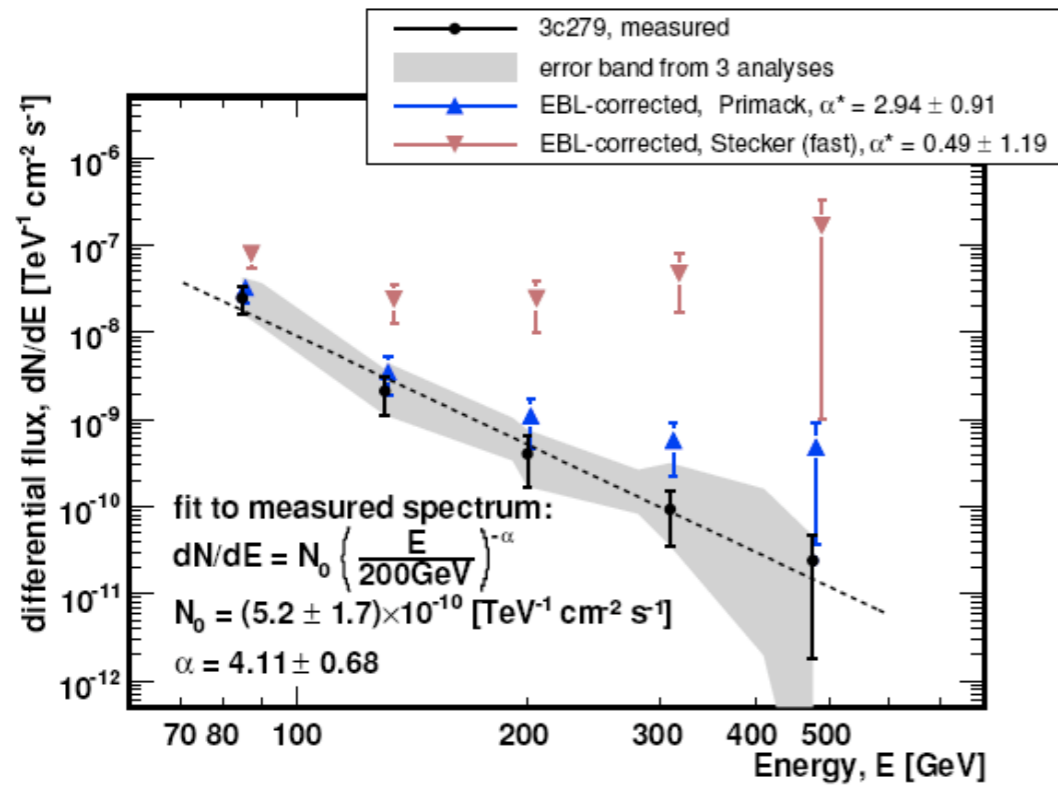
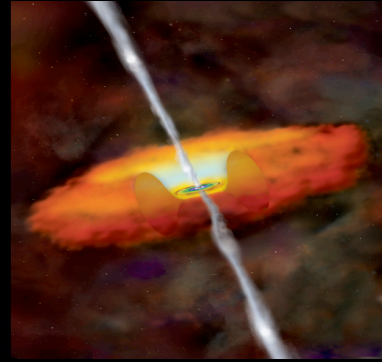


3C279 observation by MAGIC (science 2007)



By unfolding the EBL extinction => the only consistent explanation with quasar model is compatible with EBL ~ **lower limits of galaxy count**

3C279 observation by MAGIC (science 2007)



By unfolding the EBL extinction => the only consistent explanation with quasar model is compatible with EBL ~ **lower limits of galaxy count**

EBL seen by HESS

Large gamma ray dataset from 3 source at different redshift:

By evaluating the extinction factor as a function of energy it is possible to “see” the Extragalactic Background Light

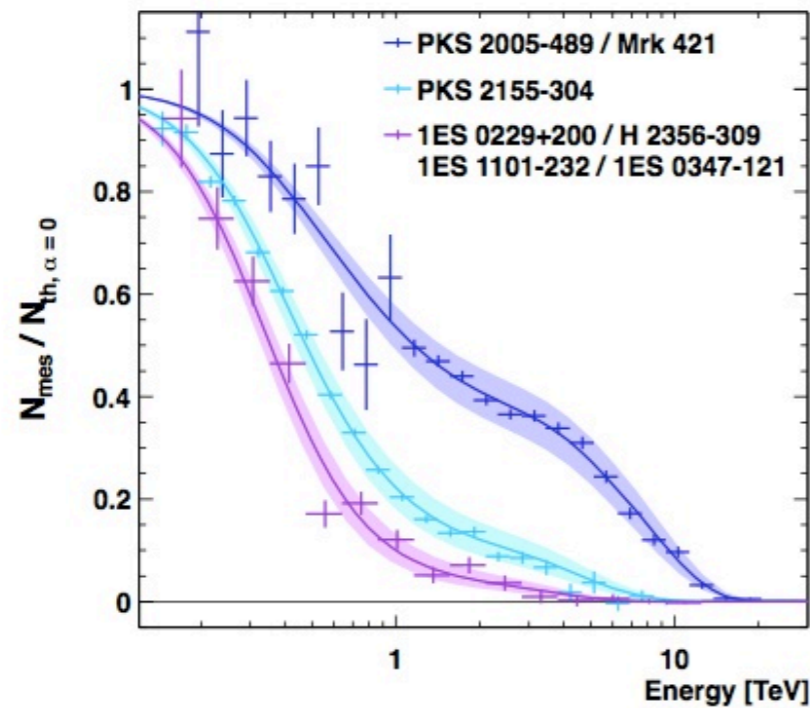


Fig. 2: Observed number of gamma-rays over number expected from the source spectra, vs. gamma-ray energy. The data sets are grouped by similar redshift: $z \sim 0.03-0.07$ (blue), $z \sim 0.12$ (green) and $z \sim 0.14-0.19$ (red), and show the attenuation at high energies increasing both with redshift and with energy. The best-fit EBL absorption is shown by the colored bands.

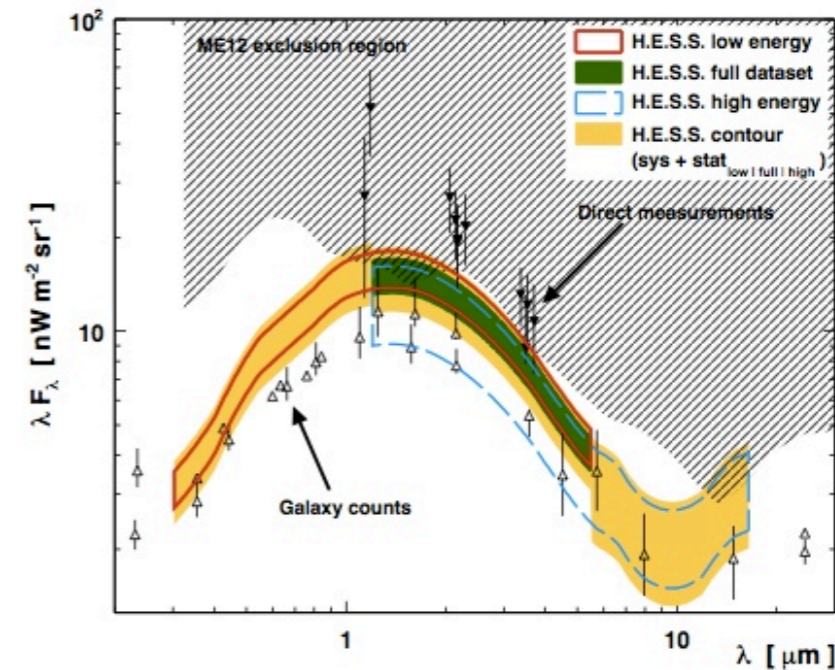
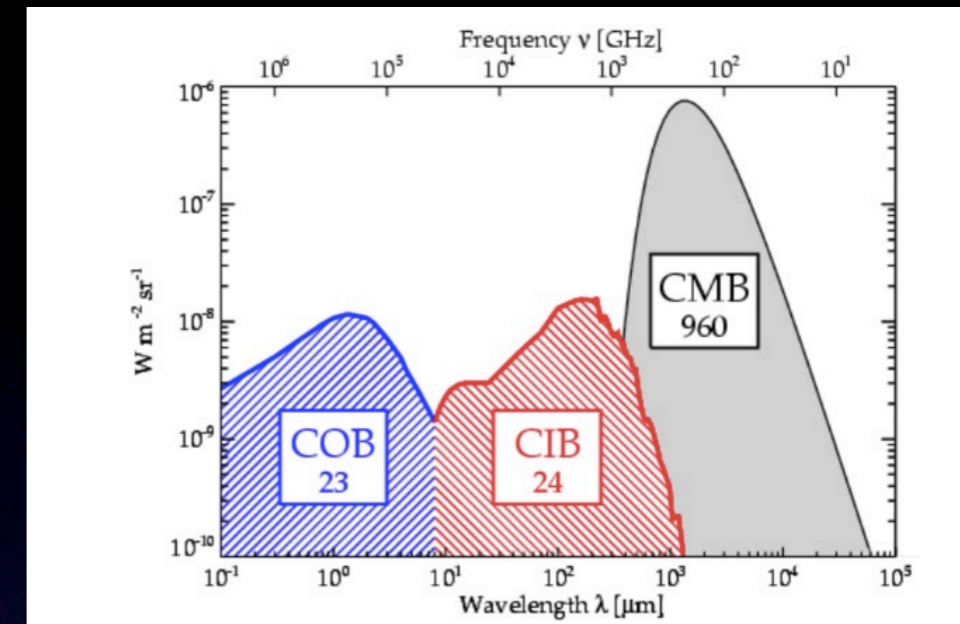


Fig. 3: Flux density of the extragalactic background light versus wavelength. The colored regions indicate the intensity levels required to match the H.E.S.S. blazar data, covering the optical bump and extending into the near infrared.

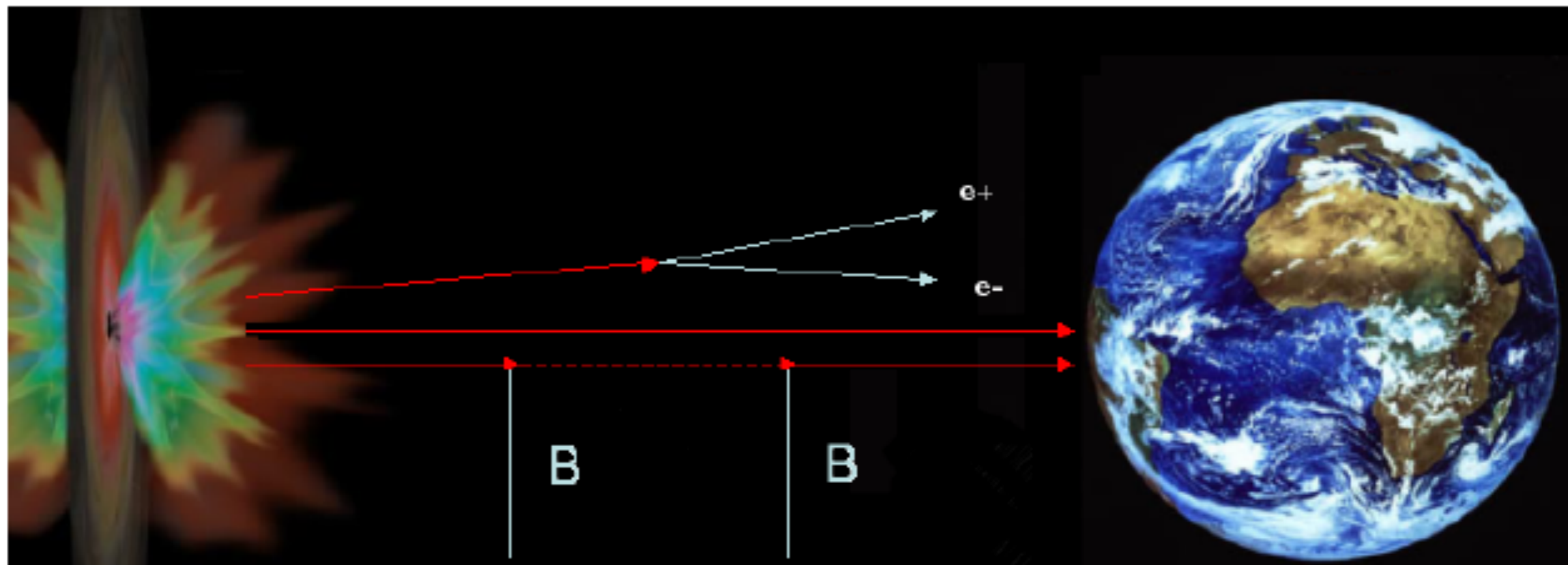
“NATURAL” WAY OUT

- photons might oscillate into a very light spin-0 neutral pseudo-scalar boson X in the presence of an external magnetic field \mathbf{B} , interacting with γ through the Lagrangian:

$$\mathcal{L} = \frac{1}{4M} F^{\mu\nu} \tilde{F}_{\mu\nu} \varphi = \frac{1}{M} \mathbf{E} \cdot \mathbf{B} \varphi$$

where φ stands for the X field.

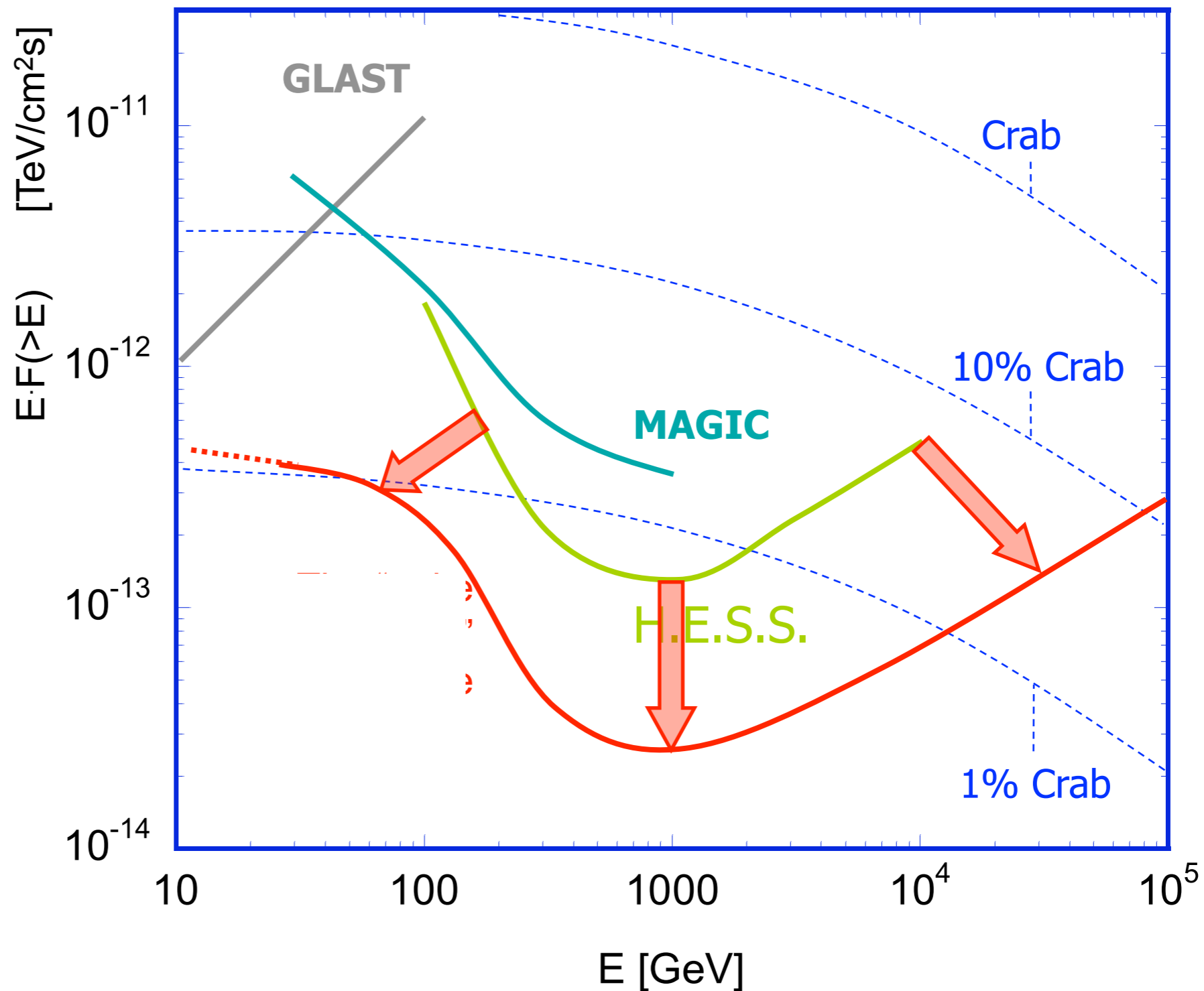
- X travels unimpeded in the EBL



The new generation of gamma ray ground based experiments

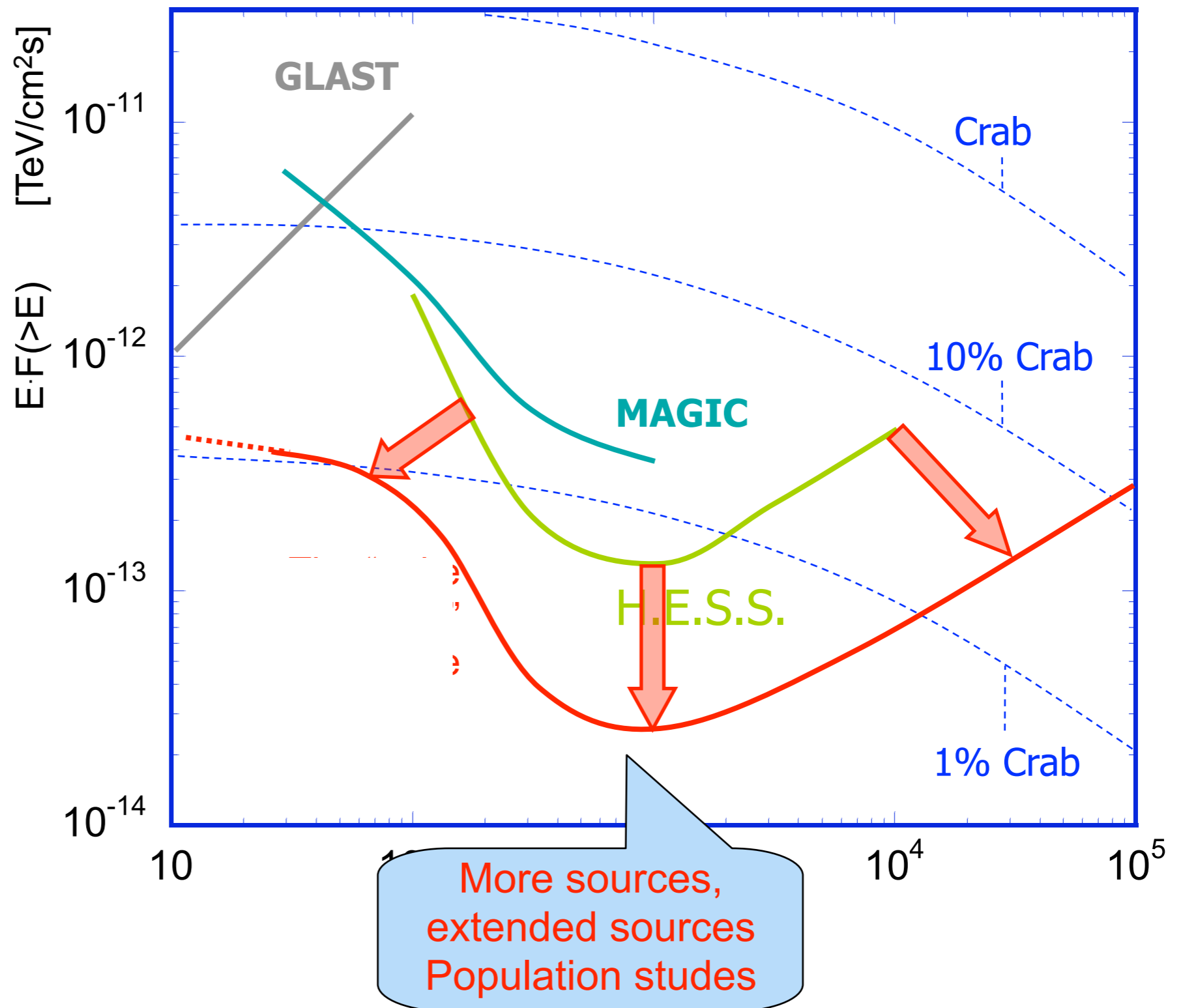


NEXT GENERATION CHERENKOV TELESCOPES.... WHISH LIST



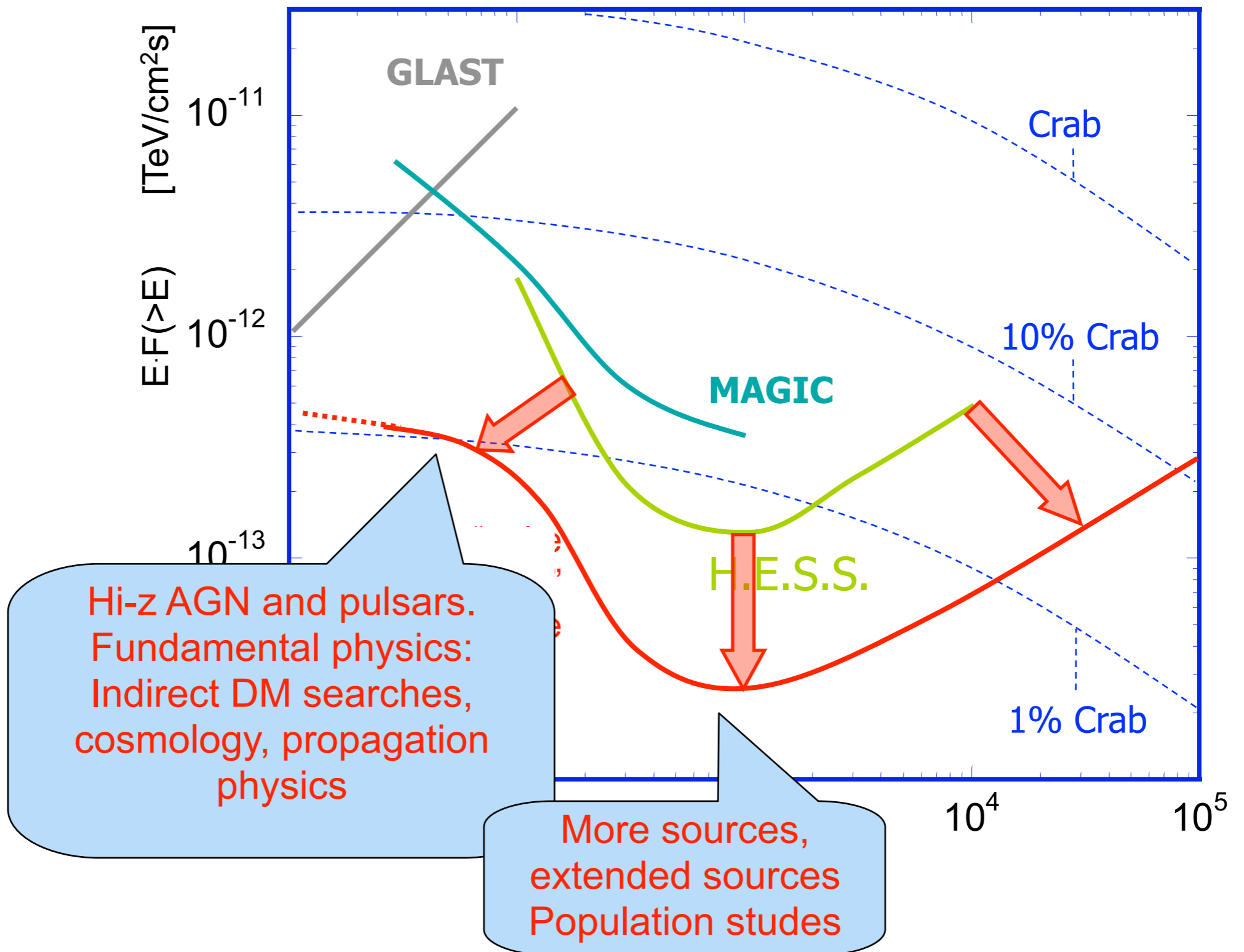


NEXT GENERATION CHERENKOV TELESCOPES.... WHISH LIST



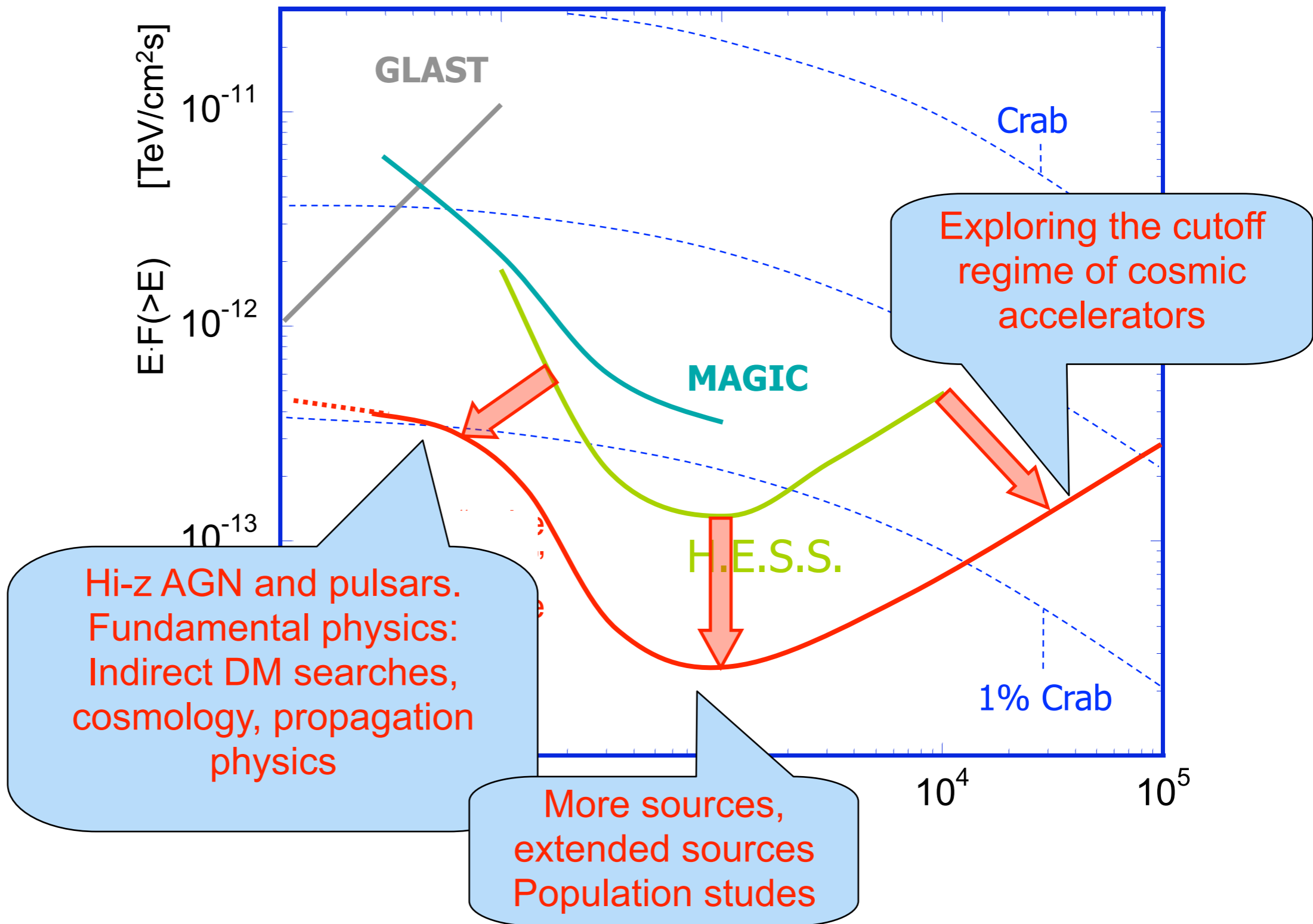


NEXT GENERATION CHERENKOV TELESCOPES.... WHISH LIST





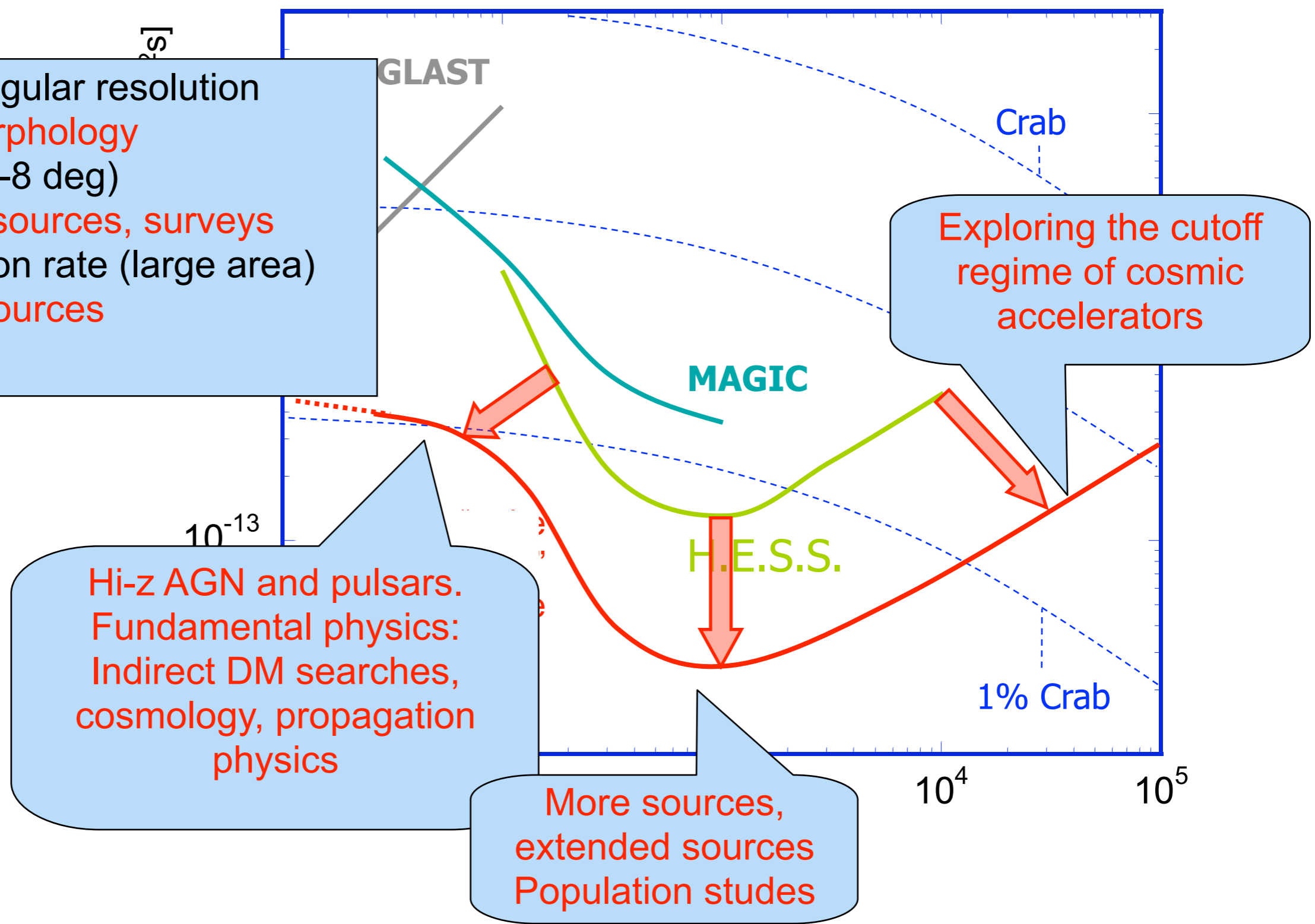
NEXT GENERATION CHERENKOV TELESCOPES.... WHISH LIST





NEXT GENERATION CHERENKOV TELESCOPES.... WHISH LIST

- Improved angular resolution
source morphology
- large FoV (6-8 deg)
extended sources, surveys
- High detection rate (large area)
transient sources



Hi-z AGN and pulsars.
Fundamental physics:
Indirect DM searches,
cosmology, propagation
physics

More sources,
extended sources
Population studies

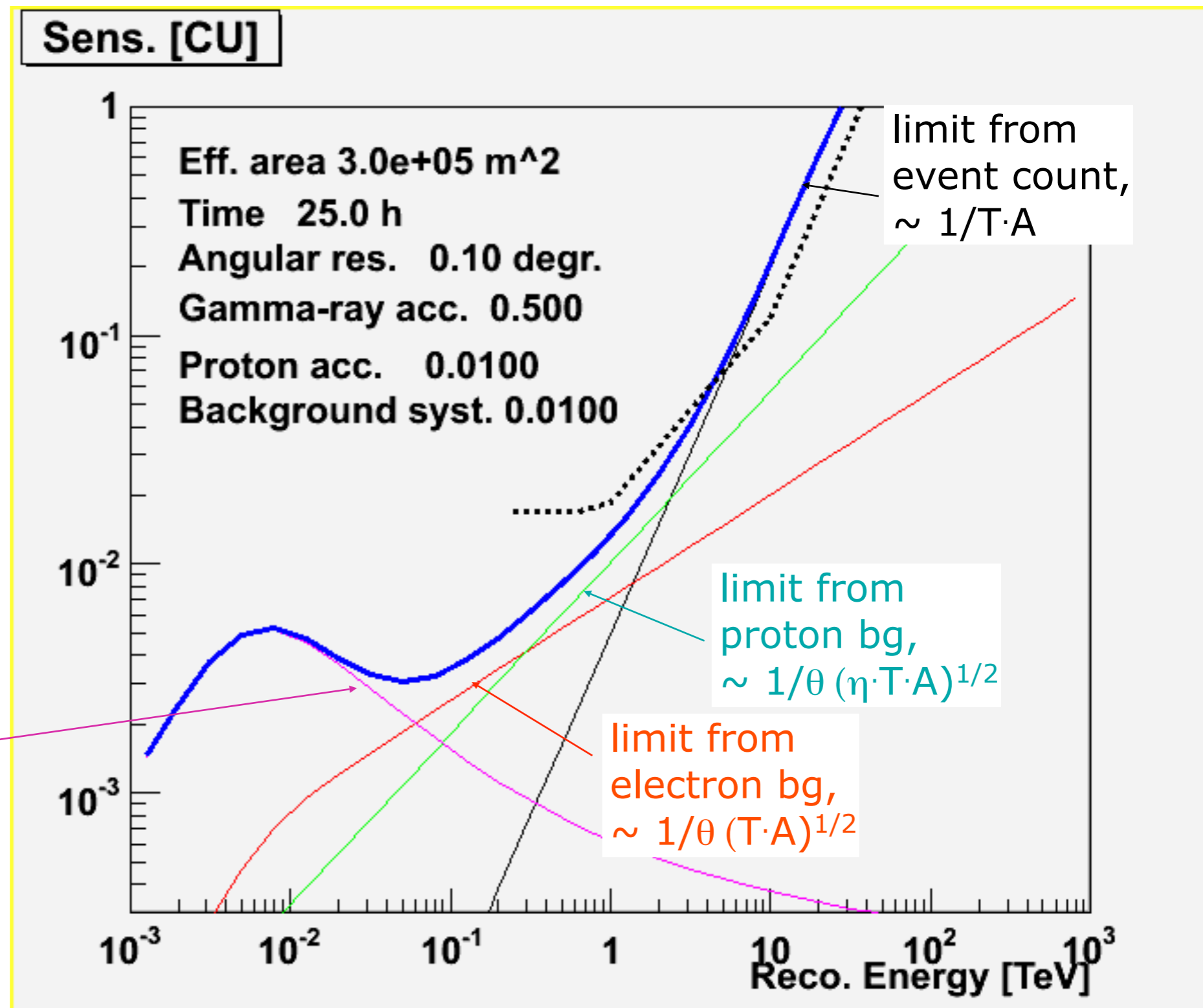
Exploring the cutoff
regime of cosmic
accelerators



Sensitivity vs energy

Minimal detectable flux per band
 $\log_{10} E = 0.2$, relative to a power-law Crab spectrum

limit from syst. error on background, indep. of T,A;

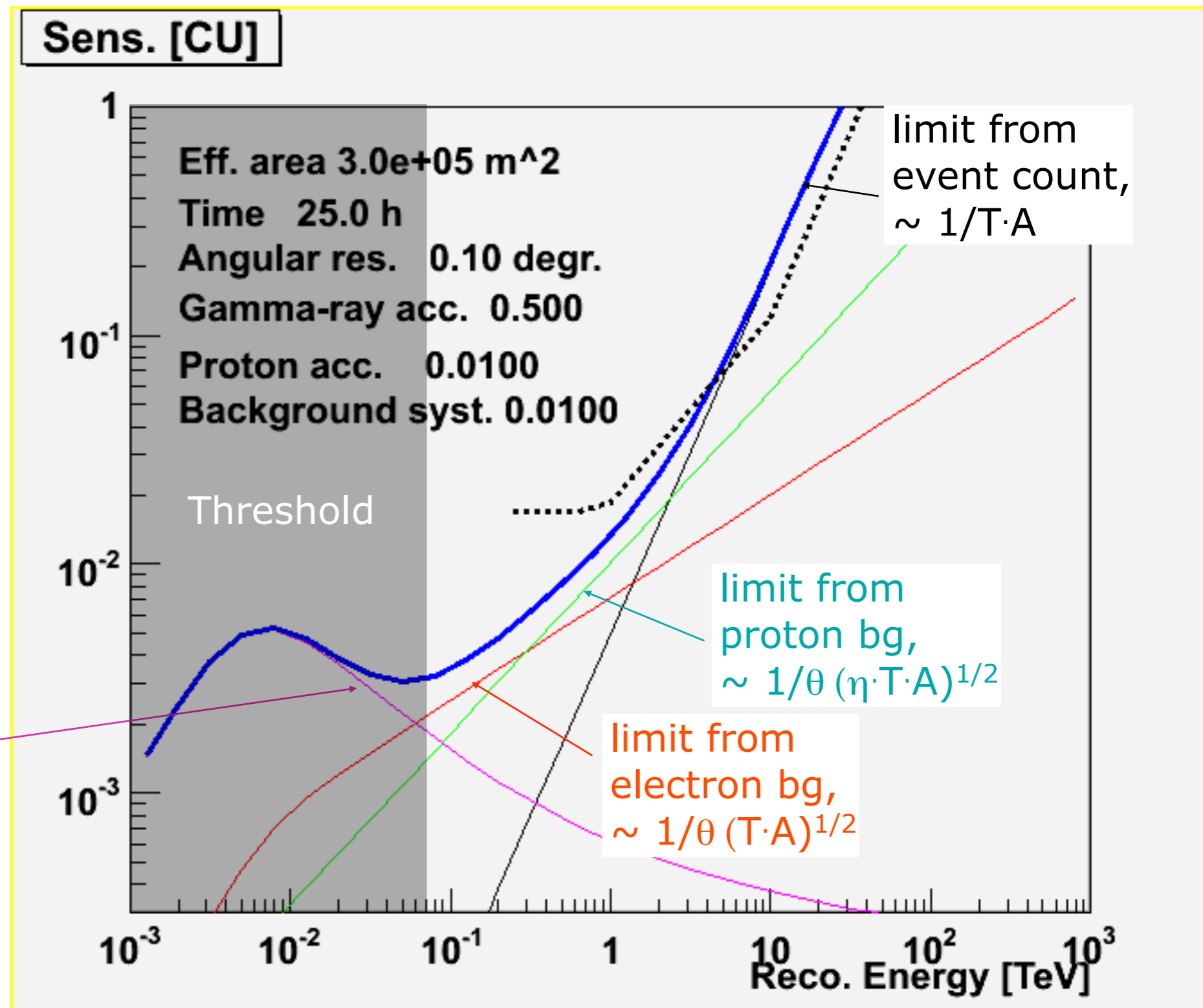


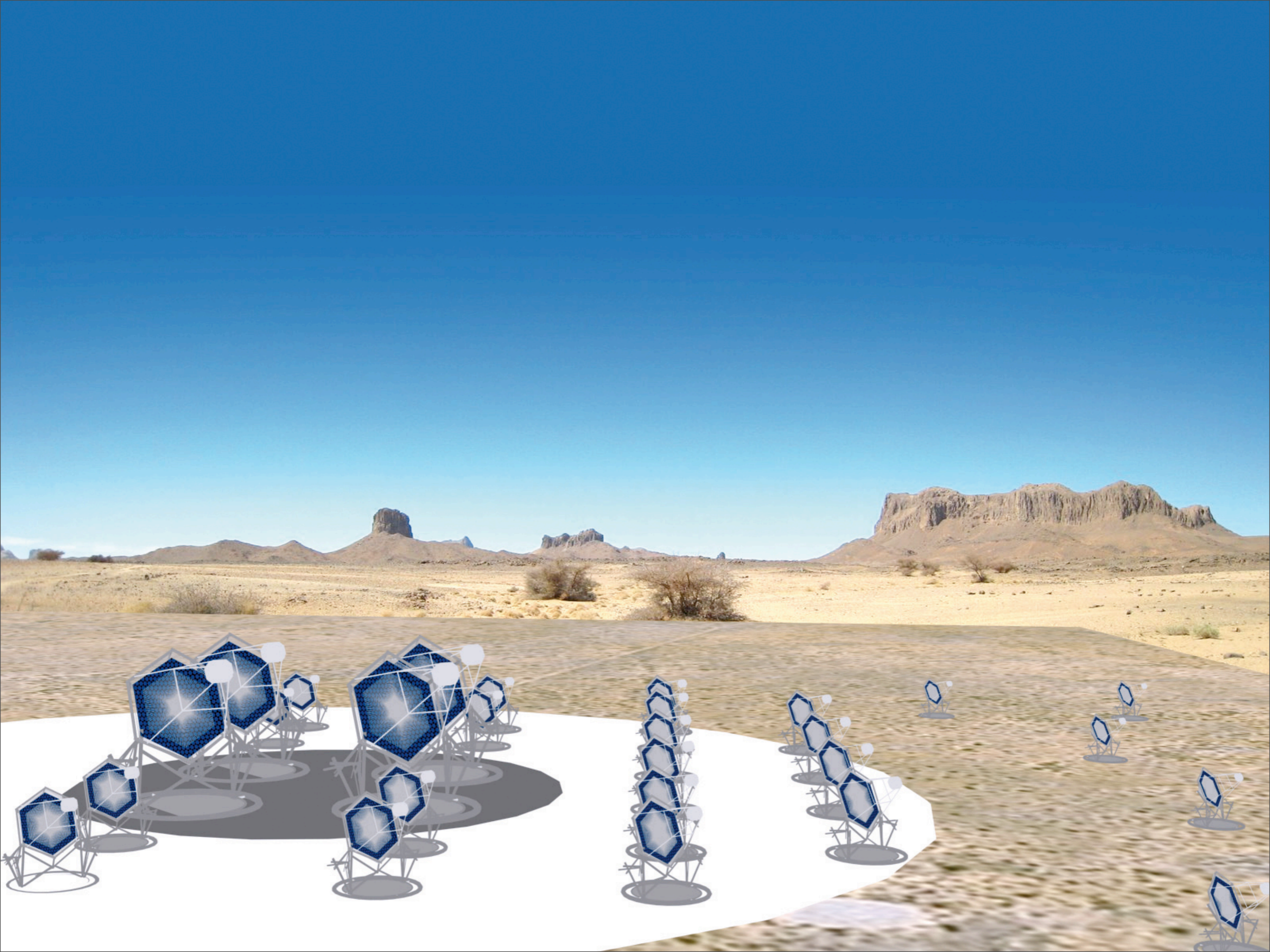


Sensitivity vs energy

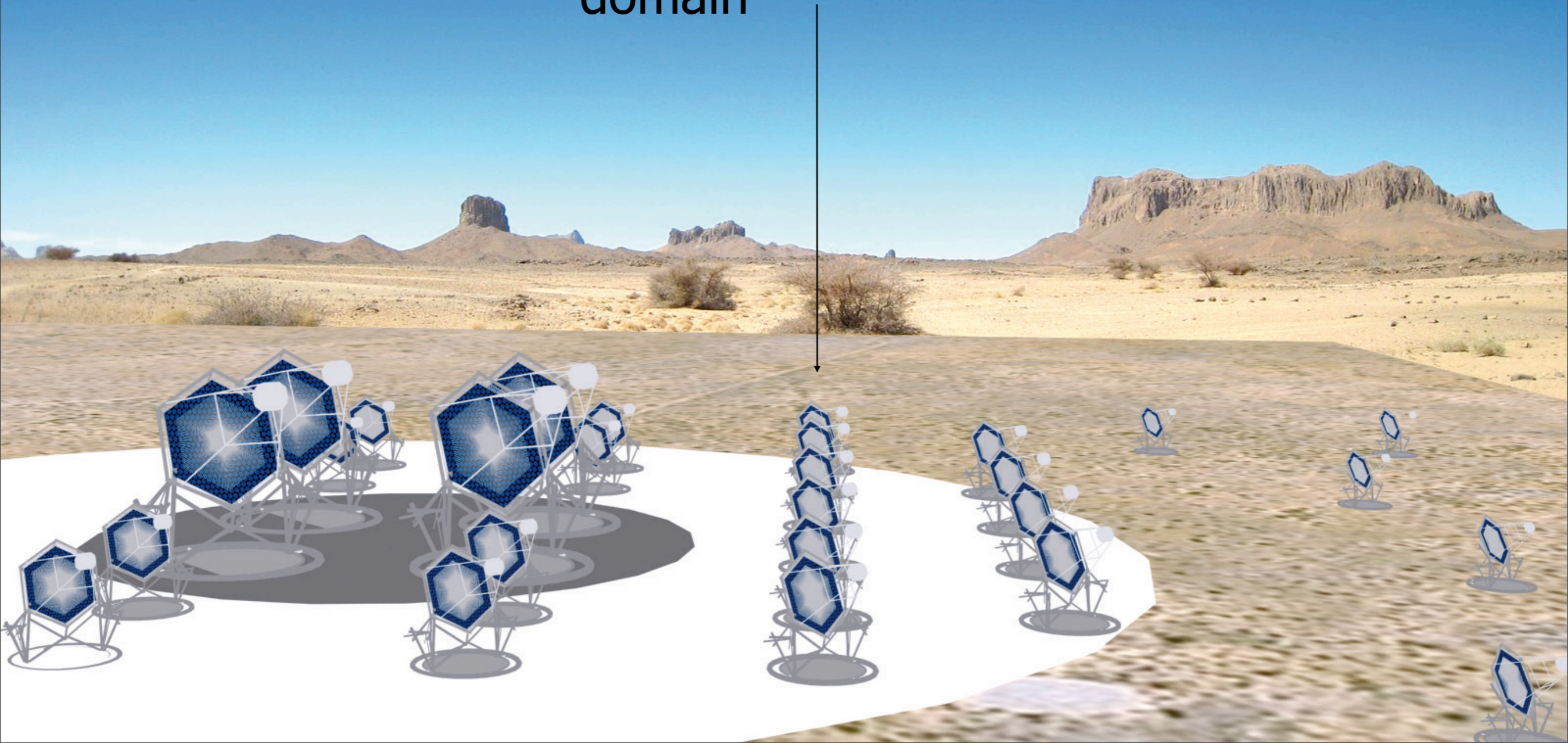
Minimal detectable flux per band
 $\log_{10} E = 0.2$, relative to a power-law Crab spectrum

limit from syst. error on background, indep. of T,A;



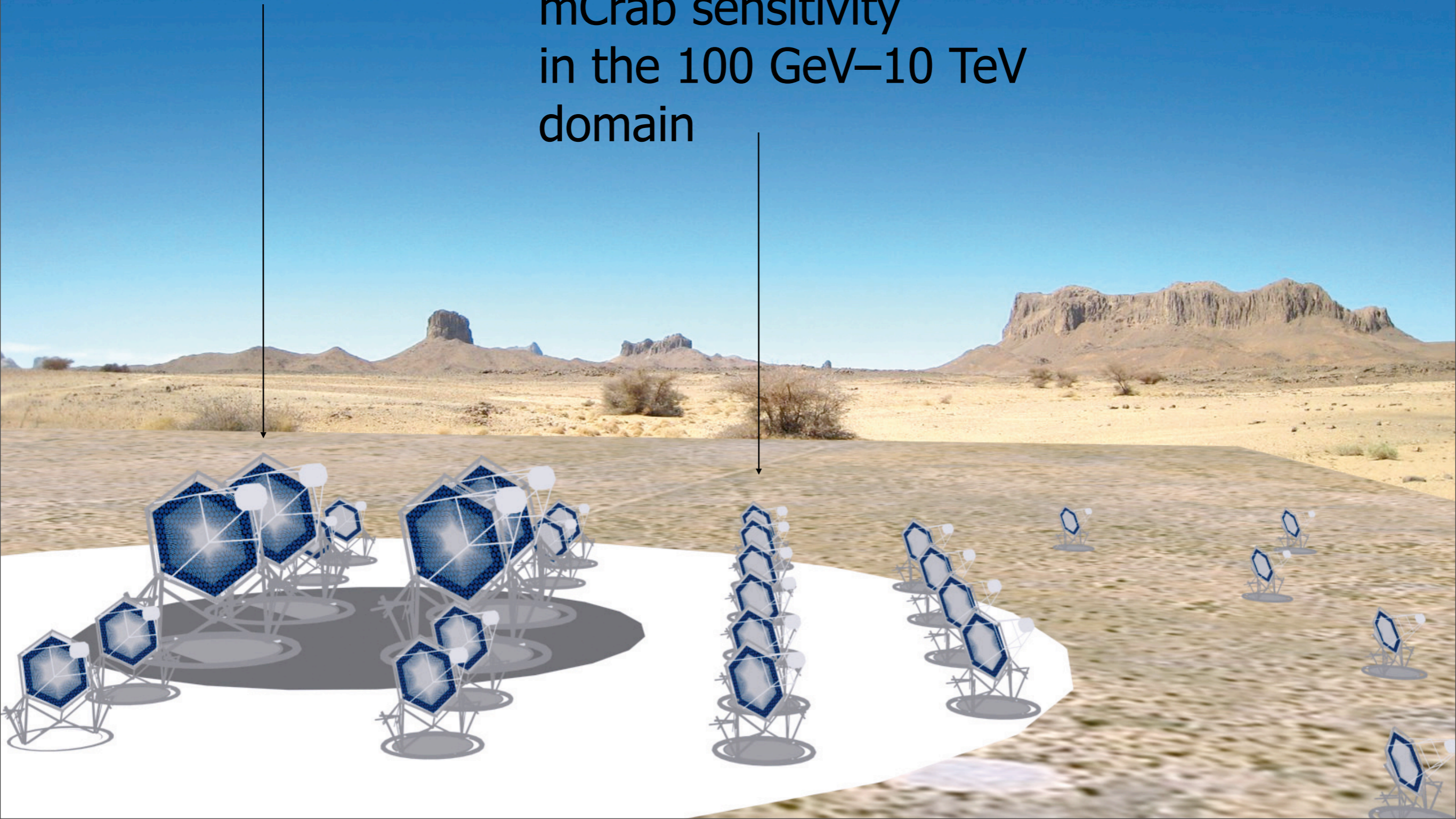


Core array:
mCrab sensitivity
in the 100 GeV–10 TeV
domain



Low-energy section
energy threshold
of some 10 GeV

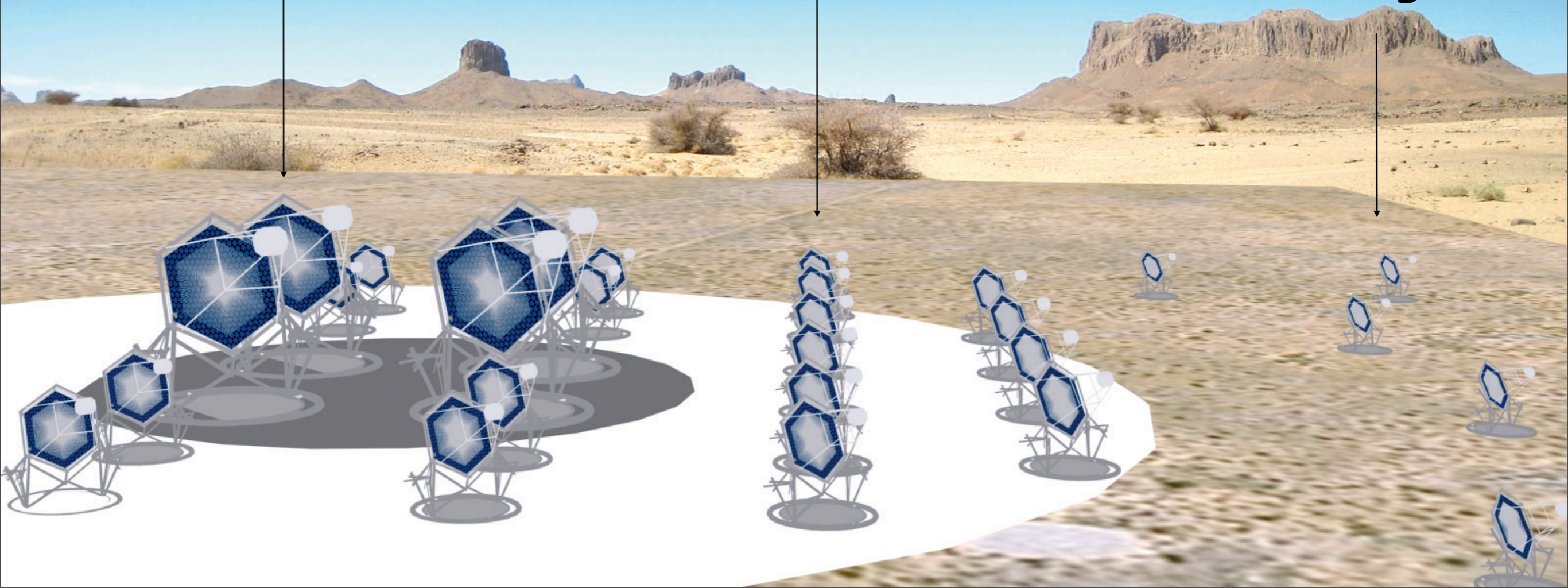
Core array:
mCrab sensitivity
in the 100 GeV–10 TeV
domain



Low-energy section
energy threshold
of some 10 GeV

Core array:
mCrab sensitivity
in the 100 GeV–10 TeV
domain

High-energy section
10 km² area at
multi-TeV energies



IACT and high altitude

Gamma-ray

Particle shower

The Cherenkov photon density **increase** with the altitude:

=> lower energy threshold

=> Higher sensitivity to low threshold

~ 10 km

Cherenkov light

~ 1°

~ 120 m

Gamma-ray

Particle shower

The Cherenkov photon density **increase** with the altitude:

=> lower energy threshold

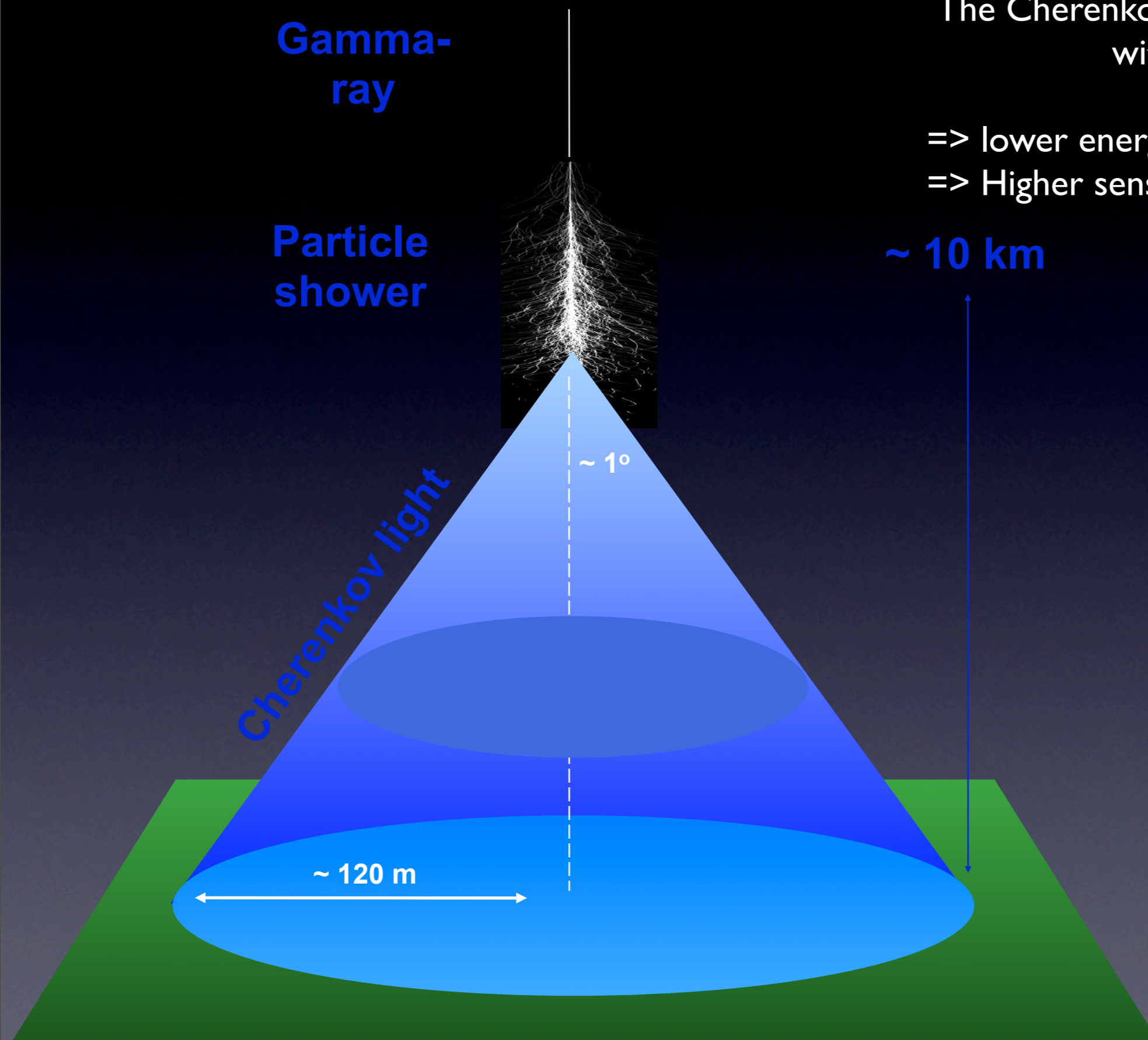
=> Higher sensitivity to low threshold

~ 10 km

Cherenkov light

~ 1°

~ 120 m



Gamma-ray

Particle shower

The Cherenkov photon density **increase** with the altitude:

=> lower energy threshold

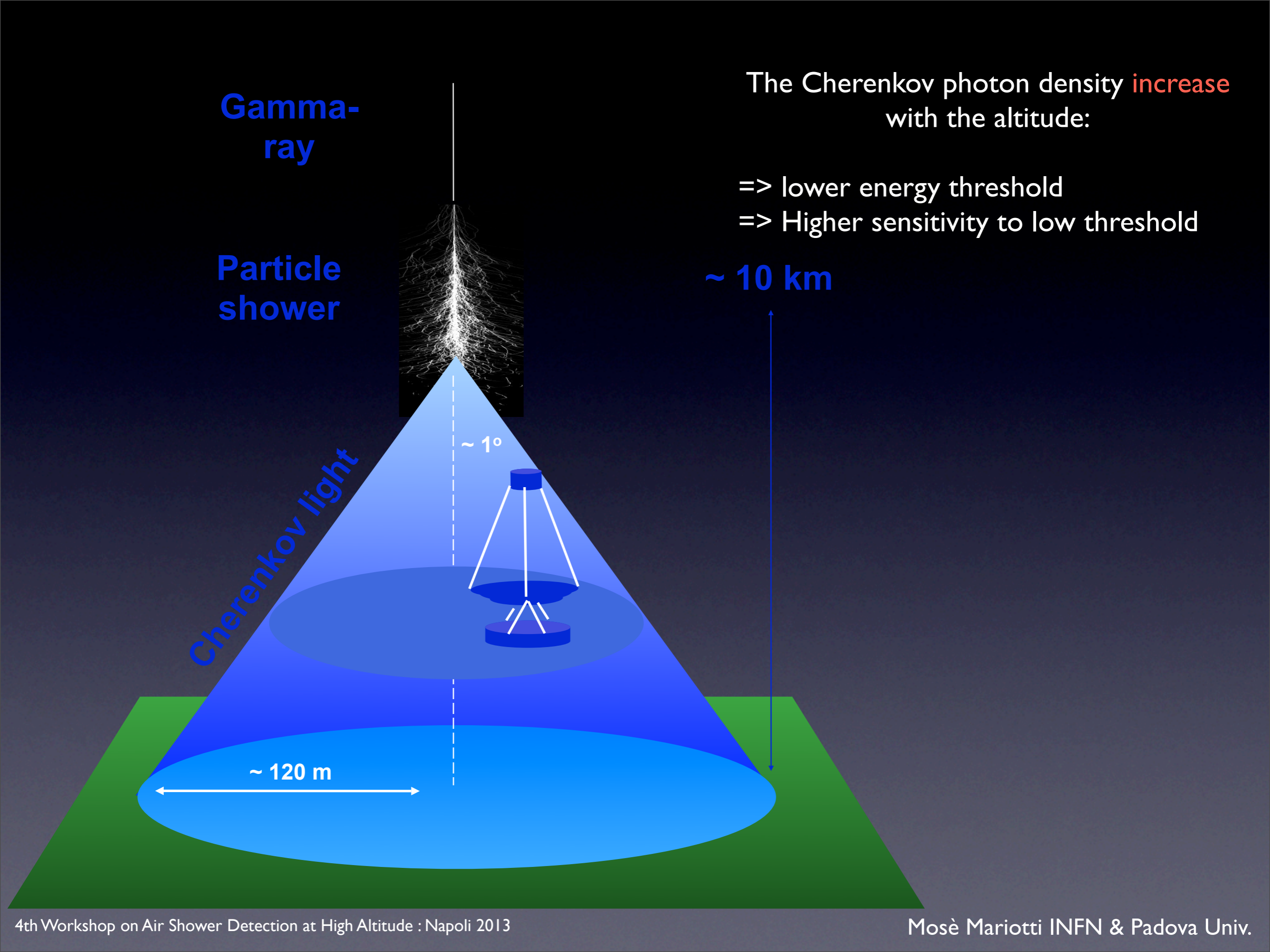
=> Higher sensitivity to low threshold

~ 10 km

Cherenkov light

~ 1°

~ 120 m



Gamma-ray

Particle shower

The Cherenkov photon density **increase** with the altitude:

=> lower energy threshold

=> Higher sensitivity to low threshold

~ 10 km

Coarse threshold reduction factor with respect a reference 2000 asl site

1.3 @3000 asl

1.8 @4000 asl

2.5 @5000 asl

Cherenkov light

~ 1°

~ 120 m

IACT at High Altitude

Unique opportunity for gamma ray astronomy to have high sensitivity at low threshold

It is not a new Idea (of course...) but the question is whether it is a priority now.....

Many discovery will be on the hand of such detector: because of the flux is increasing at low energy IACT at High altitude will be so sensitive to explore fast transient event at tenth of GeV energy regime

Astroparticle Physics, accepted for publication

**5@5 - a 5 GeV energy threshold array of
imaging atmospheric Cherenkov telescopes at
5 km altitude**

F.A. Aharonian, A.K. Konopelko, H.J. Völk

MPI für Kernphysik, D-69029 Heidelberg, Germany

IACT at High Altitude

Unique opportunity for gamma ray astronomy to have high sensitivity at low threshold

It is not a new Idea (of course...) but the question is whether it is a priority now.....

Many discovery will be on the hand of such detector: because of the flux is increasing at low energy IACT at High altitude will be so sensitive to explore fast transient event at tenth of GeV energy regime

My personal opinion:
soon or later we will do it

Astroparticle Physics, accepted for publication

**5@5 - a 5 GeV energy threshold array of
imaging atmospheric Cherenkov telescopes at
5 km altitude**

F.A. Aharonian, A.K. Konopelko, H.J. Völk

MPI für Kernphysik, D-69029 Heidelberg, Germany

Conclusions

The **High Sensitivity** IACT detectors are giving an unique opportunity to study process of high relevance for Astrophysics as well as fundamental physics

We are in the “golden ERA” of the gamma ray astronomy and new experiments are being designed and forked to empower the newly borne **experimental Astro - Particles Physics**

Likely, in a near future, IACT @ High Altitude will become a priority